

N° D'ORDRE : 7748

<p style="text-align: center;">UNIVERSITE PARIS XI UFR SCIENTIFIQUE D'ORSAY</p>

THESE

Présentée

Pour obtenir

**Le GRADE de DOCTEUR EN SCIENCES
DE L'UNIVERSITE PARIS XI ORSAY**

PAR

Béatrice DE TILIÈRE

Sujet : DIMÈRES SUR LES GRAPHEIS ISORADIAUX &
MODÈLE D'INTERFACES ALÉATOIRES EN
DIMENSION 2+2

Rapporteurs : M. Gérard BEN AROUS
M. David WILSON

Soutenue le 9 décembre 2004 devant la Commission d'examen

M. Richard KENYON (directeur de thèse)
M. Jean-François LE GALL
M. Yves LE JAN
M. Gilles SCHAEFFER
M. Wendelin WERNER

Remerciements

Merci Richard pour beaucoup de choses. D'abord d'avoir accepté de diriger mes recherches sans même m'avoir rencontrée. Merci pour toutes les discussions mathématiques qui éclairaient mes semaines de travail, et pour l'occasion que tu m'as donnée de te visiter à Princeton. Merci pour ta gentillesse, ta disponibilité, ta patience infinie avec mon incertitude chronique et mes "c'est vraiment nul ce que je suis entrain de faire...". J'ai beaucoup appris de toi, et t'en suis très reconnaissante. C'est une grande chance que d'avoir pu travailler avec toi!

Merci Professeur Werner d'avoir accepté de vous occuper de moi lors du départ de Richard. La porte de votre bureau était toujours ouverte, je vous remercie pour votre disponibilité, vos conseils et pour votre présence dans le jury.

Professor Ben Arous and Professor Wilson, thank you for having accepted to report my thesis. You both have very busy schedules, and I am grateful and honored that you have accepted to give me some of your time. Professeur Ben Arous, merci aussi de m'avoir guidée dans mes débuts mathématiques, et de m'avoir aidée à trouver ma voie. Je sens que je peux toujours compter sur vous pour un conseil, et vous en suis très reconnaissante.

Professeur Le Jan, merci pour votre présence dans le jury, et pour les discussions que nous avons eues à Saint-Flour et à Orsay, cela fait chaud au coeur de se sentir encouragée et soutenue.

Professeur Le Gall et Gilles Schaeffer, vous m'honorez beaucoup en acceptant d'être dans mon jury, merci!

Yuval, I thank you for recommending me to Richard. Without you this thesis would not have been possible, you gave me the opportunity to spend three wonderful years.

Merci aux habitants du bureau 106 anciens et nouveaux, et à ceux du couloir du 430 pour les moments passés à rire et à discuter; en particulier Graham, Estelle, Céline, Vincent, Gilles, Mina ... c'est dur de ne pas énumérer tout le monde! Madame Justin et Madame Lavigne, merci pour votre sourire, c'est un plaisir que de passer dans votre bureau (et vous avez vu que je ne m'en prive pas...). Reda, après avoir partagé le même bureau à Lausanne et à Orsay, tous les bureaux sans toi me paraîtront un peu vide. Je te remercie pour ton amitié très précieuse, et souhaite que nos chemins se recroisent le plus rapidement possible. Cédric, d'abord co-thésard, tu es devenu un très grand ami. Merci pour tes conseils et pour les nombreuses discussions mathématiques, en particulier celle de mi-août 2004. Marilyne, Hugo, outre votre amitié constante, je vous remercie particulièrement pour toutes les discussions sur notre avenir tellement plein de rêves et tellement incertain...

A ma famille, en particulier à mes parents, merci de m'avoir toujours guidée, encouragée et soutenue dans mes choix d'étude et professionnels. C'est un soutien qui compte

énormément à mes yeux, et sur lequel il fait bon s'appuyer les jours de découragement. Vos conseils me sont très précieux, merci !

A toi petite vie qui grandit au fond de moi, merci d'être là.

Guillaume, ma thèse fait une centaine de pages, mais tout ce que je veux te dire bien plus, on a donc un problème... il faut que j'abrège... Simplement, cette thèse ne serait pas là si tu n'étais pas à mes côtés. Ton ouverture d'esprit et ton respect vis à vis de ma passion me laissera toujours admirative, et je t'en remercie. Merci de me faire confiance, j'espère que je pourrai toujours en être digne.

Abstract

The dimer model represents diatomic molecules adsorbed on the surface of a crystal. We suppose that the lattice representing the surface of the crystal is infinite, periodic, and satisfies a geometric condition called *isoradiality*, moreover we assume that the *critical* weight function is assigned to edges of the lattice (weights represent the external temperature). The model then has a “critical” behavior, i.e. it can be in 2 different phases, solid or liquid, instead of 3 in general (it has no gaseous phase). Our three main results on the isoradial dimer model are the following. We prove an explicit formula for the growth rate of the partition function of the natural exhaustion of the infinite lattice, and we show an explicit formula for the minimal free energy Gibbs measure. The interesting feature of those two formulas lies in the fact that they only depend on the local structure of the graph, which makes them very simple to use. We believe this locality property to be specific of the isoradial case. Geometrically, dimer configurations can be interpreted as discrete surfaces described by one height function. We show that when the surfaces are chosen with respect to the minimal free energy Gibbs measure, the height function converges to a Gaussian free field. Classical examples of isoradial dimer models are the case of the square lattice and that of the hexagonal lattice, with uniform measure on dimer configurations.

We introduce the *triangular quadri-tile* dimer model, where quadri-tilings are tilings by quadrilaterals made of adjacent right triangles. We show that this model is the superposition of two dimer models on isoradial graphs, and interpret it geometrically as surfaces of dimension 2 in a space of dimension 4. We study this model in the “critical” phase. We prove an explicit formula for the growth rate of the *total* partition function, and for a measure on the space of *all* quadri-tilings (this requires the extension of the result of the isoradial case to a family of non-periodic graphs). It is the first random interface model in dimension $2 + 2$ for which those kind of results can be obtained.

Keywords: statistical mechanics, dimers, tilings, isoradial graphs, partition function, Gibbs measure, Gaussian free field, quadri-tilings.

MSC2000: 82B20.

Contents

1	Introduction	11
2	The dimer model	25
2.1	The dimer model	26
2.1.1	2-tilings/dimer configurations	26
2.1.2	Energy of configurations, and partition function	27
2.1.3	Boltzmann and Gibbs measures	29
2.2	Geometric features of the dimer model	30
2.2.1	Height functions	30
2.2.2	2-tilability	32
2.2.3	The space of 2-tilings	34
3	Isoradial dimer model	37
3.1	Isoradial graphs and critical weight function	38
3.1.1	Isoradial graphs	38
3.1.2	Critical weight function	38
3.2	Complex Dirac operator	39
3.2.1	Complex Dirac operator	39
3.2.2	Inverse complex Dirac operator	39
3.3	Real Dirac operator	40
3.3.1	Real Dirac operator	41
3.3.2	Inverse real Dirac operator	41
3.4	Isoradial dimer model on the torus	45
3.4.1	Toroidal partition function	45
3.4.2	Toroidal Boltzmann measure	46
3.4.3	Inverse real Dirac operator and inverse Kasteleyn matrices	47
3.5	Isoradial dimer model and height functions	48
4	Quadri-tile dimer model	49
4.1	Quadri-tiles and quadri-tilings	50
4.2	Underlying rhombus-with-diagonals tilings	50
4.2.1	Underlying rhombus-with-diagonals tilings	50
4.2.2	Properties of rhombus-with-diagonals tilings	51

4.3	Triangular quadri-tile dimer model	52
4.3.1	Definition	52
4.3.2	Critical weight function	52
4.4	Quadri-tilings as surfaces in dimension $2+2$	53
4.4.1	First height function	53
4.4.2	Second height function	54
4.4.3	Geometric interpretation	55
4.5	The space of quadri-tilings	55
5	Combinatorics of the triangular quadri-tile and isoradial dimer models	57
5.1	Growth rate of the total partition function in the case of critical weights	58
5.1.1	Definition of the total partition function	58
5.1.2	Statement of result	58
5.2	Property of the total partition function	59
5.3	Partition function for planar and toroidal graphs	63
5.3.1	Triangular lattice case	64
5.3.2	Lozenge-with-diagonals tiling case	64
5.4	Growth rate of the partition function of isoradial dimer models	74
5.4.1	Statement of result	75
5.4.2	Proof of proposition 5.8	75
5.5	Proof of theorem 5.1	77
6	Explicit Gibbs measure for isoradial dimer models and the case of quadri-tilings	79
6.1	Explicit Gibbs measure for the isoradial dimer model	80
6.1.1	Explicit Gibbs measure	80
6.1.2	Proof of theorem 6.1 under assumption 1.	82
6.1.3	Geometric property of rhombus tilings	85
6.1.4	Proof of theorem 6.1 under assumption 2.	91
6.2	The case of quadri-tilings	92
6.2.1	Total measure for the triangular quadri-tile dimer model	92
6.2.2	Asymptotics of the quadri-tile Gibbs measure and of the total measure	94
7	Height fluctuations for isoradial dimer models	99
7.1	Gaussian free field in the plane	99
7.1.1	Green's function of the plane, and Dirichlet energy	100
7.1.2	Random distributions	101
7.1.3	Gaussian free field in the plane	102
7.2	Gaussian fluctuations for the height function of the isoradial dimer model	102
7.3	Proof of theorem 7.3	103
7.3.1	Properties of the height function	103

7.3.2	Moment formula	104
7.3.3	Proof of theorem 7.3	111
Bibliography		115

Chapitre 1

Introduction

Le Modèle de dimères

Un modèle de mécanique statistique exactement soluble

La mécanique statistique a pour but d'étudier les propriétés globales d'un système mécanique. Elle souhaite prédire les relations existant entre les observables macroscopiques du système, en ne connaissant que les interactions microscopiques.

Dans ce domaine, le modèle le plus célèbre est sans doute le *modèle d'Ising*. Le système considéré est un aimant constitué de molécules contraintes à être sur un réseau régulier. Chaque molécule est elle-même vue comme un aimant microscopique qui peut pointer dans deux directions possibles. Chacune des configurations σ de molécules a une énergie $\mathcal{E}(\sigma)$, somme de deux contributions : l'énergie d'interactions intermoléculaires, et celle d'interaction avec un champ magnétique externe.

En 1871, Boltzmann dérive la probabilité d'apparition d'une configuration à partir des principes thermodynamiques, dans le cas des gaz [8]. Depuis lors, sa formule est utilisée en mécanique statistique. Dans le cas du modèle d'Ising, la probabilité d'une configuration σ est :

$$e^{\frac{-\mathcal{E}(\sigma)}{kT}} \frac{1}{Z},$$

où k est la constante de Boltzmann, et T est la température. Z est la constante normalisatrice, appelée *fonction de partition*. Son importance est capitale pour la raison suivante : Z vue comme une fonction des paramètres du modèle permet de dériver les observables macroscopiques du système, telle la magnétisation dans le cas Ising [1].

Rares sont les modèles de mécanique statistique où la fonction de partition peut être calculée exactement. Deux des plus importants sont :

- Le modèle d'Ising 2 dimensionnel avec interactions entre plus proche voisins, et champ magnétique externe nul : le calcul a été fait par Onsager [38].

- Le *modèle de dimères* : le calcul a été fait par Kasteleyn [19], et indépendamment par Temperley et Fisher [42].

Ainsi, le fait que le modèle de dimères soit un des rares qui permette d'obtenir des résultats exacts constitue une des motivations principales pour son étude.

Ses origines

Dans la littérature physique, le modèle de dimères est apparu pour la première fois en 1937 dans un article de Fowler et Rushbrooke [13]. Il sert à modéliser la répartition de molécules diatomiques à la surface d'un cristal. Les physiciens ont observé que les points favorables pour la répartition des molécules forment un réseau, et qu'une molécule diatomique occupe deux sites voisins. Le modèle de dimères fait partie d'une classe de problèmes plus grande, qui concerne la répartition de figures de tailles différentes sur un réseau. D'un point de vue physique, il est aussi utilisé dans la théorie des liquides constitués de molécules de tailles différentes [16], et dans la théorie des clusters cellulaires de l'état liquide [6].

Les mathématiciens étudient un modèle équivalent qui est celui des *2-pavages*. Deux exemples classiques sont les pavages par dominos et par losanges-60° (appelés aussi calissons). Dans le premier cas, on considère le réseau \mathbb{Z}^2 . On le recouvre de tuiles formées de deux carrés adjacents, appelées **dominos**, de sorte qu'il n'y ait pas de chevauchement et qu'il ne reste pas de trou. Dans le deuxième cas, la procédure est la même sauf que l'on considère le réseau triangulaire équilatéral \mathbb{T} , et que les tuiles formées de triangles adjacents sont appelées des **losanges-60°**. La première référence mathématique que nous avons trouvée à ce sujet est [9] et concerne le "problème des calissons", mais nous dirions que l'étude systématique du modèle débute avec Thurston [44].

Définitions

Une définition détaillée du modèle de dimères est donnée au paragraphe 2.1, en voici les points essentiels.

Le système considéré est un graphe G dans le plan. Une **2-tuile** de G est un polygone formé de deux faces intérieures de G adjacentes le long d'une arête. Un **2-pavage** de G est un recouvrement de G par des 2-tuiles qui ne se chevauchent pas, et qui ne laissent pas de trou.

Une **configuration de dimères** du graphe dual G^* est un couplage parfait de G^* , c'est à dire un ensemble d'arêtes qui couvre chaque sommet exactement une fois. Les arêtes du couplage représentent les molécules diatomiques, et le graphe G^* le réseau sur lequel elles se répartissent. On note $\mathcal{M}(G^*)$ l'ensemble des configurations de dimères du graphe G^* .

Il existe une bijection entre les 2-pavages du graphe G , et les configurations de dimères

du graphe dual G^* : soit un 2-pavage de G , à chaque tuile de G correspond l'arête duale à l'arête séparant les deux faces constituant la tuile ; l'ensemble d'arêtes ainsi défini forme un couplage parfait de G^* . Un exemple de cette bijection est donné à la figure 2.1. C'est grâce à cette correspondance que nous parlons de modèles équivalents.

Supposons le graphe G^* fini. Chaque configuration $M \in \mathcal{M}(G^*)$ possède une énergie $\mathcal{E}(M)$ déterminée par une fonction de poids ν , strictement positive, sur les arêtes de G^* :

$$\mathcal{E}(M) = - \sum_{e \in M} \log \nu(e).$$

Ceci nous permet de définir la **mesure de Boltzmann** μ^1 sur $\mathcal{M}(G^*)$. Chaque configuration $M \in \mathcal{M}(G^*)$ a une probabilité de :

$$\mu^1(M) = \frac{e^{-\mathcal{E}(M)}}{Z(G^*, \nu)},$$

où $Z(G^*, \nu) = \sum_{M \in \mathcal{M}(G^*)} e^{-\mathcal{E}(M)}$ est la **fonction de partition**. Remarquons que la température est directement incluse dans la fonction de poids.

En utilisant la bijection entre les configurations de dimères et les 2-pavages, on peut voir ν comme une fonction de poids sur les 2-tuiles, et μ^1 comme une mesure de probabilité sur les 2-pavages du graphe G .

Lorsque le graphe G est planaire, Kasteleyn [20] donne une formule explicite pour $Z(G^*, \nu)$: c'est la racine du déterminant de la matrice d'adjacence K du graphe G^* , où l'on change le signe de certains des coefficients ; K est appelée **matrice de Kasteleyn** du graphe G^* . Kenyon [21] donne une expression explicite pour la mesure de Boltzmann en fonction de la matrice de Kasteleyn et de son inverse.

Supposons le graphe G^* infini. Une **mesure de Gibbs** est une mesure de probabilité définie sur $\mathcal{M}(G^*)$ qui vérifie les propriétés suivantes : si l'on fixe un couplage parfait dans une région annulaire de G^* , alors les couplages à l'extérieur et à l'intérieur de l'anneau sont indépendants ; de plus la probabilité d'un couplage à l'intérieur de l'anneau est proportionnelle à $\prod_{e \in M} \nu(e)$.

Interprétation géométrique : interfaces en dimension 2+1

L'interprétation géométrique des 2-pavages nécessite la notion de *fonction de hauteur*. Elle a été réalisée par Thurston [44] dans le cas des losanges et des dominos. Notons que cette notion était déjà présente chez Blöte et Hilhorst [3], et Levitov [33].

En utilisant les groupes de Cayley et la fonction de hauteur, Thurston interprète les pavages par losanges du réseau triangulaire \mathbb{T} comme des surfaces dans \mathbb{Z}^3 (où les diagonales des cubes sont perpendiculaires au plan), projetées dans le plan. La fonction de hauteur associée à chaque sommet d'un pavage par losanges, la "hauteur" du sommet lui correspondant sur la surface. La figure 2.1 convaincra le lecteur de l'interprétation

des losanges comme interfaces de cubes projetés. Thurston donne une interprétation analogue des pavages par dominos du réseau \mathbb{Z}^2 , dont la représentation géométrique est toutefois moins intuitive.

Une question naturelle est de généraliser la notion de fonction de hauteur aux 2-pavages de graphes généraux. Il semblerait que lorsque le dual du graphe n'est pas biparti, il n'y ait pas de définition analogue. Dans le cas où le dual du graphe est biparti, Kenyon, Propp et Wilson [39, 30] donnent une généralisation. Nous choisissons cependant l'approche de Kenyon, Okounkov, Sheffield [29], voir aussi [5], qui utilise la notion de *flots*. La définition est donnée au paragraphe 2.2. Il existe une bijection entre les fonctions de hauteur sur les sommets d'un graphe G , et les 2-pavages de G (une fois fixée la hauteur d'un des sommets). Ainsi tout 2-pavage de G peut être interprété comme une surface discrète de dimension 2 dans un espace de dimension 3 ; on parle alors d'interface en dimension $2 + 1$.

Sujet de la thèse

Un modèle d'interfaces en dimension $2 + 2$

Le sujet de thèse proposé par Richard Kenyon est l'étude du modèle de **quadri-pavages**. Son originalité réside dans le fait qu'il s'agisse de pavages par un ensemble fixé de tuiles qui correspond à toute une famille de modèles de dimères. Une attention particulière est portée à un cas particulier de ce modèle appelé modèle de **quadri-pavages triangulaire**. C'est le premier exemple de modèle d'interfaces en dimension $2 + 2$, qui est superposition de deux modèles de dimères. En effet les modèles de dimères étudiés jusqu'alors, tels les pavages par losanges ou par dominos, sont des modèles d'interfaces en dimension $2 + 1$. On peut décrire cette propriété de deux autres manières : les quadri-pavages sont caractérisés par deux fonctions de hauteur, ou encore ce sont des surfaces de dimension 2 dans un espace de dimension 4, qui sont projetées sur le plan. La définition et les propriétés des modèles de quadri-pavages et de quadri-pavages triangulaire sont le sujet du chapitre 4, dont voici une brève description.

On considère l'ensemble des triangles rectangles dont l'hypoténuse a longueur 2. On colorie en noir le sommet de l'angle droit, et en blanc les deux autres. Une **quadri-tuile** (cf. figure 4.1) est obtenue à partir de deux tels triangles de deux manières : soit en les collant le long de l'hypoténuse, soit en les collant le long de l'une des autres arêtes (s'ils en ont une de même longueur), en identifiant les sommets noirs et blancs. Notons que chacune des quadri-tuiles est considérée comme un quadrilatère. Un **quadri-pavage** est un pavage du plan avec des quadri-tuiles, qui respecte la coloration des sommets, voir figure 4.1.

Chaque quadri-pavage Q a la propriété d'être un 2-pavage d'un unique pavage par losanges $R(Q)$, où les losanges ont leurs diagonales. On appelle $R(Q)$ le **pavage par losanges-avec-diagonales sous-jacent** ; le **pavage par losanges sous-jacent** est le pavage par losanges correspondant, on le note $R(Q)$. Réciproquement, tout 2-pavage

d'un pavage par losanges-avec-diagonales est un quadri-pavage. Ainsi, les quadri-pavages constituent un ensemble de modèles de dimères sur une famille de graphes.

Le modèle de quadri-pavages triangulaire est constitué de l'ensemble \mathcal{Q} des quadri-pavages dont le pavage par losanges sous-jacent est formé de losanges- 60° uniquement (un exemple est donné à la figure 1.1). Soit $Q \in \mathcal{Q}$, alors Q est un 2-pavage de son pavage par losanges- 60° -avec-diagonales sous-jacent $L(Q)$. De plus, $L(Q)$ est un 2-pavage du réseau triangulaire équilatéral \mathbb{T} . Ainsi le modèle de quadri-pavages triangulaire correspond à deux modèles de dimères superposés.

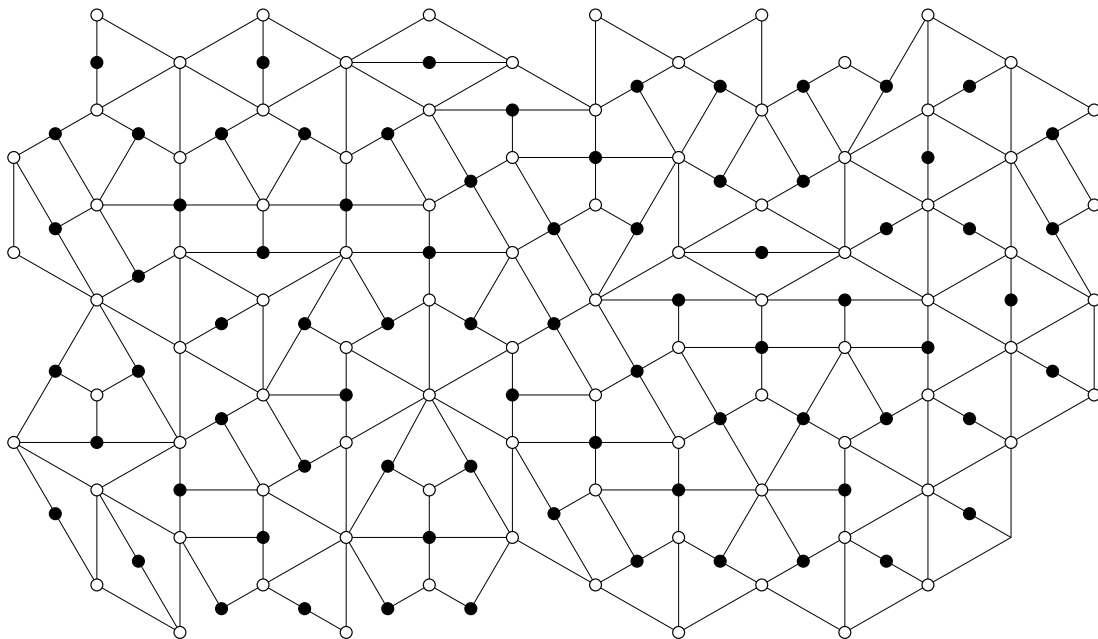


FIG. 1.1 – Exemple de pavage du modèle de quadri-pavages triangulaire

Ce fait peut être interprété géométriquement. Nous montrons que chaque quadri-pavage de \mathcal{Q} est caractérisé par deux fonctions de hauteur, et nous obtenons l'interprétation suivante. Un quadri-pavage $Q \in \mathcal{Q}$ est une surface S_1 dans un espace de dimension 4, projetée sur le plan. S_1 peut aussi être projetée sur $\tilde{\mathbb{Z}}^3$ ($\tilde{\mathbb{Z}}^3$ est l'espace \mathbb{Z}^3 où les cubes ont leurs diagonales), et l'on obtient une surface S_2 . Lorsque S_2 est projetée sur le plan, on obtient le pavage par losanges-avec-diagonales sous-jacent $L(Q)$.

Dans une dernière partie, en utilisant le théorème de Propp [39], nous caractérisons l'espace des quadri-pavages d'un sous-graphe fini et simplement connexe du réseau triangulaire.

Le modèle de dimères isoradial

Les pavages par losanges-avec-diagonales, ainsi que le réseau triangulaire \mathbb{T} ont la propriété géométrique d'être des graphes **isoradiaux**, c'est à dire que toutes leurs faces sont inscriptibles dans un cercle, et tous les cercles ont le même rayon.

Lorsque G est un graphe isoradial, Kenyon [26] définit une fonction de poids spécifique sur les arêtes de son dual G^* , appelée fonction de poids **critique**. On appelle **modèle de dimères isoradial** un modèle de dimères sur un graphe isoradial, dont les arêtes du dual sont munies de la fonction de poids critique.

Incités par l'originalité des résultats de Kenyon sur les graphes isoradiaux, nous avons voulu généraliser nos travaux à cette famille de graphes. Voici une idée de ses résultats. Soit G un graphe isoradial infini avec fonction de poids critique sur les arêtes de G^* . Supposons de plus que G^* est biparti, notons W l'ensemble des sommets blancs et B l'ensemble des sommets noirs. Kenyon définit l'opérateur de Dirac complexe K et son inverse K^{-1} . K est représenté par une matrice $K(w, b)$ ($w \in W$, $b \in B$) qui est une matrice de Kasteleyn infinie. L'inverse K^{-1} a une propriété surprenante : il ne dépend que de la géométrie locale du graphe G^* (i.e. $K^{-1}(b, w)$ ne dépend que des angles le long d'un chemin de w à b). De plus, Kenyon conjecture que K^{-1} est, dans un certain sens à préciser, la limite de la matrice de Kasteleyn inverse. Il obtient aussi une expression très simple pour ce qu'il appelle le "log normalisé du déterminant de K ", et conjecture que ce serait, dans un sens à préciser aussi, la limite de fonctions de partitions normalisées.

Il nous a paru très intéressant de donner un sens à l'opérateur de Dirac complexe et à son inverse, dans le cadre du modèle de dimères isoradial. En effet, cette propriété de "localité", qui permet d'avoir des résultats s'exprimant très simplement, est étonnante et n'apparaît pas dans les modèles de dimères sur des graphes généraux.

Les résultats principaux

Les résultats principaux se trouvent dans les chapitres 5 à 7. Nous les avons ordonnés de la manière dont on aborde un problème de dimères. La première étape est de comprendre la combinatoire, i.e. la fonction de partition, qui décrit le comportement global des configurations. La deuxième est d'obtenir une expression explicite pour une mesure sur les configurations, afin de pouvoir comprendre les statistiques locales. Et la troisième consiste à utiliser l'interprétation des configurations de dimères en surfaces discrètes, pour étudier les fluctuations des surfaces autour de leur moyenne. Il existe encore d'autres questions comme celle de comprendre les transitions de phase du modèle, que nous souhaitons aborder après la thèse.

Chacun des paragraphes suivants correspond à un des chapitres 5 à 7, et est structuré ainsi : nous donnons d'abord une description de la problématique générale et un aperçu des résultats existants ; puis nous expliquons les résultats obtenus.

Combinatoire du modèle de quadri-pavages triangulaire et du modèle de dimères isoradial

Les configurations de dimères représentent des molécules diatomiques réparties à la surface d'un cristal, ainsi il est intéressant d'étudier les modèles de dimères sur des graphes infinis. La fonction de partition d'un tel modèle est infinie, et l'étude de la combinatoire est abordée de la manière suivante. Soit un modèle de dimères sur un graphe G infini, où les arêtes du dual G^* sont munies d'une fonction de poids ν ; prendre une exhaustion $\{G_n\}$ de G constituée de graphes finis, puis calculer la limite des fonctions de partitions des graphes G_n^* correctement normalisées, c'est à dire

$$\lim_{n \rightarrow \infty} \frac{1}{|V(G_n^*)|} \log Z(G_n^*, \nu), \quad (1.1)$$

où $V(G_n^*)$ dénote l'ensemble des sommets de G_n^* . Notons que cette limite dépend de l'exhaustion choisie.

Résultats existants

- Kasteleyn [18] : calcule la limite (1.1) dans le cas d'une exhaustion du réseau \mathbb{Z}^2 par des graphes planaires, et d'une autre par des graphes toriques.
- Kasteleyn [20] : donne une formule explicite pour la fonction de partition d'un graphe fini et simplement connexe, c'est la racine du déterminant de la matrice de Kasteleyn (matrice d'adjacence avec signes modifiés).
- Kasteleyn [19] : observe les transitions de phase du modèle de dimères sur le réseau hexagonal, en étudiant la régularité de la fonction de partition comme fonction des poids sur les arêtes.
- Cohn, Kenyon, Propp [7] : entre autres, étudient précisément les transitions de phase pour le modèle de dimères sur \mathbb{Z}^2 .
- Tesler [43] : donne une formule exacte pour la fonction de partition d'un graphe plongé sur une surface orientable ou non.
- Elkies, Kuperberg, Larsen et Propp [12] : donne une formule exacte (en fonction de n) pour la fonction de partition d'un diamant aztèque de taille n .
- Kenyon, Okounkov, Sheffield [29] : considèrent un graphe G doublement périodique; donnent une formule explicite pour la limite (1.1) dans le cas d'une exhaustion naturelle par des graphes toriques. Cette limite s'exprime comme une double intégrale du "polynôme caractéristique". Les zéros de ce polynôme décrivent les phases du modèle : liquide, gazeuse, solide.

Résultats obtenus

Le chapitre 5 a pour objet la compréhension de la combinatoire du modèle de quadri-pavages triangulaire. L'approche doit être adaptée car les quadri-pavages correspondent aux 2-pavages d'une famille de graphes, et non d'un seul comme c'était le cas pour les modèles étudiés jusqu'alors.

Une quantité naturelle à introduire est la **fonction de partition totale** définie comme suit. Soit ν une fonction de poids sur les quadri-tuiles du modèle de quadri-pavages triangulaire, et soit G un sous-graphe fini et simplement connexe du réseau triangulaire \mathbb{T} . La fonction de partition totale, notée $Z(\partial G, \nu)$, est la somme des poids des quadri-pavages dont le pavage sous-jacent est un pavage par losanges-60° de G .

Le résultat principal du chapitre 5 consiste en une formule explicite pour le taux de croissance de $Z(\partial G_n, \nu)$ lorsque $\{G_n\}$ est une exhaustion particulière du réseau \mathbb{T} , et ν est la fonction de poids critique.

Théorème 1 *Supposons que ν soit la fonction de poids critique sur les quadri-tuiles, alors*

$$\lim_{n \rightarrow \infty} \frac{1}{12n^2} \log Z(\partial G_n, \nu) = \frac{1}{12} \log 3 + \frac{1}{4} \log 2 + \frac{1}{2\pi} L\left(\frac{\pi}{6}\right) + \frac{5}{4\pi} L\left(\frac{\pi}{3}\right),$$

où $\{G_n\}$ est définie au paragraphe 5.1.2 ; et L est la fonction de Lobachevsky,

$$L(x) = - \int_0^x \log 2 \sin t \, dt.$$

La preuve du théorème 1 est la combinaison de trois propositions. Chacune fait l'objet d'un paragraphe (5.2, 5.3, 5.4 respectivement), et est plus forte que ce qui est nécessaire à la preuve. Nous les citons ci-dessous étant donné qu'elles possèdent un intérêt propre, en particulier la dernière qui décrit la combinatoire des modèles de dimères isoradiaux.

Le but du paragraphe 5.2 est de ramener le calcul de la fonction de partition totale au calcul de fonctions de partitions pour des graphes fixés. Avant d'énoncer le résultat, rappelons quelques notations. Soit G un sous-graphe fini et simplement connexe du réseau triangulaire \mathbb{T} , alors $Z(G^*, 1)$ est le nombre de pavages par losanges-60° de G . Les quadri-tuiles du modèle de quadri-pavages triangulaire sont classées en 4 catégories I, II, III, IV (cf. figure 4.3). Ainsi, lorsque nous parlons d'une fonction de poids ν sur les quadri-tuiles, nous voulons dire des poids $a, b, c \in \mathbb{R}^+$ associés aux quadri-tuiles de type I, II, III et IV respectivement. Soit L un pavage par losanges-60° de G , et L^* le pavage par losanges-avec-diagonales correspondant, alors $Z(L^*, \nu)$ est la somme des poids des 2-pavages de L , autrement dit c'est la somme des poids des quadri-pavages dont le pavage sous-jacent est L .

Proposition 1 *Supposons que les poids a, b, c satisfont la relation suivante :*

$$0 < a < c, \quad b = \sqrt{a \left(\frac{a^2 + c^2 - ac}{c - a} \right)}.$$

Alors, $Z(L^, \nu)$ est indépendante du pavage par losanges L du graphe G , et la fonction de partition totale vérifie*

$$Z(\partial G, \nu) = Z(L^*, \nu) Z(G^*, 1).$$

Idée de preuve:

- La deuxième partie de la proposition est une conséquence directe de la première.
- Il est possible de passer d'un pavage par losanges-60° de G à un autre par une suite d'opérations élémentaires (opération qui consiste à "rajouter" ou "enlever" un cube, cf. paragraphe 4.5). Ainsi, nous considérons deux pavages par losanges-60° L_1 et L_2 qui diffèrent par une seule opération élémentaire, et cherchons une condition sur les poids a, b, c pour que $Z(L_1^*, \nu) = Z(L_2^*, \nu)$. \square

Le paragraphe 5.3 concerne le calcul de la limite (1.1) pour une exhaustion $\{L_n\}$ constituée de pavages par losanges-60°-avec-diagonales finis et planaires, lorsqu'une fonction de poids ν est associée aux quadri-tuiles. On ne peut calculer cette limite directement car les matrices de Kasteleyn des graphes L_n^* ne possèdent pas assez de symétries. L'objet de la proposition 2 est d'exhiber une exhaustion $\{\bar{L}_n\}$, constituée de pavages par losanges-60°-avec-diagonales *toriques*, qui a la même limite (1.1) que $\{L_n\}$. Les symétries du tore permettront alors de calculer la limite explicitement (cf. paragraphe suivant). Nous nous référons au paragraphe 5.3 pour la définition précise des exhaustions $\{L_n\}$ et $\{\bar{L}_n\}$. La preuve de la proposition 2 utilise des techniques de style combinatoire, et un argument de sous-additivité. Il est important de noter que la limite (1.1) dans le cas d'exhaustions planaires et toriques ne coïncide pas en général.

Proposition 2 *Supposons que les poids a, b, c satisfont la condition $a^2 + b^2 = c^2$, alors*

$$\lim_{n \rightarrow \infty} \frac{1}{n^2} \log Z(L_n^*, \nu) = \lim_{n \rightarrow \infty} \frac{1}{n^2} \log Z(\bar{L}_n^*, \nu).$$

Le paragraphe 5.4 a pour sujet la limite (1.1) pour le modèle de dimères isoradial. Soit G un graphe isoradial infini, dont le dual G^* est biparti. Supposons que G est Λ -doublement périodique (pour un réseau bidimensionnel Λ), et supposons que la fonction de poids critique ν est associée aux arêtes de G^* . Une exhaustion naturelle de G par des graphes toriques est $\{\bar{G}_n\}$, où $\bar{G}_n = G/n\Lambda$. La proposition 3 donne une expression explicite pour la limite (1.1) de l'exhaustion $\{G_n\}$. Le résultat est surprenant par sa simplicité d'utilisation, en effet il ne dépend que de la géométrie locale du graphe G . Dans le cas d'un modèle de dimères général, cette limite est difficile à calculer explicitement et implique l'évaluation d'intégrales elliptiques. De plus, cette proposition répond à la question de [26] qui est d'interpréter, en terme de modèle de dimères, le "log normalisé du déterminant de l'opérateur de Dirac complexe K ".

Proposition 3

$$\lim_{n \rightarrow \infty} \frac{1}{|V(\bar{G}_n^*)|} \log Z(\bar{G}_n^*, \nu) = \frac{1}{|V(\bar{G}_1^*)|} \sum_{i=1}^m \left(\frac{\theta_i}{\pi} \log 2 \sin \theta_i + \frac{1}{\pi} L(\theta_i) \right). \quad (1.2)$$

où $\theta_1, \dots, \theta_m$ sont les angles des losanges associés aux arêtes e_1, \dots, e_m de \bar{G}_1^* (cf. paragraphe 5.4), et L est la fonction de Lobachevsky, $L(x) = -\int_0^x \log 2 \sin t \, dt$.

Idée de preuve:

Le terme de droite de l'équation (1.2) a été calculé par Kenyon [26]. La preuve consiste à passer par le modèle de dimères sur les graphes toriques \tilde{G}_n , et de montrer qu'à la limite, on obtient la même quantité. Certaines des étapes de la preuve sont proches de [26]. \square

Mesure de Gibbs explicite pour le modèle de dimères isoradial et le cas des quadri-pavages

La définition d'une mesure de Gibbs sur les configurations de dimères $\mathcal{M}(G^*)$ d'un graphe G^* infini est une extension naturelle de la définition d'une mesure de Boltzmann. Une telle mesure permet de connaître les statistiques locales du modèle, d'où l'importance d'obtenir une expression explicite. De plus, elle permet de calculer les corrélations asymptotiques, et ainsi de connaître la phase du modèle dans laquelle on se trouve.

Résultats existants

- Kenyon [21] : donne une formule explicite pour la mesure de Boltzmann pour un graphe G fini planaire (resp. torique), en fonction de la matrice (resp. des 4 matrices) de Kasteleyn et de son inverse.
- Kenyon, Okounkov, Sheffield [29] : donnent une formule explicite pour la famille à deux paramètres de mesure de Gibbs d'un modèle de dimères sur un graphe infini doublement périodique dont le dual est biparti, en fonction des matrices de Kasteleyn et de la limite de leurs inverses.

Résultats obtenus

Soit G un graphe doublement périodique dont le dual G^* est biparti. L'expression explicite pour la famille à deux paramètres de mesure de Gibbs, obtenue dans [29] utilise la limite des matrices de Kasteleyn inverses. Cette limite est en général difficile à calculer exactement. Le théorème 2 montre que lorsque G est isoradial, et que la fonction de poids critique est associée aux arêtes de G^* , on peut remplacer la limite des matrices de Kasteleyn inverses par l'inverse de l'opérateur de Dirac complexe K^{-1} . Ceci répond à une conjecture de [26]. Rappelons que $K^{-1}(b, w)$ ne dépend que d'un chemin de w à b . Utilisant cette propriété de localité, le théorème 2 donne aussi une expression explicite pour une mesure de Gibbs sur des graphes qui ne sont pas forcément périodiques - les pavages par losanges-avec-diagonales. Nous pensons que ce théorème peut se généraliser à tous les graphes isoradiaux non périodiques avec fonction de poids critique.

Théorème 2 *Soit G un graphe isoradial infini dont le dual G^* est biparti. Supposons que la fonction de poids critique ν est associée aux arêtes de G^* , et soit K l'opérateur de Dirac complexe indicé par les sommets de G^* . Supposons que*

1. G est périodique,
 2. G est un pavage par losanges-avec-diagonales (qui n'est pas forcément périodique)
- alors, il existe une unique mesure de probabilité μ sur $(\mathcal{M}(G^*), \sigma(\mathcal{A}))$ qui vérifie,

$$\mu(e_1, \dots, e_k) = \left(\prod_{i=1}^k K(w_i, b_i) \right) \det_{1 \leq i, j \leq k} (K^{-1}(b_i, w_j)). \quad (1.3)$$

De plus, μ est une mesure de Gibbs.

Idée de preuve:

Cas périodique

- On part de l'expression explicite pour la mesure de Boltzmann du modèle de dimères sur les graphes toriques $\tilde{G}_n = G/n\Lambda$ [21], cette expression utilise les matrices de Kasteleyn toriques et leurs inverses.

- La proposition 3.11 donne la convergence sur une sous-suite de n des matrices de Kasteleyn toriques des graphes \tilde{G}_n^* , vers l'inverse de l'opérateur de Dirac réel (introduit au paragraphe 3.3). Combiné avec l'unicité de la limite donnée par le théorème de Sheffield [41], ceci implique la convergence des mesures de Boltzmann vers (1.3) où l'opérateur de Dirac complexe est remplacé par l'opérateur de Dirac réel.

- Nous montrons que l'expression (1.3) est la même si on considère l'opérateur de Dirac réel ou complexe, et concluons en appliquant le théorème d'extension de Kolmogorov. La propriété de Gibbs découle directement du fait que ce soit une extension de mesures de Boltzmann.

Cas non périodique

L'aspect probabiliste est essentiellement le même une fois que l'on démontre en plus le fait géométrique suivant :

Proposition 4 *Tout sous-graphe P fini et simplement connexe d'un pavage par losange du plan peut être plongé dans un pavage par losanges du plan périodique.*

Une première étape consiste à montrer que l'on peut compléter P par un nombre fini de losanges, de sorte à obtenir un polygone convexe Q dont les côtés opposés sont parallèles. On montre ensuite qu'en rajoutant un nombre fini de losanges à Q , on obtient un hexagone "déformé" qui pave le plan périodiquement (cf. figure 6.3). \square

Le paragraphe 6.2 se concentre sur les quadri-pavages. On considère d'abord le modèle de quadri-pavages triangulaire. En utilisant le théorème 2, nous donnons une expression explicite pour une mesure totale sur l'ensemble des quadri-pavages du plan. Nous nous référons au paragraphe 6.2.1 pour la définition exacte des termes de la proposition suivante.

Proposition 5 *Il existe une unique mesure de probabilité μ sur $(\mathcal{M}, \sigma(\mathcal{B}))$ qui vérifie :*

$$\mu(e_1, \dots, e_m) = \mu_L(e_1, \dots, e_m) \nu(\mathbf{k}_{e_1}, \dots, \mathbf{k}_{e_m}),$$

où L est le pavage par losanges-avec-diagonales correspondant à un pavage par losange \mathcal{L} qui contient les losanges l_{e_1}, \dots, l_{e_m} .

Ensuite nous considérons un pavage par losanges-avec-diagonales R , et nous notons K_R l'opérateur de Dirac indicé par les sommets de R^* . Nous montrons une propriété étonnante de l'asymptotique de l'inverse K_R^{-1} . Lorsque $|b - w| \rightarrow \infty$, $K_R^{-1}(b, w)$ ne dépend que des deux losanges auxquels appartiennent les sommets b et w . C'est à dire que $K_R^{-1}(b, w)$ ne dépend plus des angles le long d'un chemin de w à b . L'énoncé exact est le suivant,

Théorème 3 $K_R^{-1}(b, w)$ est donné par,

$$\frac{1}{2\pi} \left(\frac{1}{b-w} + \frac{e^{-i(\theta_1+\theta_2)}}{\bar{b}-\bar{w}} \right) + \frac{1}{2\pi} \left(\frac{e^{2i\theta_1} + e^{2i\theta_2}}{(b-w)^3} + \frac{e^{-i(3\theta_1+\theta_2)} + e^{-i(\theta_1+3\theta_2)}}{(\bar{b}-\bar{w})^3} \right) + O\left(\frac{1}{|b-w|^3}\right),$$

où θ_1 et θ_2 sont définis au paragraphe 6.2.2.

Nous déduisons des propriétés asymptotiques pour la mesure de Gibbs μ_R donnée par le théorème 2, et pour la mesure totale μ .

Fluctuations de la hauteur du modèle de dimères isoradial

Rappelons que, grâce à la fonction de hauteur, les 2-pavages d'un graphe G peuvent être interprétés comme des surfaces discrètes projetées sur le plan. Une question intéressante est d'étudier les fluctuations de la surface autour de sa moyenne.

Résultats existants

- Kenyon [24, 25] : démontre que les fluctuations de la fonction de hauteur des pavages par dominos de régions simplement connexes convergent vers un champ libre Gaussien (lorsque la maille du réseau tend vers 0).
- Kenyon [27] : étudie les fluctuations de la hauteur pour le modèle de dimères sur le réseau hexagonal.

Résultats obtenus

Soit G un graphe isoradial infini dont le dual est G^* est biparti, avec la fonction de poids critique sur les arêtes de G^* . Considérons la fonction de hauteur h sur les 2-pavages de G (définie au paragraphe 3.5). Soit G^ε le graphe G où la longueur des arêtes est multipliée par un facteur ε . Soit h la fonction de hauteur sur les 2-pavages de G^ε (notons que h n'est pas normalisée). Définissons,

$$\begin{aligned} H^\varepsilon : C_{c,0}^\infty(\mathbb{R}^2) &\rightarrow \mathbb{R} \\ \varphi &\mapsto H^\varepsilon \varphi = \varepsilon^2 \sum_{v \in V(G^\varepsilon)} \varphi(v) h(v), \end{aligned}$$

Supposons que G est soit périodique, soit un pavage par losanges-avec-diagonales. Notons μ la mesure de Gibbs donnée par le théorème 2. Le théorème 4 décrit les fluctuations de H^ε lorsque $\varepsilon \rightarrow \infty$. L'objet limite est un champ libre Gaussien, défini au paragraphe 7.1 : il s'agit d'une distribution aléatoire Gaussienne dont la fonction de covariance est donnée par l'énergie de Dirichlet.

Comme application directe du théorème 4, nous obtenons la convergence de la fonction de hauteur des pavages du plan par dominos, losanges, et quadri-tuiles vers un champ libre Gaussien.

Utilisant la formule asymptotique pour l'opérateur de Dirac inverse [26], et la caractérisation des phases d'un modèle de dimères de [29], nous déduisons que le modèle de dimères isoradial est toujours dans la phase liquide. Nous pensons que le théorème 4 reste vrai pour tous les modèles de dimères dans la phase liquide.

Théorème 4 H^ε converge faiblement en distribution vers $\frac{1}{\sqrt{\pi}}$ fois un champ libre Gaussien. C'est à dire, pour tout $\varphi_1, \dots, \varphi_k \in C_{c,0}^\infty(\mathbb{R}^2)$, $(H^\varepsilon \varphi_1, \dots, H^\varepsilon \varphi_k)$ converge en loi (quand $\varepsilon \rightarrow 0$) vers $\frac{1}{\sqrt{\pi}}(F\varphi_1, \dots, F\varphi_k)$, où F est un champ libre Gaussien.

Idée de preuve:

Les étapes de la preuve sont essentiellement celles de [24], sauf le lemme 7.14 qui est nouveau. Cependant, étant donné que nous travaillons avec un graphe isoradial général, et non pas avec le réseau \mathbb{Z}^2 , chacune des étapes a dû être adaptée de manière non triviale. □

Chapter 2

The dimer model

The *dimer model* belongs to the field of statistical mechanics (as do the *Ising model* and the *percolation model*). It has been introduced by statistical physicists in order to model diatomic molecules adsorbed on the surface of a crystal [20]. This model is in bijection with the *2-tiling model*, which is a random interface model. Both approaches are used throughout this thesis. To simplify terminology, when we speak of the dimer model, we also refer to the corresponding 2-tiling model. The aim of the first chapter is to define the dimer model, and some of its features in a quite general setting. We also try to give a little insight into three papers which, in our opinion, form the groundwork of this theory. In chronological order, they are Kasteleyn [20], Thurston [44], Kenyon [21]. Kasteleyn solves some fundamental combinatorial questions; Thurston gives an essential geometric interpretation; Kenyon works out a simple expression for a measure on the model, and so opens the path for probabilistic studies of the model.

Section 2.1 consists in the description of the dimer model using the terminology of *statistical mechanics*. The *system* considered is a graph G satisfying condition (*) below:

- (*) $\left\{ \begin{array}{l} \text{The graph } G \text{ is finite or infinite, planar, and simple (} G \text{ has no loops and} \\ \text{no multiple edges); its vertices are of degree } \geq 3. G \text{ is } \textit{simply connected}, \\ \text{i.e. it is the one-skeleton of a simply connected union of faces. When} \\ G \text{ is infinite, it is made of finitely many different faces, up to isometry.} \end{array} \right.$

Configurations of the system are 2-tilings of the graph G , or equivalently *perfect matchings* - also called *dimer configurations* - of the dual graph G^* of G . Assume that the graph G is finite. Each configuration has an *energy* determined by a weight function on the edges of G^* . The *partition function* counts the weighted sum of dimer configurations of the graph G^* . The probability of a dimer configuration occurring when chosen with respect to the *Boltzmann measure*, is given by the exponential of minus its energy, normalized by the partition function. A *Gibbs measure* is defined to be a natural extension of the Boltzmann measure to infinite graphs. After having defined the above terms in more details, we state Kasteleyn result for the partition function [20], and Kenyon's result for the Boltzmann measure [21].

Section 2.2 is about Thurston's discrete surface interpretation of 2-tilings via height functions: in [44] he describes lozenge tilings as surfaces in \mathbb{Z}^3 projected to the plane. Following [29], we use flows to generalize Thurston's notion of height function to 2-tilings of quite general graphs. This allows us to extend Thurston's criteria for the existence of a lozenge tiling of a simply connected subgraph of the triangular lattice, to graphs which have a height function. We finish by giving Propp's theorem [39], which states that the space of 2-tilings of a finite simply connected graph, has a structure of distributive lattice.

2.1 The dimer model

The *dimer model* represents diatomic molecules adsorbed on the surface of a crystal (see [20] for references). The most favorable points for the adsorption of atoms on such a surface form a two-dimensional lattice, in which a dimer, if it is of the right size, can occupy two neighboring sites. In subsection 2.1.1, we define the equivalent *2-tiling model*, and the bijection to the dimer model. In subsection 2.1.2, we introduce the *energy of configurations* and the *partition function*, and give some insight into Kasteleyn's result [20]. In subsection 2.1.3, we define the *Boltzmann* and *Gibbs* measures, and state Kenyon's explicit expression for the Boltzmann measure [21].

2.1.1 2-tilings/dimer configurations

The *system* we consider is a graph G satisfying condition (*). *Configurations* of the system are 2-tilings of the graph G , and are defined as follows. A **2-tile** of G is a polygon consisting of two adjacent inner faces of G , glued together. A **2-tiling** of G is a covering of G with 2-tiles, such that there are no holes and no overlapping.

There is an alternative and equivalent way of defining the system and its configurations. In this view, let us recall two definitions from graph theory. The **dual graph** of G , denoted by G^* , is the graph whose vertices correspond to the inner faces of G (that is, there is no vertex of G^* corresponding to the outer face of G), two vertices of G^* being joined by an edge if the corresponding faces of G are adjacent. A **perfect matching** of G^* is a subset of edges of G^* which covers each vertex exactly once. In the physics literature, perfect matchings are referred to as **dimer configurations**. A **dimer** is a di-atomic molecule represented by an edge of the perfect matching [20].

2-tilings of the graph G are in bijection with dimer configurations of the dual graph G^* , as explained by the following correspondence. Denote by F^* the dual vertex of a face F of G , and consider an edge $F_1^*F_2^*$ of G^* . We say that the 2-tile of G made of the adjacent faces F_1, F_2 is the **2-tile corresponding to the edge $F_1^*F_2^*$** . Then, 2-tiles corresponding to edges of a dimer configuration of G^* form a 2-tiling of G . Let us denote by $\mathcal{M}(G^*)$ the set of perfect matchings of the graph G^* .

Here is a classical example, see figure 2.1: take G to be the equilateral triangular lattice

\mathbb{T} . 2-tiles of \mathbb{T} consist of 60° -rhombi, called **lozenges** (sometimes also **calissons**), and 2-tilings of \mathbb{T} are referred to as **lozenge tilings**. By the above bijection, 2-tilings of \mathbb{T} correspond to perfect matchings of the dual graph \mathbb{T}^* , also known as the honeycomb lattice. Another classical example is given by the square lattice \mathbb{Z}^2 . 2-tiles of \mathbb{Z}^2 are rectangles, also called **dominos**, and 2-tilings of \mathbb{Z}^2 are referred to as **domino tilings**. They are in bijection with perfect matchings of the dual graph \mathbb{Z}^{2*} (which is isomorphic to \mathbb{Z}^2).

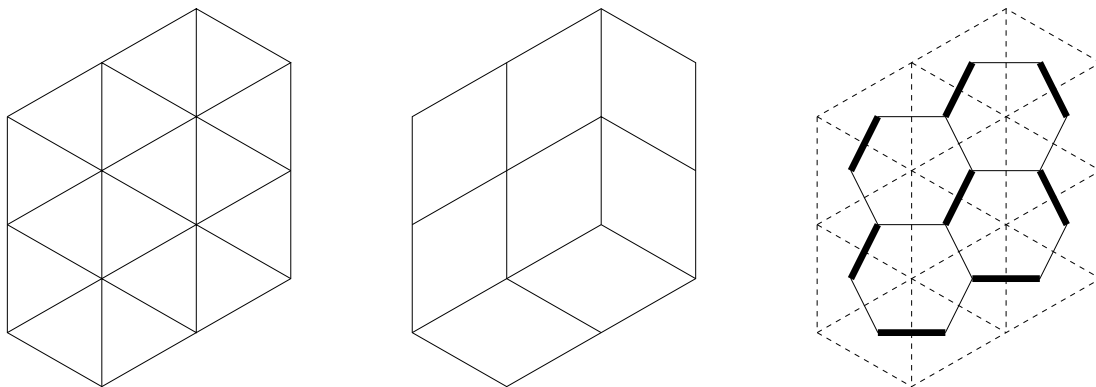


Figure 2.1: The equilateral triangular lattice \mathbb{T} , a 2-tiling of \mathbb{T} , and the corresponding perfect matching of the honeycomb lattice.

2.1.2 Energy of configurations, and partition function

Let G be a graph satisfying (*). Consider a positive **weight function** ν on the edges of the dual graph G^* , that is an edge e of G^* has weight $\nu(e)$. Assume that G^* is finite and simply connected. The **energy** of a dimer configuration M of G^* , is $\mathcal{E}(M) = -\sum_{e \in M} \log \nu(e)$. The **weight** of a dimer configuration M of G^* , denoted by $\nu(M)$, is given by the exponential of minus its energy:

$$\nu(M) = e^{-\mathcal{E}(M)} = \prod_{e \in M} \nu(e).$$

Note that by the correspondence between dimer configurations and 2-tilings, the function ν can be seen as weighting 2-tiles of G , $\nu(M)$ is then the weight of the 2-tiling corresponding to M .

The **partition function**, denoted by $Z(G^*, \nu)$, is defined to be the weighted sum of dimer configurations of G^* , weighted as above, that is

$$Z(G^*, \nu) = \sum_{M \in \mathcal{M}(G^*)} \nu(M).$$

For example, when $\nu \equiv 1$, $Z(G^*, 1)$ counts the number of dimer configurations of the graph G^* , or equivalently the number of 2-tilings of the graph G .

Kasteleyn gives an explicit formula for the partition function [20]. Here is a brief outline of his methods and results. Suppose that the edges of the graph G^* are oriented, and that G^* has n vertices u_1, \dots, u_n . The **weighted adjacency matrix** associated to G^* and ν , is the matrix A whose entry $A(u_i, u_j) = \pm\nu(u_i u_j)$, if the vertices u_i and u_j are adjacent, the sign being determined by the orientation of the edge $u_i u_j$; and 0 if the vertices u_i and u_j are not adjacent. The matrix A is skew-symmetric. The **Pfaffian** of a skew-symmetric matrix is defined by

$$\text{Pf } A = \sum_{\pi} \text{sgn } \sigma(\pi) A(u_{\pi(1)}, u_{\pi(2)}) \cdots A(u_{\pi(n-1)}, u_{\pi(n)}),$$

where the sum is over all partitions π of the numbers $1, \dots, n$ into $n/2$ unordered pairs, and $\sigma(\pi)$ is a permutation such that $|u_{\sigma(\pi)(1)} u_{\sigma(\pi)(2)}| \cdots |u_{\sigma(\pi)(n-1)} u_{\sigma(\pi)(n)}|$ is a description of the partition π . Because of skew-symmetry, the definition is independent of the choice of permutation $\sigma(\pi)$.

Note that each non zero term in the expansion of $\text{Pf } A$ corresponds to the weight of a dimer configuration, but not all terms are counted with the same sign. Kasteleyn introduces the following definition: an orientation of the edges of the graph G^* is said to be **admissible** if all terms in the expansion of $\text{Pf } A$ have the same sign. He then proves

Lemma 2.1 [20] *Every finite, simply connected, planar, simple graph has an admissible orientation of its edges.*

A **Kasteleyn matrix** \tilde{K} associated to a graph G^* is the weighted adjacency matrix corresponding to an admissible orientation of the graph G^* . Using the fact that, if A is a skew-symmetric matrix, then $\det A = (\text{Pf } A)^2$, Kasteleyn deduces the following,

Theorem 2.2 [20] *The partition function of the graph G^* is given by*

$$Z(G^*, \nu) = \sqrt{\det \tilde{K}} = |\text{Pf } \tilde{K}|.$$

When the graph G^* is bipartite, one simplifies the expression for $Z(G^*, \nu)$ in the following way. Vertices of G^* can be divided into two subsets $B \cup W$, where B denotes the black vertices, W the white ones, and vertices in B are only adjacent to vertices in W . We suppose that $|B| = |W|$, for otherwise there is no perfect matching on the graph G^* . Let K be the sub-matrix of \tilde{K} whose line correspond to the white vertices, and columns to the black ones. Then, \tilde{K} can be written as

$$\tilde{K} = \begin{pmatrix} 0 & K \\ -K^t & 0 \end{pmatrix}.$$

We deduce,

Theorem 2.3 [20] *Suppose that the dual graph G^* of the graph G is bipartite, then the partition function of the graph G^* is given by*

$$Z(G^*, \nu) = |\det K|.$$

An expression using a sum of four determinants can be obtained for the partition function of toroidal graphs [20, 43]. More generally, the partition function of graphs embedded on surfaces of genus g can be obtained using the sum of 2^g determinants. In order to avoid repetition, and since our interest focuses more on isoradial graphs [26] (see chapter 3), we postpone giving the formula for the toroidal partition function until subsection 3.4.1. Although isoradial graphs are specific graphs, the expression for the partition function is similar to that of the general case.

2.1.3 Boltzmann and Gibbs measures

Let G be a finite graph satisfying (*). Suppose that a weight function ν is assigned to the edges of G^* . The **Boltzmann measure** μ^1 is a probability measure on the set of dimer configurations $\mathcal{M}(G^*)$, defined by

$$\mu^1(M) = \frac{e^{-\mathcal{E}(M)}}{Z(G^*, \nu)} = \frac{\prod_{e \in M} \nu(e)}{Z(G^*, \nu)},$$

for every perfect matching $M \in \mathcal{M}(G^*)$.

Assume that the dual graph G^* is bipartite. Let K be a Kasteleyn matrix associated to G^* , and let $e_1 = w_1 b_1, \dots, e_k = w_k b_k$ be a subset of edges of G^* . Kenyon [21] derives an explicit expression for the probability $\mu^1(e_1, \dots, e_k)$ of these edges occurring in a dimer configuration of G^* chosen with respect to the Boltzmann measure.

Theorem 2.4 [21]

$$\mu^1(e_1, \dots, e_k) = \left| \left(\prod_{i=1}^k K(w_i, b_i) \right) \det_{1 \leq i, j \leq k} K^{-1}(b_i, w_j) \right|.$$

An expression for the Boltzmann measure on the set of dimer configurations of toroidal graphs is given in [21]. We state it in subsection 3.4.2 in the case of isoradial graphs. The expression is similar to that of the general case.

Let G be an infinite graph satisfying (*). Assume that a weight function ν is assigned to the edges of G^* . A **Gibbs measure** is a probability measure on $\mathcal{M}(G^*)$ defined as follows. If the perfect matching in an annular region of G^* is fixed, the matchings inside and outside of the annulus are independent, and the probability of any interior matching M is proportional to $\prod_{e \in M} \nu(e)$.

2.2 Geometric features of the dimer model

By means of the *height function*, Thurston interprets lozenge tilings as discrete surfaces in \mathbb{Z}^3 projected to the plane; he gives a similar interpretation of domino tilings [44]. In subsection 2.2.1, following [29], we use flows to define height functions on 2-tilings of quite general graphs, see also [5] for a similar approach. This leads to the surface interpretation of 2-tilings, whereby each 2-tiling is the projection to the plane of a discrete surface, whose “height” is given by the height function. In subsection 2.2.2, we generalize Thurston’s necessary and sufficient condition for the existence of a 2-tiling of a simply connected subgraph of \mathbb{T} , to graphs which have a height function. Under some regularity assumption, Propp shows that the set of 2-tilings of a finite simply connected graph G has a structure of distributive lattice [39]. His theorem is stated in subsection 2.2.3.

Let G be a graph. In the whole of this section, we make the following assumptions and use the following notations. Suppose that the dual graph G^* of G is bipartite, B denotes the set of black vertices, and W the set of white ones. Orient the edges of G^* from the white vertices to the black vertices. The bipartite coloring of the vertices of G^* induces an orientation of the edges of G : color the dual faces of the black (resp. white) vertices of G^* black (resp. white); orient the boundary edges of the black faces of G cclw (counterclockwise), the boundary edges of the white faces of G are then oriented cw (clockwise).

2.2.1 Height functions

Assume that the graph G satisfies condition (*). We define a set of reference flows $\Omega(G^*)$ on the edges of G^* . Supposing that $\Omega(G^*) \neq \emptyset$, and fixing a flow $\omega_0 \in \Omega(G^*)$, we define a height function h on the vertices of every 2-tiling T of G . By means of this height function, T can be interpreted as the projection to the plane of a discrete surface.

Let us first introduce some notations. Consider a flow ω on the edges of G^* , and let e be an oriented edge of G^* , denote by $\omega(e)$ the amount of flow ω which flows from the white vertex of e to the black vertex of e (note that $\omega(e)$ may be positive or negative). Suppose that the graph G is infinite. Define $\Omega(G^*)$ to be the set of white-to-black flows on the edges of G^* , which have divergence 1 at every white vertex of G^* , and -1 at every black vertex of G^* . That is, a flow ω_0 belongs to $\Omega(G^*)$, if

$$\forall e \in G^*, \omega_0(e) \geq 0; \forall w \in W, \sum_{b: b \sim w} \omega_0(wb) = 1; \forall b \in B, \sum_{w: w \sim b} \omega_0(wb) = 1.$$

Suppose that the graph G is finite, and denote by G^* the dual graph G^* which contains the dual edges of the boundary edges of G . Then we define $\Omega(G^*)$ to be the set of white-to-black flows on the edges of G^* , which have divergence 1 at every white vertex of G^* , and -1 at every black vertex of G^* .

$\Omega(G^*)$ is called the set of **reference flows** of the graph G^* . Here are some examples of graphs G^* whose set $\Omega(G^*) \neq \emptyset$.

Examples

1. G^* has a perfect matching M : define ω_0 to be a white-to-black flow, which flows by 1 along every edge of M .
2. G^* is infinite and has vertices of degree n : define ω_0 to be a white-to-black flow, which flows by $1/n$ along every edge of G^* .
3. G^* is infinite and isoradial: refer to section 3.5 for the definition of a flow $\omega_0 \in \Omega(G^*)$.

Consider a graph G (finite or infinite) such that $\Omega(G^*) \neq \emptyset$, and let $\omega_0 \in \Omega(G^*)$. Consider a 2-tiling T of G . Let us define an \mathbb{R} -valued function h on the vertices of T , called the **height function**, which depends on the reference flow ω_0 , and on the choice of a vertex v_0 of G^* . Denote by M the perfect matching of G^* corresponding to T , then M defines a white-to-black unit flow ω on the edges of G^* : flow by 1 along every edge of M . The difference $\omega_0 - \omega$ is a divergence free flow, which means that the quantity of flow which enters any vertex of G^* equals the quantity of flow which exits that same vertex. Choose a vertex v_0 of G , and fix $h(v_0) = 0$. For every other vertex v of T , take an edge-path γ of G from v_0 to v . If an edge uv of γ is oriented in the direction of the path, and if we denote by e its dual edge, then h increases by $\omega_0(e) - \omega(e)$ along uv ; if an edge uv of γ is oriented in the opposite direction, then h decreases by the same quantity along uv . As a consequence of the fact that $\omega_0 - \omega$ is a divergence free flow, the height function h is well defined.

The following lemma gives a correspondence between height functions defined on the vertices of an infinite graph G , and 2-tilings of G . A similar result holds when the graph G is finite.

Lemma 2.5 *Consider an infinite graph G such that $\Omega(G^*) \neq \emptyset$, and let $\omega_0 \in \Omega(G^*)$. Let \tilde{h} be an \mathbb{R} -valued function on the vertices of G satisfying*

- $\tilde{h}(v_0) = 0$,
- $\tilde{h}(v) - \tilde{h}(u) = \omega_0(e)$ or $\omega_0(e) - 1$ for any edge uv oriented from u to v , where e denotes the dual edge of uv .

Then, there is a bijection between functions \tilde{h} satisfying these two conditions, and 2-tilings of G .

Proof:

Let T be a 2-tiling of G , M be the corresponding matching, and ω be the unit white-to-black flow defined by M . Then, the height function h satisfies the conditions of the lemma: consider an edge uv of G oriented from u to v and denote by e its dual edge,

then $h(v) - h(u) = \omega_0(e) - \omega(e)$, and by definition $\omega(e) = 0$ or 1 .

Conversely, consider an \mathbb{R} -valued function \tilde{h} as in the lemma. Let us construct a 2-tiling T whose height function is \tilde{h} . Consider a black face F of G , and let e_1, \dots, e_m be the dual edges of its boundary edges. Then $\sum_{i=1}^m \omega_0(e_i) = 1$, so that there is exactly one boundary edge uv along which $\tilde{h}(v) - \tilde{h}(u)$ is $\omega_0(e_i) - 1$ (where e_i is the dual edge of uv). To the face F , we associate the 2-tile of G which is crossed by the edge uv . Repeating this procedure for all black faces of G , we obtain T . \square

Let us return to the classical examples of lozenge tilings of \mathbb{T} , and domino tilings of \mathbb{Z}^2 . The honeycomb lattice \mathbb{T}^* is bipartite and has vertices of degree 3, so that we define the reference flow ω_0 to be a white-to-black flow, which flows by $1/3$ along every edge of G^* . The height function of a lozenge tiling of G corresponding to the flow ω_0 , changes by $1/3$ or $-2/3$ along every positively oriented edge; it is $1/3$ of Thurston's height function on lozenge tilings [44]. The square lattice \mathbb{Z}^{2*} is bipartite and has vertices of degree 4, so that we define the reference flow ω_0 to be a white-to-black flow, which flows by $1/4$ along every edge of G^* . The height function of a domino tiling of G corresponding to the flow ω_0 , changes by $1/4$ or $-3/4$ along every positively oriented edge. It is $1/4$ of Thurston's height function on domino tilings [44].

2.2.2 2-tilability

We extend Thurston's lozenge tilability condition, to graphs G that satisfy condition (*), and whose set of flows $\Omega(G^*) \neq \emptyset$.

Suppose that the graph G is infinite, and consider a reference flow $\omega_0 \in \Omega(G^*)$. Let G_1 be a finite simply connected subgraph of G , and denote by ∂G_1 the cycle of G_1 consisting of its boundary edges. Consider the flow ω_0 restricted to the edges of G_1^* (recall that G_1^* is the dual graph G_1^* which contains the dual edges of the edges of ∂G_1), then $\omega_0 \in \Omega(G_1^*)$. If the region G_1 is 2-tilable, then edges of ∂G_1 bound 2-tiles of G_1 . This allows us to compute the height function h along ∂G_1 : fix a vertex v_0 of ∂G_1 , and set $h(v_0) = 0$. Travel around ∂G_1 cclw, if an edge uv is oriented in the direction of the path, h increases by $\omega_0(e)$ along uv (where e is the dual edge of uv); else if it is oriented in the opposite direction, it decreases by $\omega_0(e)$. Denote by $h(v_0)'$ the value of the height function at v_0 obtained after one cclw loop around ∂G_1 .

Lemma 2.6

$$h(v_0)' - h(v_0) = |B(G_1)| - |W(G_1)|,$$

where $B(G_1)$ and $W(G_1)$ denote the set of black and white faces of G_1 respectively.

Proof:

Suppose that G_1 consists of a single white face. Denote by e_1, \dots, e_m the dual edges of the edges of ∂G_1 . Then, $h(v_0)' - h(v_0) = -\sum_{i=1}^m \omega_0(e_i)$. By definition of the flow ω_0 , this quantity is equal to -1 . Similarly, if G_1 consists of a single black face, $h(v_0)' - h(v_0) = 1$. The proof is completed by induction on the number of faces included

in G_1 , and by linearity of the height function. \square

As a consequence of this lemma, we obtain a necessary condition for the region G_1 to be 2-tilable.

Corollary 2.7 *If G_1 is 2-tilable, then h is well defined on ∂G_1 , that is $h(v_0)' = h(v_0)$.*

Proof:

Since each 2-tile of a 2-tiling of G_1 consists of a black and of a white face, we have $|B(G_1)| = |W(G_1)|$. \square

In order to state the extension of Thurston's condition, let us introduce the notion of weighted distance between vertices of G_1 (it is a generalization of the notion of distance of [44]). Consider two vertices u, v of G_1 , and let Γ be the set of positively oriented paths of G_1 from u to v , which have no loops. Let $\gamma \in \Gamma$, then γ can be written as $\gamma = \{u = u_0, u_1, \dots, u_m = v\}$; denote by e_i the dual edge of the edge $u_{i-1}u_i$. The **weighted distance** from u to v , denoted by $d(u, v)$, is defined by

$$d(u, v) = \min_{\gamma \in \Gamma} \sum_{i=1}^m \omega_0(e_i). \quad (2.1)$$

Assume that the graph G_1 satisfies $|B(G_1)| = |W(G_1)|$, and consider the height function h on ∂G_1 . The following proposition extends Thurston's condition.

Proposition 2.8 *The graph G_1 is 2-tilable if and only if,*

$$\forall u, v \in \partial G_1, \quad h(v) - h(u) \leq d(u, v).$$

Proof:

We use the following necessary and sufficient condition of Hall [34]: there exists a perfect matching of the bipartite graph G_1^* if and only if, for every subset S of black vertices of G_1^* , $|N(S)| \geq |S|$, where $N(S)$ denotes the set of neighbors of vertices in S , ($N(S)$ consists of white vertices).

Assume there are vertices $u, v \in \partial G_1$, such that $h(v) - h(u) > d(u, v)$. Consider the path $\gamma \in \Gamma$ from u to v , for which the minimum (2.1) is attained. Without loss of generality, we can suppose that the path γ consists of edges of $G_1 \setminus \partial G_1$ exclusively. Indeed, if the path γ uses edges of ∂G_1 , say between vertices u' and v' , then $h(v') - h(u') = d(u', v')$, hence there exists a sub-path of γ using edges of $G_1 \setminus \partial G_1$ exclusively, which satisfies the above. Consider the cycle ∂G_2 of G_1 which consists of the path γ , and the part of ∂G_1 which is on the right of γ . Let G_2 be the subgraph of G_1 whose boundary is ∂G_2 . Let $h(u)' - h(u)$ be the height change around ∂G_2 , starting from u going cclw. Then,

$$h(u)' - h(u) = h(v) - h(u) - d(u, v).$$

Using our assumption, we obtain $h(u)' - h(u) > 0$. By lemma 2.6, this implies that $|W(G_2)| < |B(G_2)|$. Moreover, the graph G_2 is simply connected, because the path γ has no loop, and contains no edges of ∂G_1 ; the faces of G_2 adjacent to γ are white because the path γ is positively oriented. Hence, white faces of G_1 that are adjacent to black faces of G_2 are exactly the white faces of G_2 . Denote by S the dual vertices of the black faces of G_2 , then $N(S)$ consists of the dual vertices of the white faces of G_2 . We deduce that S is a subset of black vertices of G_1^* , which satisfies $|N(S)| < |S|$. By Hall's condition, this implies that there is no perfect matching on G_1^* .

Conversely, let us assume that the graph G_1^* has no perfect matching, then by Hall's condition there exists a subset of black vertices of G_1^* such that $|N(S)| < |S|$. Consider the subgraph G_2 of G_1 consisting of the dual faces of the black vertices of S , and of dual faces of the white vertices of $N(S)$. G_2 can be written as the disjoint union of its simply connected components C_1, \dots, C_n . Suppose there is a simply connected component C_j which is strictly included in G_1 , that is $\partial C_j \cap \partial G_1 = \emptyset$. Then all faces of C_j adjacent to ∂C_j are white faces. Let us compute the height change along ∂C_j starting from a vertex v_0 , and going cclw. Recall that white faces of G_1 are oriented cw, so that using the definition of the height function, we obtain $h(v_0)' - h(v_0) = -\sum_{i=1}^m \omega_0(e_i)$, where e_1, \dots, e_m denote the dual edges of the edges of ∂C_j . Using the definition of the reference flow ω_0 , we deduce that $h(v_0)' - h(v_0) \leq 0$; by lemma 2.6 this implies $|W(C_j)| \geq |B(C_j)|$. By assumption $|N(S)| < |S|$, so that there exists a connected component of G_2 , say C_1 which is adjacent to ∂G_1 , and which satisfies $|W(C_1)| < |B(C_1)|$. C_1 cannot be the whole of G_1 , because $|W(G_1)| = |B(G_1)|$. If C_1 is an annulus, an argument similar to the one above shows $|W(C_1)| \geq |B(C_1)|$. Hence C_1 is bounded by a positively oriented path γ which runs from a vertex u to a vertex v of ∂G_1 , and by the part of ∂G_1 which is on the right of γ . Let us compute the height change along ∂C_1 , starting from u , and going cclw. By lemma 2.6, we have $h(u)' - h(u) = |B(C_1)| - |W(C_1)| > 0$. If f_1, \dots, f_n denote the dual edges of the edges of γ , the definition of the height function yields $h(u)' - h(u) = h(v) - h(u) - \sum_{i=1}^n \omega_0(f_i)$. Moreover, $d(u, v) \leq \sum_{i=1}^n \omega_0(f_i)$, so $0 < h(u)' - h(u) = h(v) - h(u) - \sum_{i=1}^n \omega_0(f_i) \leq h(v) - h(u) - d(u, v)$. Hence, we have found vertices u, v of ∂G_1 that satisfy $h(v) - h(u) > d(u, v)$. \square

2.2.3 The space of 2-tilings

Consider a graph G whose dual graph G^* has the following properties (apart from being bipartite): G^* is finite and simply connected, and it has no loops (multiple edges are allowed), moreover every edge of G^* belongs to at least one perfect matching of the graph G^* . Under these assumptions, Propp proves that the set of perfect matchings of G^* has a structure of distributive lattice [39]. His theorem is in fact true in more generality (for the set of d -factors), but we restrict the statement to the topic of this chapter.

Before stating Propp's theorem, let us give the following definitions of [39]. An **elementary cycle** of G^* is a simple cycle that encircles a single face. An **alternating cycle** of G^* relative to a perfect matching M of G^* is an elementary cycle of G^* in which the edges alternately belong to M and M^C . Call the cycle **positive** if the edges in the cycle and M , when directed from black vertices to white vertices, circle the face in cclw direction, and **negative** if they circle in the cw direction. A **face twist** is the operation of removing from a perfect matching some edges that form an alternating cycle, and inserting the complementary edges. More specifically, **twisting down** is the operation that converts a positive alternating cycle into a negative alternating cycle around the same face, and **twisting up** is the reverse operation. Note that twisting converts a perfect matching into another perfect matching.

A partially ordered set (L, \leq) is a **lattice** if for all elements x and y of L , the set $\{x, y\}$ has both a least upper bound (join), and a greatest lower bound (meet). The join and the meet are denoted by $x \vee y$ and $x \wedge y$ respectively. A lattice is **distributive** if for all $x, y, z \in L$, $x \vee (y \wedge z) = (x \vee y) \wedge (x \vee z)$ and $x \wedge (y \vee z) = (x \wedge y) \vee (x \wedge z)$.

Theorem 2.9 [39] *Let $\mathcal{M}(G^*)$ be the (non empty) set of perfect matchings of the graph G^* . If we say that a perfect matching M covers a perfect matching N exactly, when N is obtained from M by twisting down at a face other than the outer face, then the covering relation makes $\mathcal{M}(G^*)$ into a distributive lattice.*

The proof uses the notion of height function, which is the reason why this theorem is stated in the section concerning geometric features of the dimer model. Applications of this theorem are given in section 4.5.

Chapter 3

Isoradial dimer model

This chapter is devoted to a subclass of all dimer models, called *isoradial* dimer models, introduced by R. Kenyon in [26]. The system, that is the graph G , of such a model satisfies a geometric condition called *isoradiality*, and the energy of configurations is determined by a specific weight function called the *critical weight function*, see section 3.1 for definitions. In this case, Kenyon conjectured that many quantities of the dimer model can be computed in terms of the local geometry of the system [26]. Our interest in the isoradial dimer model is motivated by the *quadri-tile* dimer model (chapter 4), which was proposed by R. Kenyon as subject of this thesis. Indeed, most of the results obtained for the quadri-tile dimer model can be generalized to the isoradial dimer model (section 5.4, chapters 6 and 7).

Let G be an infinite isoradial graph, whose dual graph G^* is bipartite. Sections 3.2 and 3.3 have a parallel structure. In the first one, we introduce the *complex Dirac operator* K [26], and in the second we define the *real Dirac operator* K . Both operators are represented by an infinite weighted adjacency matrix indexed by the vertices of G^* . For K , edges of G^* are un-oriented and weighted by their critical weight times a complex number of modulus one. For K , edges of G^* are oriented with a *clockwise odd* orientation, and are weighted by their critical weight. Both weight functions yield the same probability distribution on finite subgraphs of G^* . Then, we give the definition and results of [26] for the inverse complex Dirac operator K^{-1} , and prove similar statements for the inverse real Dirac operator K^{-1} ; both inverses can be expressed in terms of the local geometry of G^* . As we will see in section 5.4, chapters 6 and 7, the Dirac operator is the right object to obtain explicit expressions for the dimer model on infinite isoradial graphs with critical weights.

Suppose that the graph G is Λ -periodic (for a 2-dimensional lattice Λ). Consider the toroidal graphs $\tilde{G}_n = G/n\Lambda$. In section 3.4, we state the expression of [20] for the partition function of the dual graph \tilde{G}_n^* , and the formula of [21] for the Boltzmann measure on $\mathcal{M}(\tilde{G}_n^*)$. Both expressions involve the restriction of the real Dirac operator K to \tilde{G}_n^* . Note that the two weight functions defined for K and K do not yield the same

probability measure on toroidal graphs, that is we cannot use the restriction of K to \bar{G}_n^* to obtain the above quantities. This explains why we introduce both operators: we use K for the dimer model on toroidal graphs, and \bar{K} because it is easier to handle since it does not involve an orientation of the edges of G^* . In the last part of section 3.4, we prove that the inverse of the restriction of K to \bar{G}_n^* , converges to K^{-1} on a subsequence of n 's.

Section 3.5 concerns height functions for 2-tilings of isoradial graphs. Recall that the definition of a height function depends on the existence of a reference flow (subsection 2.2.1). We prove that such a flow always exists in the case of isoradial graphs, and give an explicit construction.

3.1 Isoradial graphs and critical weight function

The following definitions are taken from [26].

3.1.1 Isoradial graphs

A graph G is said to be **isoradial** if it has an isoradial embedding, that is an embedding such that all faces are inscribable in a circle, and all circumcircles have the same radius. The common radius is taken to be 1. Moreover all circumcenters of the faces are contained in the closure of the faces. An isoradial embedding of the dual graph G^* of an isoradial graph G is obtained by sending dual vertices to the center of the corresponding faces. Note that if the circumcenters of two adjacent faces lie on their common edge, then the dual vertices of these two faces have the same image in the plane, so that the corresponding dual edge has length 0. From now on, when we speak of an isoradial graph, we shall actually mean an isoradial embedding of the graph.

Examples of isoradial graphs are the square lattice \mathbb{Z}^2 , the equilateral triangular lattice \mathbb{T} , and rhombus-with-diagonals tilings (see subsection 4.2.2).

3.1.2 Critical weight function

Recall that the energy of a dimer configuration depends on the weight function associated to the edges of the dual graph G^* . In the case of isoradial graphs, we consider a specific weight function ν , called the **critical weight function**, defined as follows. To each edge e of G^* , we associate a unit side-length rhombus $R(e)$ whose vertices are the vertices of e and the vertices of its dual edge ($R(e)$ may be degenerate). Let $\tilde{R} = \cup_{e \in G^*} R(e)$. Then, define $\nu(e) = 2 \sin \theta$, where 2θ is the angle of the rhombus $R(e)$ at the vertex it has in common with e ; θ is called the **rhombus angle** of the edge e . Note that $\nu(e)$ is the length of e^* , the dual edge of e .

When the graph considered for a dimer model is isoradial, and when the energy of configurations is determined by the critical weight function, we speak of an **isoradial**

dimer model.

In the remaining of this chapter, we let G be an infinite isoradial graph satisfying condition (*). Suppose that its dual graph G^* is bipartite, B denotes the set of black vertices, and W the set of white ones. Assume that the critical weight function ν is assigned to the edges of G^* .

3.2 Complex Dirac operator

This section follows [26]. In subsection 3.2.1, we define the *complex Dirac operator* K . In subsection 3.2.2, we define the inverse complex Dirac operator K^{-1} , and state an existence and uniqueness theorem; then we give an asymptotic formula for K^{-1} .

3.2.1 Complex Dirac operator

Results in this subsection are due to Kenyon [26], see also Mercat [36]. Define the Hermitian matrix K indexed by the vertices of G^* as follows. If v_1 and v_2 are not adjacent, $K(v_1, v_2) = 0$. If $w \in W$ and $b \in B$ are adjacent vertices, then $K(w, b) = \overline{K(b, w)}$ is the complex number of modulus $\nu(wb)$ and direction pointing from w to b . Another useful way to say this is as follows. Let $R(wb)$ be the rhombus associated to the edge wb , and denote by w, x, b, y its vertices in cclw (counterclockwise) order, then $K(w, b)$ is i times the complex vector $x - y$. If w and b have the same image in the plane, then $|K(w, b)| = 2$, and the direction of $K(w, b)$ is that which is perpendicular to the corresponding dual edge, and has sign determined by the local orientation. The infinite matrix K defines the **complex Dirac operator** $K: \mathbb{C}^{V(G^*)} \rightarrow \mathbb{C}^{V(G^*)}$, by

$$(Kf)(v) = \sum_{u \in G^*} K(v, u)f(u),$$

where $V(G^*)$ denotes the set of vertices of the graph G^* . Since K maps \mathbb{C}^B to \mathbb{C}^W and \mathbb{C}^W to \mathbb{C}^B , it really consists of two operators $K_{WB}: \mathbb{C}^W \rightarrow \mathbb{C}^B$, and its conjugate transpose $K_{BW}: \mathbb{C}^B \rightarrow \mathbb{C}^W$. Both operators K_{WB} and K_{BW} contain all the information about K , hence we restrict ourselves to the study of K_{BW} . To simplify notations, we denote K_{BW} by K and also call it the complex Dirac operator.

3.2.2 Inverse complex Dirac operator

The **inverse complex Dirac operator** K^{-1} is defined to be the operator which satisfies

1. $KK^{-1} = \text{Id}$,
2. $K^{-1}(b, w) \rightarrow 0$, when $|b - w| \rightarrow \infty$.

Kenyon [26] obtains an expression for the inverse complex Dirac operator. Before stating his theorem, we need to define the rational functions $f_{wv}(z)$. Let w be a white vertex of G^* . For every other vertex v , define $f_{wv}(z)$ as follows. Let $w = v_0, v_1, v_2, \dots, v_k = v$ be an edge-path of \tilde{R} from w to v . Each edge $v_j v_{j+1}$ has exactly one vertex of G^* (the other is a vertex of G). Direct the edge away from this vertex if it is white, and towards this vertex if it is black. Let $e^{i\alpha_j}$ be the corresponding vector in \tilde{R} (which may point contrary to the direction of the path). f_{wv} is defined inductively along the path, starting from

$$f_{ww}(z) = 1.$$

If the edge leads away from a white vertex, or towards a black vertex, then

$$f_{wv_{j+1}}(z) = \frac{f_{wv_j}(z)}{z - e^{i\alpha_j}},$$

else, if it leads towards a white vertex, or away from a black vertex, then

$$f_{wv_{j+1}}(z) = f_{wv_j}(z) \cdot (z - e^{i\alpha_j}).$$

The function $f_{wv}(z)$ is well defined (i.e. independent of the edge-path of \tilde{R} from w to v), because the multipliers for a path around a rhombus of \tilde{R} come out to 1. For a black vertex b the value $K^{-1}(b, w)$ will be the sum over the poles of $f_{wb}(z)$ of the residue of f_{wb} times the angle of z at the pole. However, there is an ambiguity in the choice of angle, which is only defined up to a multiple of 2π . To make this definition precise, angles are assigned to the poles of $f_{wb}(z)$. Working on the branched cover of the plane, branched over w , so that for each black vertex b in this cover, a real angle θ_0 is assigned to the complex vector $b - w$, which increases by 2π when b winds once around w . In the branched cover of the plane, a real angle in $[\theta_0 - \pi + \Delta, \theta_0 + \pi - \Delta]$ can be assigned to each pole of f_{wb} , for some small $\Delta > 0$.

Theorem 3.1 [26] *There exists a unique K^{-1} satisfying the above two properties, and K^{-1} is given by*

$$K^{-1}(b, w) = \frac{1}{4\pi^2 i} \int_C f_{wb}(z) \log z \, dz,$$

where C is a closed contour surrounding cclw the part of the circle $\{e^{i\theta} \mid \theta \in [\theta_0 - \pi + \Delta, \theta_0 + \pi - \Delta]\}$, which contains all the poles of f_{wb} , and with the origin in its exterior.

Theorem 3.2 [26] *Asymptotically, as $|b - w| \rightarrow \infty$,*

$$K^{-1}(b, w) = \frac{1}{2\pi} \left(\frac{1}{b - w} + \frac{f_{wb}(0)}{b - \bar{w}} \right) + O\left(\frac{1}{|b - w|^2}\right).$$

3.3 Real Dirac operator

The structure of this section is similar to that of the previous one. In subsection 3.3.1, we define the *real Dirac operator*. In subsection 3.3.2, we define the inverse real Dirac operator; we give an explicit expression for it, as well as an asymptotic formula. The proofs use the results for the inverse complex Dirac operator.

3.3.1 Real Dirac operator

Let us define an orientation of the edges of the graph G^* . To do this, we need to go a little bit deeper into Kasteleyn's work [20], see also subsection 2.1.2.

Consider an orientation of the edges of G^* . An elementary cycle C of G^* is said to be **clockwise odd** if, when travelling cw (clockwise) around the edges of C , the number of co-oriented edges is odd. Note that since G^* is bipartite, cycles are of even length, so that the number of contra-oriented edges is also odd. Kasteleyn defines the orientation of the graph G^* to be **clockwise odd** if all elementary cycles of G^* are clockwise odd.

Lemma 3.3 [20] *There exists a clockwise odd orientation of the edges of G^* . Moreover, if G_1^* is a finite simply connected subgraph of G^* , the orientation of the edges of G_1^* is admissible.*

Consider a clockwise odd orientation of the edges of G^* . Define K to be the infinite adjacency matrix of the graph G^* , weighted by the critical weight function ν . That is, if v_1 and v_2 are not adjacent, $K(v_1, v_2) = 0$. If $w \in W$ and $b \in B$ are adjacent vertices, then $K(w, b) = -K(b, w) = (-1)^{\mathbb{I}_{(w,b)}} \nu(wb)$, where $\mathbb{I}_{(w,b)} = 0$ if the edge wb is oriented from w to b , and 1 if it is oriented from b to w . The infinite matrix K defines the **real Dirac operator** $K: \mathbb{C}^{V(G^*)} \rightarrow \mathbb{C}^{V(G^*)}$, by

$$(Kf)(v) = \sum_{u \in G^*} K(v, u)f(u),$$

The matrix K is also called a **Kasteleyn matrix** for the underlying dimer model. As in the complex case, K consists of two operators K_{WB} and K_{BW} . We again restrict ourselves to the study of K_{BW} , denote it by K , and call it the real Dirac operator.

3.3.2 Inverse real Dirac operator

The **inverse real Dirac operator** K^{-1} is defined to be the unique operator satisfying

1. $KK^{-1} = \text{Id}$,
2. $K^{-1}(b, w) \rightarrow 0$, when $|b - w| \rightarrow \infty$.

Let us define the rational functions $f_{wx}(z)$. They are the analogous of the rational functions $f_{wv}(z)$, but are defined for vertices $x \in G^*$ (whereas the functions $f_{wv}(z)$ were defined for vertices $v \in \tilde{R}$). Let $w \in W$, and let $x \in B$ (resp. $x \in W$); consider the edge-path $w = w_1, b_1, \dots, w_k, b_k = x$ (resp. $w = w_1, b_1, \dots, w_k, b_k, w_{k+1} = x$) of G^* from w to x . Let $R(w_j b_j)$ be the rhombus associated to the edge $w_j b_j$, and denote by w_j, x_j, b_j, y_j its vertices in cclw order; $e^{i\alpha_j}$ is the complex vector $y_j - w_j$, and $e^{i\beta_j}$ is the complex vector $x_j - w_j$. In a similar way, denote by w_{j+1}, x'_j, b_j, y'_j the vertices of the rhombus $R(w_{j+1} b_j)$ in cclw order, then $e^{i\alpha'_j}$ is the complex vector $y'_j - w_{j+1}$, and

$e^{i\beta'_j}$ is the complex vector $x'_j - w_{j+1}$. $f_{wx}(z)$ is defined inductively along the path,

$$\begin{aligned} f_{ww}(z) &= 1, \\ f_{wb_j}(z) &= f_{ww_j}(z) \frac{(-1)^{\mathbb{I}(w_j, b_j)} e^{i\frac{\alpha_j + \beta_j}{2}}}{(z - e^{i\alpha_j})(z - e^{i\beta_j})}, \\ f_{ww_{j+1}}(z) &= f_{wb_j}(z) (-1)^{\mathbb{I}(w_{j+1}, b_j)} e^{-i\frac{\alpha'_j + \beta'_j}{2}} (z - e^{i\alpha'_j})(z - e^{i\beta'_j}). \end{aligned}$$

Remark 3.4 We have the following relations between the real and the complex case.

1. $\forall w \in W, \forall x \in B \cup W, f_{wx}(z) = \overline{f_{wx}(0)} f_{wx}(z)$.
2. $\forall w \in W, \forall b \in B$, such that w is adjacent to b , $K(w, b) = f_{wb}(0)K(w, b)$.

Proof:

1. This is a direct consequence of the definitions of the functions f_{wx} and f_{wx} .
2. Let $R(wb)$ be the rhombus associated to the edge wb , and let w, x, b, y be its vertices in cclw order. Denote by $e^{i\alpha}$ the complex vector $y - w$, and by $e^{i\beta}$ the complex vector $x - w$. Let θ be the rhombus angle of the edge wb . By definition we have,

$$\begin{aligned} K(w, b) &= (-1)^{\mathbb{I}(w, b)} 2 \sin \theta = (-1)^{\mathbb{I}(w, b)} \frac{e^{i\frac{\alpha - \beta}{2}} - e^{-i\frac{\alpha - \beta}{2}}}{i}, \\ K(w, b) &= i(e^{i\beta} - e^{i\alpha}), \\ f_{wb}(0) &= (-1)^{\mathbb{I}(w, b)} e^{-i\frac{\alpha + \beta}{2}}. \end{aligned}$$

Combining the above three equations yields 2. □

Lemma 3.5 *The function f_{wx} is well defined.*

Proof:

Showing that the function f_{wx} is well defined amounts to proving that f_{wx} is independent of the edge-path of G^* from w to x . This is equivalent to proving the following: let $w_1, b_1, \dots, w_k, b_k, w_{k+1} = w_1$ be the vertices of an elementary cycle C of G^* , where vertices are enumerated in cclw order; if $f_{w_1 w_1}(z) = 1$ then $f_{w_1 w_{k+1}}(z) = 1$. Let us use the notations introduced in the definition of f_{wx} (see also figure 3.1), and denote indices cyclically, that is $k + 1 \equiv 1$. By remark 3.4, we have

$$f_{w_1 w_{k+1}}(z) = \overline{f_{w_1 w_{k+1}}(0)} f_{w_1 w_{k+1}}(z).$$

Since the function f_{wx} is well defined, $f_{w_1 w_{k+1}}(z) = 1$. Hence, it remains to prove that $\overline{f_{w_1 w_{k+1}}(0)} = 1$.

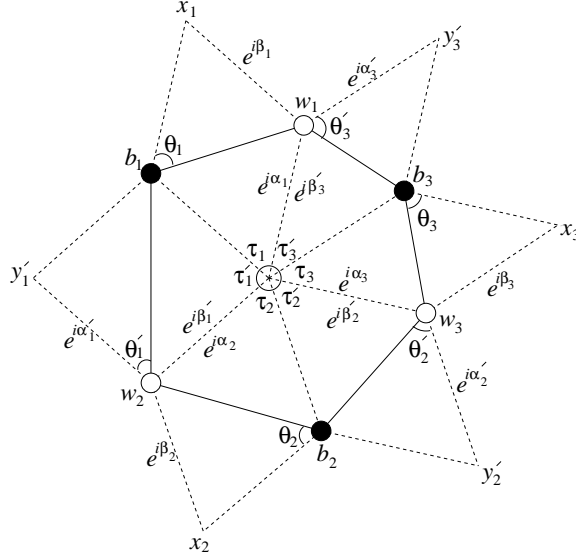


Figure 3.1: Notations

By definition of \mathbf{f}_{wx} , we have

$$\overline{\mathbf{f}_{w_1 w_{k+1}}(0)} = \prod_{j=1}^k \left((-1)^{(\mathbb{I}_{(w_j, b_j)} + \mathbb{I}_{(w_{j+1}, b_j)})} e^{i \frac{\alpha_j + \beta_j}{2}} e^{-i \frac{\alpha'_j + \beta'_j}{2}} \right).$$

Moreover for every j , $\alpha'_j = \beta_j$ (see figure 3.1), so that

$$\overline{\mathbf{f}_{w_1 w_{k+1}}(0)} = \prod_{j=1}^k \left((-1)^{(\mathbb{I}_{(w_j, b_j)} + \mathbb{I}_{(w_{j+1}, b_j)})} e^{i \frac{\alpha_j - \beta_j}{2}} e^{i \frac{\alpha'_j - \beta'_j}{2}} \right).$$

Let θ_j (resp. θ'_j) be the rhombus angle of the edge $w_j b_j$ (resp. $w_{j+1} b_j$), then

$$\overline{\mathbf{f}_{w_1 w_{k+1}}(0)} = (-1)^{\sum_{j=1}^k (\mathbb{I}_{(w_j, b_j)} + \mathbb{I}_{(w_{j+1}, b_j)})} e^{i \sum_{j=1}^k (\theta_j + \theta'_j)}. \quad (3.1)$$

The cycle C corresponds to a face of the graph G^* . Let c be the circumcenter of this face, and let τ_j (resp. τ'_j) be the angle of the rhombus $R(w_j b_j)$ (resp. $R(w_{j+1} b_j)$) at the vertex c . Then $\tau_j = \pi - 2\theta_j$, and $\tau'_j = \pi - 2\theta'_j$ (see figure 3.1). Since $\sum_{j=1}^k (\tau_j + \tau'_j) = 2\pi$, we deduce $\sum_{j=1}^k (\theta_j + \theta'_j) = \pi(k-1)$. Hence,

$$e^{i \sum_{j=1}^k (\theta_j + \theta'_j)} = -(-1)^k. \quad (3.2)$$

Moreover $\mathbb{I}_{(w_{j+1}, b_j)} = 1 - \mathbb{I}_{(b_j, w_{j+1})}$, and $(-1)^{1 - \mathbb{I}_{(b_j, w_{j+1})}} = (-1)^{\mathbb{I}_{(b_j, w_{j+1})} - 1}$, so

$$(-1)^{\sum_{j=1}^k (\mathbb{I}_{(w_j, b_j)} + \mathbb{I}_{(w_{j+1}, b_j)})} = (-1)^{\sum_{j=1}^k (\mathbb{I}_{(w_j, b_j)} + \mathbb{I}_{(b_j, w_{j+1})} - k)}.$$

Note that $\sum_{j=1}^k (\mathbb{I}_{(w_j, b_j)} + \mathbb{I}_{(b_j, w_{j+1})})$ is the number of co-oriented edges encountered when travelling cclw around the cycle C . Since the orientation of the edges of G^* is clockwise odd, it is also counterclockwise odd, and so this number is odd. This implies

$$(-1)^{\sum_{j=1}^k (\mathbb{I}_{(w_j, b_j)} + \mathbb{I}_{(w_{j+1}, b_j)})} = -(-1)^{-k}. \quad (3.3)$$

The proof is completed by combining equations (3.1), (3.2) and (3.3). \square

As in the complex case, a real angle in $[\theta_0 - \pi + \Delta, \theta_0 + \pi - \Delta]$ can be assigned to each pole of f_{wb} , for some small $\Delta > 0$; where θ_0 is the real angle assigned to the vector $b - w$.

Proposition 3.6 *The inverse real Dirac operator is given by*

$$\mathbb{K}^{-1}(b, w) = \frac{1}{4\pi^2 i} \int_C f_{wb}(z) \log z \, dz, \quad (3.4)$$

where C is a closed contour surrounding cclw the part of the circle $\{e^{i\theta} \mid \theta \in [\theta_0 - \pi + \Delta, \theta_0 + \pi - \Delta]\}$, which contains all the poles of f_{wb} , and with the origin in its exterior.

Proof:

Let $\mathbb{F}(b, w)$ be the right hand side of (3.4). Fix a vertex $w_0 \in W$, and let us prove that $\sum_{b \in B} \mathbb{K}(w_0, b) \mathbb{F}(b, w) = \delta_{w_0}(w)$. Denote by b_1, \dots, b_k the black neighbors of w_0 . Using remark 3.4, we obtain for every j ,

$$\begin{aligned} \mathbb{K}(w_0, b_j) &= f_{w_0 b_j}(0) K(w_0, b_j), \\ f_{w b_j}(z) &= \overline{f_{w b_j}(0)} f_{w b_j}(z). \end{aligned}$$

Moreover $\forall w \in W, \forall b \in B$, we have $\overline{f_{wb}(0)} = f_{wb}(0)^{-1} = f_{bw}(0)$, so that $f_{w_0 b_j}(0) \overline{f_{w b_j}(0)} = f_{w_0 b_j}(0) f_{b_j w}(0) = f_{w_0 w}(0)$. Hence, using theorem 3.1, we obtain for every j ,

$$\mathbb{K}(w_0, b_j) \mathbb{F}(b_j, w) = f_{w_0 w}(0) K(w_0, b_j) K^{-1}(b_j, w).$$

Since $\mathbb{K}(w_0, b) = 0$ when w_0 and b are not adjacent, and since K^{-1} is the inverse complex Dirac operator, we obtain

$$\sum_{b \in B} \mathbb{K}(w_0, b) \mathbb{F}(b, w) = \sum_{j=1}^k \mathbb{K}(w_0, b_j) \mathbb{F}(b_j, w) = f_{w_0 w}(0) \sum_{j=1}^k K(w_0, b_j) K^{-1}(b_j, w) = f_{w_0 w}(0) \delta_{w_0}(w) = \delta_{w_0}(w).$$

To prove that $\mathbb{F}(b, w) \rightarrow 0$ as $|b - w| \rightarrow \infty$, see proposition 3.7 below. \square

Proposition 3.7 *Asymptotically, as $|b - w| \rightarrow \infty$,*

$$\mathbb{K}^{-1}(b, w) = \frac{1}{2\pi} \left(\frac{\overline{f_{wb}(0)}}{b - w} + \frac{f_{wb}(0)}{\overline{b} - \overline{w}} \right) + O\left(\frac{1}{|b - w|^2}\right).$$

Proof:

Using proposition 3.6, remark 3.4, and the asymptotic formula for $K^{-1}(b, w)$ of theorem 3.2, we obtain

$$\begin{aligned} \mathbb{K}^{-1}(b, w) &= \frac{1}{4\pi^2 i} \int_C f_{wb}(z) \log z dz = \overline{f_{wb}(0)} K^{-1}(b, w), \\ &= \overline{f_{wb}(0)} \left(\frac{1}{2\pi} \left(\frac{1}{b-w} + \frac{f_{wb}(0)}{\bar{b}-\bar{w}} \right) + O\left(\frac{1}{|b-w|^2}\right) \right), \\ &= \frac{1}{2\pi} \left(\overline{f_{wb}(0)} \frac{1}{b-w} + \frac{f_{wb}(0)}{\bar{b}-\bar{w}} \right) + O\left(\frac{1}{|b-w|^2}\right). \end{aligned}$$

□

Proposition 3.8 *The inverse real Dirac operator \mathbb{K}^{-1} is unique.*

Proof:

This follows from the uniqueness of the complex inverse Dirac operator K^{-1} . □

3.4 Isoradial dimer model on the torus

Let Λ be a two-dimensional lattice. Suppose that the graph G is Λ -periodic, and assume that the bipartite coloring of the vertices of G^* is preserved by Λ -translations, that is black vertices are mapped to black ones, and white vertices to white ones. Let us call **horizontal** and **vertical** the directions given by two basis vectors of Λ . Define \bar{G}_n to be the toroidal graph $G/n\Lambda$, then the graph \bar{G}_n^* is bipartite. In subsection 3.4.1, we give Tesler's result for the partition function of the toroidal graph \bar{G}_n^* [43]. In subsection 3.4.2, we state Kenyon's expression for the Boltzmann measure on $\mathcal{M}(\bar{G}_n^*)$ [21]. In subsection 3.4.3, we prove that the inverse Kasteleyn matrices of the graph \bar{G}_n^* converge on a subsequence of n 's to the inverse real Dirac operator indexed by the vertices of G^* .

3.4.1 Toroidal partition function

The **toroidal partition function** $Z(\bar{G}_n^*, \nu)$ is defined to be the weighted sum of dimer configurations of the graph \bar{G}_n^* . Before giving an explicit expression for $Z(\bar{G}_n^*, \nu)$, let us orient the edges of G^* . Consider the graph \bar{G}_1^* , it is a bipartite graph on the torus. Fix a reference matching M_0 of \bar{G}_1^* . For every other perfect matching M of \bar{G}_1^* , consider the superposition $M \cup M_0$ of M and M_0 , then $M \cup M_0$ consists of doubled edges and cycles. Let us define four parity classes for perfect matchings M of \bar{G}_1^* : (e,e) consists of perfect

matchings M , for which cycles of $M \cup M_0$ circle the torus an even number of times horizontally and vertically; (e,o) consists of perfect matchings M , for which cycles of $M \cup M_0$ circle the torus and even number of times horizontally, and an odd number of times vertically; (o,e) and (o,o) are defined in a similar way. By Tesler [43], one can construct an orientation of the edges of \bar{G}_1^* , so that the corresponding adjacency matrix K_1^1 has the following property: perfect matchings which belong to the same parity class have the same sign in the expansion of the determinant; moreover of the four parity classes, three have the same sign and one the opposite sign. By an appropriate choice of sign, we can make the (e,e) class have the plus sign in $\det K_1^1$, and the other three have minus sign. Consider a horizontal and a vertical cycle of \bar{G}_1 . Then define K_2^1 (resp. K_3^1) to be the matrix K_1^1 where the sign of the coefficients corresponding to edges crossing the horizontal (resp. vertical) cycle is reversed; and define K_4^1 to be the matrix K_1^1 where the sign of the coefficients corresponding to the edges crossing both cycles are reversed. By Kasteleyn [20] (in the domino case), and Tesler [43] (in the general case), we have the following,

$$Z(\bar{G}_1^*, \nu) = \frac{1}{2}(-\det K_1^1 + \det K_2^1 + \det K_3^1 + \det K_4^1).$$

The orientation of the edges of \bar{G}_1^* defines a periodic orientation of the graph G^* . For every n , consider the graph \bar{G}_n^* , and the four matrices $K_1^n, K_2^n, K_3^n, K_4^n$ defined as above. These matrices are called the **Kasteleyn matrices** of the graph \bar{G}_n^* .

Theorem 3.9 [20, 43]

$$Z(\bar{G}_n^*, \nu) = \frac{1}{2}(-\det K_1^n + \det K_2^n + \det K_3^n + \det K_4^n).$$

The orientation defined on the edges of the graph G^* is a clockwise odd orientation. Let K be the real Dirac operator indexed by the vertices of G^* , corresponding to the critical weight function ν , and to this clockwise odd orientation. Note that except for edges crossing the horizontal and the vertical cycle, the coefficients of the Kasteleyn matrices K_ℓ^n and of the real Dirac operator agree on edges they have in common.

3.4.2 Toroidal Boltzmann measure

Let μ^n be the Boltzmann measure on the set of dimer configurations $\mathcal{M}(\bar{G}_n^*)$ of the toroidal graph \bar{G}_n^* . Let $e_1 = w_1 b_1, \dots, e_k = w_k b_k$ be a subset of edges of \bar{G}_n^* which do not cross the horizontal and the vertical cycle of \bar{G}_n . Kenyon [21] derives an explicit expression for the probability $\mu^n(e_1, \dots, e_k)$ of these edges occurring in a dimer configuration of \bar{G}_n^* chosen with respect to the Boltzmann measure.

Theorem 3.10 [21] *The probability $\mu^n(e_1, \dots, e_k)$ is given by*

$$\left(\prod_{i=1}^k K(w_i, b_i) \right) \left(-\frac{\det K_1^n}{2Z(\bar{G}_n^*, \nu)} \det_{1 \leq i, j \leq k} ((K_1^n)^{-1}(b_i, w_j)) + \sum_{\ell=2}^4 \frac{\det K_\ell^n}{2Z(\bar{G}_n^*, \nu)} \det_{1 \leq i, j \leq k} ((K_\ell^n)^{-1}(b_i, w_j)) \right).$$

3.4.3 Inverse real Dirac operator and inverse Kasteleyn matrices

The inverse real Dirac operator K^{-1} indexed by the vertices of the graph G^* can be seen as the limit on a subsequence of n 's of each of the inverse Kasteleyn matrices of the graphs \tilde{G}_n^* .

Proposition 3.11 *For every $w \in W$, $b \in B$, we have*

$$\forall \ell = 1, \dots, 4, \lim'_{n \rightarrow \infty} (\mathsf{K}_\ell^n)^{-1}(b, w) = \mathsf{K}^{-1}(b, w),$$

where \lim' means the limit is taken along a subsequence (n_j) of n 's.

Proof:

The following theorem of [29] gives the convergence on a subsequence of n 's of the inverse Kasteleyn matrices of the graph \tilde{G}_n^* .

Theorem 3.12 [29] *For every $w \in W, b \in B$,*

$$\forall \ell = 1, \dots, 4, \lim'_{n \rightarrow \infty} (\mathsf{K}_\ell^n)^{-1}(b, w) = \frac{1}{(2\pi)^2} \int_{S^1 \times S^1} \frac{Q_{b,w}(z, u) u^x z^y}{P(z, u)} \frac{dz du}{z u}, \quad (3.5)$$

where $Q_{b,w}$ and P are polynomials ($Q_{b,w}$ only depends on the equivalence class of w and b), and x (resp. y) is the horizontal (resp. vertical) translation from the fundamental domain of b to the fundamental domain of w .

Denote by $F(b, w)$ the right hand side of (3.5). In [29], it is proved that $F(b, w)$ converges to 0 as $|b - w| \rightarrow \infty$, as long as the dimer model is not in its frozen phase. Moreover, it is proved in [28] that the isoradial dimer model is never in its frozen phase when the weights associated to the edges of the graph G^* are the critical weights. Hence, we deduce that $F(b, w)$ converges to 0 as $|b - w| \rightarrow \infty$.

Let us prove that for every $b \in B, w \in W$, $F(b, w) = \mathsf{K}^{-1}(b, w)$. Consider two white vertices w_1, w_2 of G^* , and denote by b_1, \dots, b_k the neighbors of w_1 . Assume n is large enough so that the graph \tilde{G}_n^* contains $w_1, w_2, b_1, \dots, b_k$, and so that the edges $w_1 b_j$ do not cross the horizontal and vertical cycle of \tilde{G}_n . Then, for every $\ell = 1, \dots, 4$,

$$\sum_{b \in B} \mathsf{K}_\ell^n(w_1, b) (\mathsf{K}_\ell^n)^{-1}(b, w_2) = \sum_{j=1}^k \mathsf{K}_\ell^n(w_1, b_j) (\mathsf{K}_\ell^n)^{-1}(b_j, w_2) = \delta_{w_1 w_2}.$$

Moreover, $\mathsf{K}_\ell^n(w_1, b_j) = \mathsf{K}(w_1, b_j)$, so that taking the limit on a subsequence of n 's, and using theorem 3.12, we obtain

$$\sum_{j=1}^k \mathsf{K}(w_1, b_j) F(b_j, w_2) = \delta_{w_1 w_2}.$$

This is true for all white vertices $w_1, w_2 \in G^*$. Moreover, $\lim_{|b-w| \rightarrow \infty} F(b, w) = 0$. Using the definition of the inverse real Dirac operator, and the uniqueness proposition 3.8, we deduce that for all $b \in B, w \in W$, $F(b, w) = \mathsf{K}^{-1}(b, w)$. \square

3.5 Isoradial dimer model and height functions

By subsection 2.2.1, we know that the definition of a height function h on the vertices of 2-tilings of G depends on the existence of a reference flow $\omega_0 \in \Omega(G^*)$ on the edges of G^* . The following lemma states that such a flow always exists when G is an infinite isoradial graph. An explicit construction is given in the proof.

Lemma 3.13 *If G is an infinite isoradial graph satisfying condition (*), then $\Omega(G^*) \neq \emptyset$.*

Proof:

Consider an edge wb of G^* , let $R(wb)$ be the rhombus associated to wb , and let θ_{wb} be the corresponding rhombus angle. Define ω_0 to be a white-to-black flow, which flows by θ_{wb}/π along every edge wb . Then $\omega_0 \in \Omega(G^*)$, indeed we have

$$\forall w \in W, \sum_{b: b \sim w} 2\theta_{wb} = 2\pi; \forall b \in B, \sum_{w: w \sim b} 2\theta_{wb} = 2\pi.$$

□

Chapter 4

Quadri-tile dimer model

The aim of the first two chapters was to introduce the dimer model in all of its generality. To go deeper in our study, the third chapter is dedicated to the particular model which was proposed by R. Kenyon as subject for this thesis: the *quadri-tile dimer model*. In general, choosing a model amounts to choosing a graph G (the system). For instance, when G is the square lattice \mathbb{Z}^2 , or the equilateral triangular lattice \mathbb{T} , we obtain the domino and the lozenge dimer model respectively (see subsection 2.1.1). In the case of the quadri-tile dimer model, the process is slightly different.

In section 4.1, we define a set of tiles which are quadrilaterals made of adjacent right triangles. Quadri-tilings are tilings obtained from this set of tiles.

In section 4.2, we prove that quadri-tilings correspond to 2-tilings of a family of graphs which are rhombus-with-diagonals tilings. Hence, quadri-tilings actually consist of a family of dimer models, this is precisely the interest of the model.

Section 4.3 is about a sub-family \mathcal{Q} of the set of all quadri-tilings, consisting of quadri-tilings that are 2-tilings of lozenge-with-diagonals tilings. Quadri-tilings of \mathcal{Q} correspond to two superposed dimer models: let $Q \in \mathcal{Q}$, then Q is a 2-tiling of its underlying lozenge-with-diagonals tiling, and the corresponding lozenge tiling is a 2-tiling of the equilateral triangular lattice \mathbb{T} . We refer to this sub-family as the *triangular quadri-tile dimer model*.

The triangular quadri-tile dimer model is interpreted geometrically in section 4.4. We prove that quadri-tilings of \mathcal{Q} are characterized by two height functions, that is quadri-tilings are seen as discrete surfaces of dimension 2 in a space of dimension 4. Hence, the triangular quadri-tile dimer model is a random interface model in dimension $2 + 2$. This is the first model of the kind obtained as superposition of 2 dimer models.

In section 4.5, using Propp's result [39] (see also subsection 2.2.3), we describe the space of quadri-tilings of the triangular quadri-tile dimer model restricted to a simply connected subgraph of \mathbb{T} .

4.1 Quadri-tiles and quadri-tilings

Consider the set of right triangles whose hypotenuses have length two. Color the vertex at the right angle black, and the other two vertices white. A **quadri-tile** is a quadrilateral obtained from two such triangles in two different ways: either glue them along the hypotenuse, or supposing they have a leg of the same length, glue them along this edge matching the black (white) vertex to the black (white) one, see figure 4.1. Both types of quadri-tiles have four vertices.

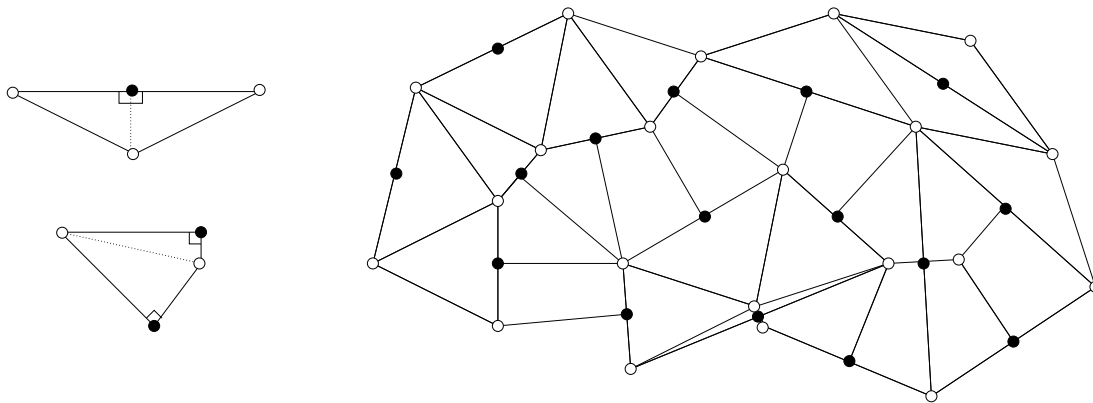


Figure 4.1: Two types of quadri-tiles (left), and a quadri-tiling (right).

A **quadri-tiling** of the plane is an edge-to-edge tiling of the plane by quadri-tiles that respects the coloring of the vertices, that is black (resp. white) vertices are matched to black (resp. white) ones. An example of quadri-tiling is given in figure 4.1. In all that follows, we consider quadri-tilings that use finitely many different quadri-tiles, up to isometry.

4.2 Underlying rhombus-with-diagonals tilings

In this section, we prove that each quadri-tiling is a 2-tiling of a unique rhombus-with-diagonals tiling. Then we give two properties of rhombus-with-diagonals tilings.

4.2.1 Underlying rhombus-with-diagonals tilings

Lemma 4.1 *Quadri-tilings are in one-to-one correspondence with 2-tilings of graphs which are rhombus-with-diagonals tilings of the plane, and which use finitely many different rhombi, up to isometry.*

Proof:

Consider a rhombus-with-diagonals tiling of the plane R . Color the vertices at the

crossing of the diagonals of the rhombi black, and the boundary vertices of the rhombi white, then 2-tilings of R are quadri-tilings. Conversely, consider a quadri-tiling of the plane Q . Denote by R the tiling of the plane obtained from Q by drawing, for each quadri-tile, the edge separating the two right triangles. Let b be a black vertex of R , denote by w_1, \dots, w_k the neighbors of b in cclw (counterclockwise) order. In each right triangle, the black vertex is adjacent to two white vertices, and since the gluing respects the coloring of the vertices, w_1, \dots, w_k are white vertices. Moreover, b is at the right angle, so $k = 4$ and the edges $w_1w_2, w_2w_3, w_3w_4, w_4w_1$ are hypotenuses of right triangles. Therefore w_1, \dots, w_4 form a side-length 2 rhombus, and b stands at the crossing of its diagonals. This is true for any black vertex b of R , so R is a rhombus-with-diagonals tiling of the plane, and Q is a 2-tiling of R . \square

As a consequence of lemma 4.1, a quadri-tiling Q is a 2-tiling of a unique rhombus-with-diagonals tiling, which we call the **underlying rhombus-with-diagonals tiling**, and which we denote by $R(Q)$.

4.2.2 Properties of rhombus-with-diagonals tilings

Consider a rhombus-with-diagonals tiling of the plane R , and denote by R the rhombus tiling corresponding to R , that is R is the tiling R without the diagonals.

Property 4.2

1. *The graph R^* is bipartite.*
2. *The graph R is isoradial.*

Proof:

1. Cycles corresponding to the faces of the graph R have length four, hence R has a bipartite coloring of its vertices, say black and white. Consider a face of R , and orient its boundary edges cclw. If the white vertex of the hypotenuse-edge comes before the black one, assign color black to the face, else assign color white. This defines a bipartite coloring of the faces of R , which is also a bipartite coloring of the vertices of R^* (see figure 4.2).

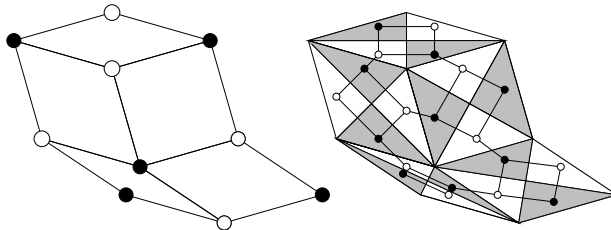


Figure 4.2: Bipartite coloring of the vertices of R (left), and corresponding bipartite coloring of the faces of R and of the vertices of R^* (right).

2. Faces of R are right triangles, so that circumcenters are at the mid-point of the hypotenuse edges. The radius of the circumcenters is equal to half the edge-length of the rhombi, that is 1. □

Note that the circumcenters of the faces of R are on the boundary of the faces, so that in the isoradial embedding of the dual graph R^* , some dual edges have length 0.

4.3 Triangular quadri-tile dimer model

We explain how the triangular quadri-tile dimer model consists of two superposed dimer models. Then, we compute the critical weights for quadri-tiles of this model.

4.3.1 Definition

Let \mathcal{Q} be the set of quadri-tilings of the plane whose underlying tilings are lozenge-with-diagonals tilings, \mathcal{Q} is a sub-family of all quadri-tilings of the plane. Our interest in \mathcal{Q} lies in the fact that it consists of two superposed dimer models. More precisely, let $Q \in \mathcal{Q}$ be a quadri-tiling, and let $L(Q)$ be its underlying lozenge-with-diagonals tiling, then Q is a 2-tiling of $L(Q)$. Now, denote by $\mathbb{L}(Q)$ the lozenge tiling corresponding to $L(Q)$, then $\mathbb{L}(Q)$ is a 2-tiling of the equilateral triangular lattice \mathbb{T} . The model which considers quadri-tilings of \mathcal{Q} is called the **triangular quadri-tile dimer model**.

Let us write \mathcal{M} for the set of dimer configurations corresponding to quadri-tilings of \mathcal{Q} ; if \mathcal{L} denotes the set of lozenge-with-diagonals tiling of the plane, up to isometry, then \mathcal{M} can be written as $\mathcal{M} = \cup_{L \in \mathcal{L}} \mathcal{M}(L^*)$.

Up to isometry, we classify quadri-tiles of quadri-tilings of \mathcal{Q} in four types, denoted by I, II, III, IV see figure 4.3.

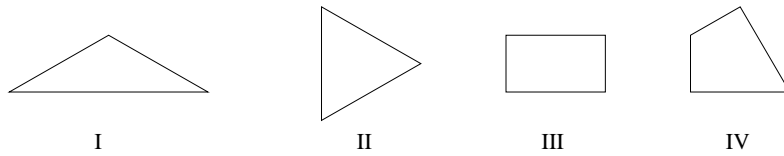


Figure 4.3: Four types of quadri-tiles for quadri-tilings of \mathcal{Q} .

4.3.2 Critical weight function

Consider a quadri-tiling $Q \in \mathcal{Q}$. By property 4.2, the lozenge-with-diagonals tiling $L(Q)$ is an isoradial graph. Let us compute the critical weight function ν associated to edges of $L(Q)^*$. Classify edges of $L(Q)^*$ in four types I, II, III, IV, where for $i = \text{I}, \dots, \text{IV}$, an edge of type i corresponds to a quadri-tile of type i . Figure 4.4 represents the rhombus

$R(e_i)$ associated to an edge e_i of type i . Note that edges e_{III} and e_{IV} have length zero, so that their rhombus is degenerate, and they have the same weight. The rhombus angle of the edge e_i allows us to compute the critical weights:

$$\nu(e_{\text{I}}) = 1, \nu(e_{\text{II}}) = \sqrt{3}, \nu(e_{\text{III}}) = \nu(e_{\text{IV}}) = 2.$$

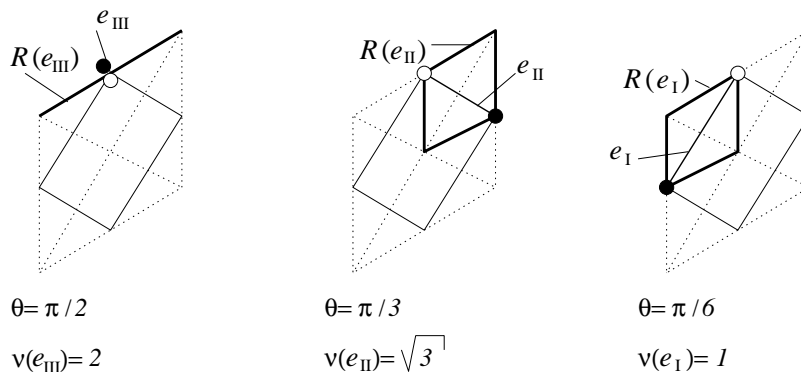


Figure 4.4: Critical weight function for $L(Q)^*$.

The graph \mathbb{T} is also isoradial, and the critical weight function for \mathbb{T}^* associates weight $\sqrt{3}$ to every edge.

4.4 Quadri-tilings as surfaces in dimension 2+2

We define a first height function on the vertices of every quadri-tiling Q , interpreted as a 2-tiling of its underlying rhombus-with-diagonals tiling. When $Q \in \mathcal{Q}$, we define a second height function on the vertices of Q , which corresponds to the height of its underlying lozenge-with-diagonals tiling, interpreted as a 2-tiling of the triangular lattice \mathbb{T} . This leads to the interpretation of Q as a 2-dimensional surface in a 4-dimensional space.

4.4.1 First height function

Consider a quadri-tiling of the plane Q , and let $R(Q)$ be its underlying rhombus-with-diagonals tiling. Then Q is a 2-tiling of $R(Q)$, and the dual graph $R(Q)^*$ of $R(Q)$ is bipartite. Fix a vertex v_0 of $R(Q)$ on a boundary edge of one of the rhombi. By subsection 2.2.1, the definition of a height function on the vertices of Q depends on the existence of a reference flow ω_0 on the edges of $R(Q)^*$. Note that vertices of $R(Q)^*$ are of degree 3, so that we define ω_0 to be a white-to-black flow, which flows by $1/3$ along every edge of $R(Q)^*$; then $\omega_0 \in \Omega(R(Q)^*)$ (the set of reference flows). This defines a height function on the vertices of Q , which we call the **first height function**, and denote by h^R . Consider the orientation on the edges of $R(Q)$ induced by the bipartite coloring of its faces, and let uv be an edge of Q oriented from u to v . If uv bounds

a quadri-tile, then h^R increases by $1/3$ along uv , else if it lies across a quadri-tile, it decreases by $2/3$. An example of computation of h^R is given in figure 4.5.

4.4.2 Second height function

Consider a quadri-tiling $Q \in \mathcal{Q}$, and let $L(Q)$ be its underlying lozenge-with-diagonals tiling. Let us assign the first height function h^L to the vertices of Q . We define a second height function on the vertices of $L(Q)$ (which are the same as the vertices of Q). It is just $1/3$ of Thurston's classical height function on lozenges [44] (see also subsection 2.2.1).

The lozenge tiling $L(Q)$ corresponding to $L(Q)$ is a 2-tiling of the triangular lattice \mathbb{T} . The honeycomb lattice \mathbb{T}^* is bipartite and has vertices of degree 3, so that we define ω_0 to be a white-to-black flow, which flows by $1/3$ along every edge of \mathbb{T}^* ; then $\omega_0 \in \Omega(\mathbb{T}^*)$. Take v_0 to be the vertex chosen for the height function h^L (it is also a vertex of \mathbb{T}). This defines a height function on the vertices of $L(Q)$, which we call the **second height function**, and denote by h . Consider the orientation on the edges of \mathbb{T} induced by the bipartite coloring of its faces, and let uv be an edge of $L(Q)$ oriented from u to v . If uv bounds a lozenge, then h increases by $1/3$ along uv , else if it lies across a lozenge, it decreases by $2/3$.

There is a natural way of defining a value for h at the vertex at the crossing of the diagonals of the lozenges of $L(Q)$. When going cclw around the vertices of a lozenge ℓ of $L(Q)$, starting from the smallest value, say α , vertices take on successive values $\alpha, \alpha + 1/3, \alpha + 2/3, \alpha + 1/3$, so that we assign value $\alpha + 1/3$ to the vertex at the center of the lozenge ℓ . An example of computation of h is given in figure 4.5.

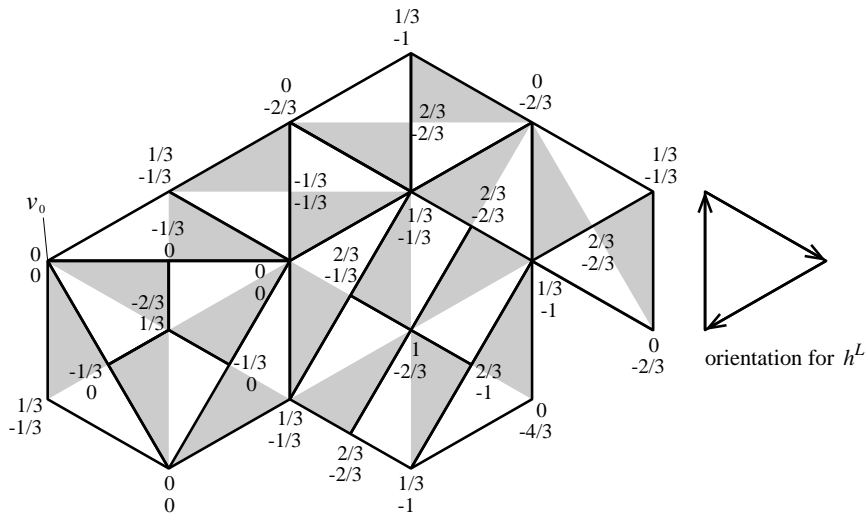


Figure 4.5: Quadri-tiling of an underlying lozenge tiling with height function h^L (above) and h (below).

4.4.3 Geometric interpretation

In Thurston's geometric interpretation of the second height function h [44], a lozenge tiling is seen a surface S in $\frac{1}{3}\mathbb{Z}^3$ (where the diagonals of the cubes are orthogonal to the plane), that has been projected orthogonally to the plane. S is determined by the height function h . In a similar way, a quadri-tiling of the plane $Q \in \mathcal{Q}$ can be seen as a surface S_1 in a 4-dimensional space that has been projected orthogonally to the plane. S_1 can also be projected to $\frac{1}{3}\tilde{\mathbb{Z}}^3$ ($\tilde{\mathbb{Z}}^3$ is the space \mathbb{Z}^3 where cubes are drawn with diagonals on their faces), and one obtains a surface S_2 . When projected to the plane, S_2 is the underlying lozenge-with-diagonals tiling $L(Q)$.

4.5 The space of quadri-tilings

Consider a finite simply connected subgraph G of the equilateral triangular lattice \mathbb{T} , and let ∂G be the cycle of G consisting of its boundary edges. Denote by $\mathcal{Q}(\partial G)$ the set of quadri-tilings of ∂G whose underlying tilings are lozenge tilings of G . As a consequence of theorem 2.9 [39], we obtain

Lemma 4.3 *Let L be a lozenge tiling of G , and let L be the corresponding lozenge-with-diagonals tiling. Then every quadri-tiling of L can be transformed into any other by a finite sequence of the following moves, (in brackets is the number of possible orientations for the graph corresponding to the move):*

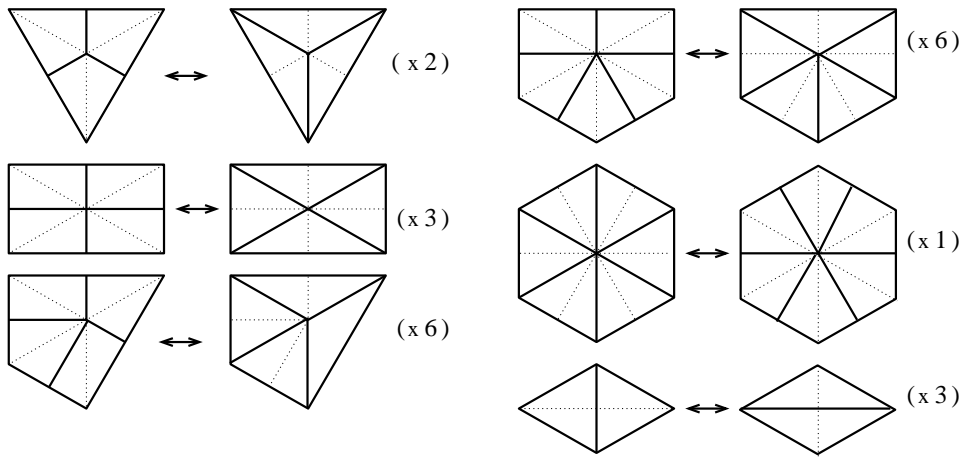


Figure 4.6: Quadri-tile moves.

Proof:

Denote by L^* the dual graph of L . Every edge of L^* belongs to at least one perfect matching, so that by theorem 2.9 [39], one can transform any matching of L^* into

any other by a finite sequence of inner face twists (see subsection 2.2.3). Using the bijection between dimer configurations and 2-tilings, the twisting (up or down) of a face of a perfect matching of the graph L^* can be represented on the graph L , we then speak of the dual representation of a face twist. The moves represented in figure 4.6 are exactly the duals of the face twists that occur in L^* . \square

Up to isometry, let us refer to the moves pictured in figure 4.6 as **first, second, ..., sixth quadri-tile move**, going from left to right and from top to bottom.

In [12], Elkies, Kuperberg, Larsen and Propp proved the next lemma in the case of dominos, the same proof can be applied to the case of lozenges. The next lemma can also be seen as a consequence of Propp's theorem 2.9 [39] (which came one year later, but is more general).

Lemma 4.4 *Every lozenge tiling of the graph G can be transformed into any other by a finite sequence of **lozenge moves**:*

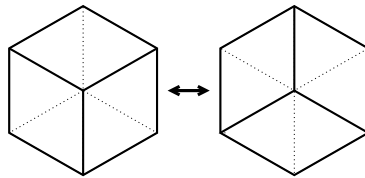


Figure 4.7: Lozenge moves.

Define the first lozenge tiling of figure 4.7 to be the **full cube**, and the second to be the **empty cube**.

Note that if L is any lozenge tiling of G , then L is quadri-tilable with quadri-tiles obtained by cutting in two every lozenge along one of its diagonals. Moreover, when one performs a lozenge move on such a quadri-tiling, one still obtains a quadri-tiling of $\mathcal{Q}(\partial G)$. Let us call **elementary moves** the quadri-tile moves and the lozenge moves performed on quadri-tilings as described above. Then we have:

Lemma 4.5 *Every quadri-tiling of $\mathcal{Q}(\partial G)$ can be transformed into any other by a finite sequence of elementary moves.*

Proof:

This results from lemmas 4.3, 4.4, and the above observation. \square

Chapter 5

Combinatorics of the triangular quadri-tile and isoradial dimer models

The first natural step in the study of a dimer model on a graph G is to understand its combinatorics. This amounts to computing the partition function - the weighted sum of dimer configurations of the graph G^* - introduced in subsection 2.1.2. Let us recall that dimer configurations represent diatomic molecules adsorbed on the surface of a crystal. This motivates the study of dimer models on infinite graphs. The partition function is then infinite, and the question is to understand its rate of growth. The classical way to approach this problem is to take an exhaustion $\{G_n\}$ by finite graphs of the infinite graph G , and to take a limit of the partition functions of the graphs G_n , normalizing them by an appropriate factor. In the case of the dimer model, this limit is highly dependent on the choice of the exhaustion: boundary effects are very important, and are at the heart of the phase transition phenomenon [7], [29].

The goal of this chapter is to understand the combinatorics of the triangular quadri-tile dimer model, in the case where the critical weight function is associated to quadri-tiles. Combinatorics of this model are complicated by the fact that quadri-tilings do not correspond to dimer configurations of a fixed graph. A natural quantity to introduce is the *total partition function*: fixing a finite simply connected subgraph G of the equilateral triangular lattice \mathbb{T} , it is defined to be the weighted sum of quadri-tilings whose underlying tiling is a lozenge tiling of G . The main result of this chapter is theorem 5.1 of section 5.1: it is an explicit formula for the growth rate of the total partition function, in the case of a specific exhaustion. It is proved in section 5.5. The proof is a combination of propositions 5.2, 5.4, 5.8 of sections 5.2, 5.3, 5.4. Each of these results is stronger than what is actually needed in the proof of theorem 5.1, and has an interest of its own.

Suppose there is a weight function ν associated to quadri-tiles of the triangular quadri-

tile dimer model. Referring to subsection 4.3.1, this amounts to assigning weights a, b, c to quadri-tiles of type I, II, III and IV respectively.

Consider a finite simply connected subgraph G of \mathbb{T} . Proposition 5.2 states that, when the weights a, b, c satisfy a simple condition, the quadri-tile partition function is the same for all lozenge-with-diagonals tilings of G . As a consequence, the total partition function is the product of the quadri-tile partition function, and of the lozenge partition function.

In section 5.3, we consider two exhaustions $\{L_n\}$ and $\{\bar{L}_n\}$ by lozenge-with-diagonals tilings, the first one by planar graphs, the second by toroidal graphs. Proposition 5.4 states that when the weights a, b, c satisfy another simple condition, the quadri-tile partition functions of these two exhaustions have the same growth rate.

In section 5.4, we consider an infinite Λ -periodic isoradial graph G (for a 2-dimensional lattice Λ), with critical weights on the edges of G^* . A natural exhaustion of G by toroidal graphs is $\{\bar{G}_n\}$, where $\bar{G}_n = G/n\Lambda$. Using a result of [26], proposition 5.8 gives an explicit formula for the growth rate of the partition function of this exhaustion.

5.1 Growth rate of the total partition function in the case of critical weights

5.1.1 Definition of the total partition function

Let us define the *total partition function* for the triangular quadri-tile dimer model. Recall that dual edges corresponding to quadri-tiles of this model are classified in four types (see subsection 4.3.2). Let us assign weight a to edges of type I, b to those of type II, c to those of type III and IV; this defines a weight function on quadri-tiles which we denote by ν .

Consider the equilateral triangular lattice \mathbb{T} , let G be a finite simply connected subgraph of \mathbb{T} , and let ∂G be the cycle consisting of its boundary edges. Recall that $\mathcal{Q}(\partial G)$ denotes the set of quadri-tilings of ∂G whose underlying tilings are lozenge tilings of G (see section 4.5).

Define the **total partition function** of ∂G to be the weighted sum of quadri-tilings of $\mathcal{Q}(\partial G)$, that is

$$Z(\partial G, \nu) = \sum_{Q \in \mathcal{Q}(\partial G)} \nu(M_Q),$$

where M_Q is defined as follows: Q is a 2-tiling of its underlying lozenge-with-diagonals tiling $L(Q)$, and M_Q is the perfect matching of $L(Q)^*$ corresponding to Q .

5.1.2 Statement of result

Consider the following exhaustion of \mathbb{T} . Let G_1 be the hexagon made of six adjacent equilateral triangles, and denote by x_1, \dots, x_6 its boundary vertices in cclw (counter-

clockwise) order, as in figure 5.1. Let e_1 be the vector $x_3 - x_1$, and e_2 the vector $x_5 - x_1$. Define G_n to be the graph made of the $ie_1 + je_2$ translates of G_1 for $i, j = 1, \dots, n$.

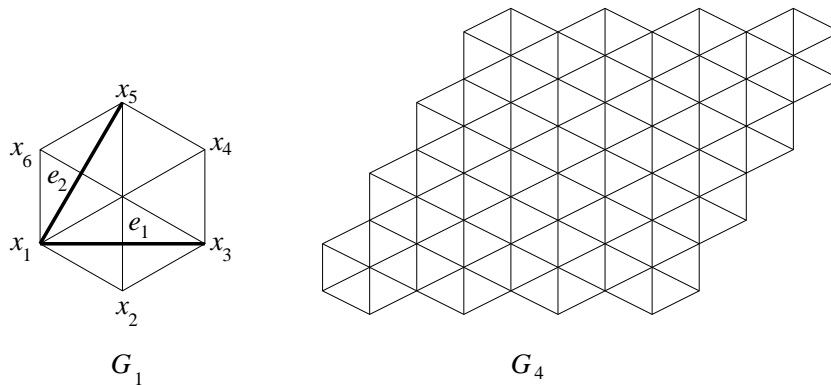


Figure 5.1: The exhaustion $\{G_n\}$ of \mathbb{T} .

Theorem 5.1 *Suppose that ν is the critical weight function on quadri-tiles, then*

$$\lim_{n \rightarrow \infty} \frac{1}{12n^2} \log Z(\partial G_n, \nu) = \frac{1}{12} \log 3 + \frac{1}{4} \log 2 + \frac{1}{2\pi} L\left(\frac{\pi}{6}\right) + \frac{5}{4\pi} L\left(\frac{\pi}{3}\right),$$

where L is the Lobachevsky function, $L(x) = -\int_0^x \log 2 \sin t \, dt$.

Recall that the critical weight function for the triangular quadri-tile dimer model is computed in subsection 4.3.2, it corresponds to weights $a = 1$, $b = \sqrt{3}$, $c = 2$. We postpone the proof of theorem 5.1 to section 5.5.

5.2 Property of the total partition function

The setting is that of subsection 5.1.1. That is, we consider a weight function ν on dual edges corresponding to quadri-tiles of the triangular quadri-tile dimer model, i.e. we consider weights a, b, c on edges of type I, II, III and IV respectively.

Let G be a finite simply connected subgraph of \mathbb{T} . Recall that $Z(G^*, 1)$ is the number of lozenge tilings of G ; recall also that if \mathbb{L} is a lozenge tiling of G , and if L is its corresponding lozenge-with-diagonals tiling, then $Z(L^*, \nu)$ is the quadri-tile partition function of the graph L^* . The total partition function satisfies the following.

Proposition 5.2 *Assume that the weights a, b, c , satisfy the condition*

$$0 < a < c, \quad b = \sqrt{a \left(\frac{a^2 + c^2 - ac}{c - a} \right)}. \quad (5.1)$$

Then, $Z(L^*, \nu)$ is independent of the lozenge tiling L of G , and the total partition function of ∂G satisfies

$$Z(\partial G, \nu) = Z(L^*, \nu)Z(G^*, 1).$$

Proof:

Let us prove the second part of the statement assuming the first one. By definition of the total partition function, and of the set $\mathcal{Q}(\partial G)$, we have

$$\begin{aligned} Z(\partial G, \nu) &= \sum_{Q \in \mathcal{Q}(\partial G)} \nu(M_Q), \\ &= \sum_{\text{lozenge tilings } L \text{ of } G} Z(L^*, \nu), \\ &= Z(L^*, \nu)Z(G^*, 1), \text{ (using the first part of the statement).} \end{aligned}$$

Let us prove that $Z(L^*, \nu)$ is independent of the lozenge tiling L of G . By lemma 4.4 we can reach any lozenge tiling of G from any other by a finite sequence of lozenge moves (see section 4.5), hence it suffices to consider two lozenge tilings L_1, L_2 of G which differ by a lozenge move, and prove that

$$Z(L_1^*, \nu) = Z(L_2^*, \nu). \tag{5.2}$$

Let us assume that the hexagon of the lozenge move lies in the interior of G . The argument is similar when it is adjacent to the boundary of G . Denote by E_1, E_2 the lozenge tilings called the full and the empty cube respectively (see section 4.5 and figure 4.7). For $i = 1, 2$ let E_i be the lozenge-with-diagonals tiling corresponding to E_i , and let E_i^* be the dual graph of E_i , which contains the dual edges of the boundary edges of E_i . Note that the boundary edges of E_1 and E_2 are the same, so that their dual edges are also the same, let us denote them by $\{e_1, \dots, e_6\}$ in cw (clockwise) order (see figure 5.2).

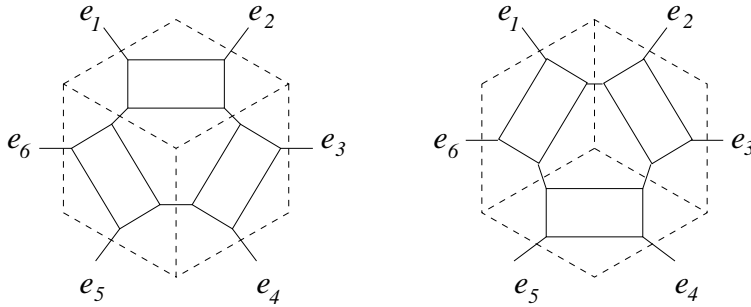


Figure 5.2: Left: E_1 (dotted line), and E_1^* (full line). Right: E_2 (dotted line), and E_2^* (full line).

Let \mathfrak{E} be a subset of the edges $\{e_1, \dots, e_6\}$ (which might be the empty set). For $i = 1, 2$ define $Z(L_i^*, \mathfrak{E}, \nu)$ to be the weighted sum of dimer configurations of L_i^* , which contain the edges of \mathfrak{E} , but not those of $\{e_1, \dots, e_6\} \setminus \mathfrak{E}$, then

$$Z(L_i^*, \nu) = \sum_{\text{subsets } \mathfrak{E} \text{ of } \{e_1, \dots, e_6\}} Z(L_i^*, \mathfrak{E}, \nu).$$

Let us prove that condition (5.1) is obtained by imposing, for every subset \mathfrak{E} , the following:

$$Z(L_1^*, \mathfrak{E}, \nu) = Z(L_2^*, \mathfrak{E}, \nu). \quad (5.3)$$

Equation (5.2) is then a consequence of (5.3).

For $i = 1, 2$ consider the graph $(L_i^* \setminus E_i^*) \cup \mathfrak{E}$. Since L_1^* and L_2^* only differ by one lozenge move, these graphs are the same. Note that the edges $\{e_1, \dots, e_6\}$ are of type III or IV, so that in E_1^* and E_2^* they have weight equal to c . This implies that the above graphs have the same edge-weights. Define $C_{\mathfrak{E}}$ to be the partition function of this graph. For $i = 1, 2$ consider the graph \widetilde{E}_i^* which is the graph $E_i^* \setminus \{e_1, \dots, e_k\}$, from which we have removed the edges adjacent to vertices of \mathfrak{E} (see figures 5.3 and 5.4 for examples of such graphs). Let $Z(\widetilde{E}_i^*, \mathfrak{E}, \nu)$ be the partition function of the graph \widetilde{E}_i^* . Then we have

$$Z(L_i^*, \mathfrak{E}, \nu) = Z(\widetilde{E}_i^*, \mathfrak{E}, \nu) C_{\mathfrak{E}}.$$

In order to obtain condition (5.3), let us find weights a, b, c such that, for every subset \mathfrak{E} of $\{e_1, \dots, e_6\}$, we have

$$Z(\widetilde{E}_1^*, \mathfrak{E}, \nu) = Z(\widetilde{E}_2^*, \mathfrak{E}, \nu). \quad (5.4)$$

Case 1: $\mathfrak{E} = \emptyset$, or $\mathfrak{E} = \{e_1, \dots, e_6\}$.

The graphs \widetilde{E}_1^* and \widetilde{E}_2^* are isomorphic, so that condition (5.4) is verified $\forall a, b, c$.

Case 2: \mathfrak{E} consists of two edges.

Let us first assume that \mathfrak{E} consists of the edges e_1 and e_2 , then (see figure 5.3):

$$\begin{aligned} Z(\widetilde{E}_1^*, \mathfrak{E}, \nu) &= a(a^2 + b^2)^2 + c^3 a^2, \\ Z(\widetilde{E}_2^*, \mathfrak{E}, \nu) &= cb^2(a^2 + b^2). \end{aligned}$$

Condition (5.4) is then equivalent to

$$a(a^2 + b^2)^2 + c^3 a^2 = cb^2(a^2 + b^2). \quad (5.5)$$

When \mathfrak{E} consists of any two adjacent edges, we again obtain equation (5.5). When \mathfrak{E} consists of edges which are opposite, the graphs \widetilde{E}_1^* and \widetilde{E}_2^* are isomorphic, so that equation (5.4) is verified $\forall a, b, c$. In all other cases there are no dimer configurations of the graphs \widetilde{E}_1^* and \widetilde{E}_2^* .



Figure 5.3: Left: \tilde{E}_1^* . Right: \tilde{E}_2^* .

Case 3: \mathfrak{E} consists of four edges.

When \mathfrak{E} consists of the edges e_1, e_2, e_3, e_4 , then (see figure 5.4):

$$\begin{aligned} Z(\tilde{E}_1^*, \mathfrak{E}, \nu) &= a^2(a^2 + b^2) + c^3a, \\ Z(\tilde{E}_2^*, \mathfrak{E}, \nu) &= b^2c^2. \end{aligned}$$

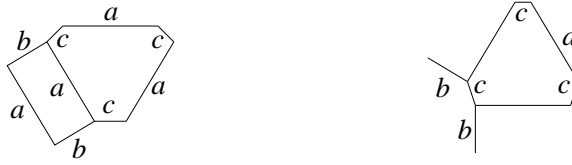


Figure 5.4: Left: \tilde{E}_1^* . Right: \tilde{E}_2^* .

Condition (5.4) is then equivalent to

$$a^2(a^2 + b^2) + c^3a = b^2c^2. \quad (5.6)$$

When \mathfrak{E} consists of any four adjacent edges, we again obtain equation (5.6). In all other cases there are no dimer configurations of the graphs \tilde{E}_1^* and \tilde{E}_2^* .

Case 4: \mathfrak{E} consists of one, three or five edges.

There are no dimer configurations of the graphs \tilde{E}_1^* and \tilde{E}_2^* , since both graphs have an odd number of vertices.

Condition (5.4) is then equivalent to solving the system

$$\begin{aligned} a(a^2 + b^2)^2 + c^3a^2 &= cb^2(a^2 + b^2), \\ a^2(a^2 + b^2) + c^3a &= b^2c^2. \end{aligned}$$

This system can be rewritten as

$$b^4(a - c) + b^2(2a^3 - a^2c) + a^2(c^3 + a^3) = 0, \quad (5.7)$$

$$b^2(a^2 - c^2) + a(c^3 + a^3) = 0. \quad (5.8)$$

Weight functions are assumed to be positive, so that we are looking for solutions $a, b, c > 0$ of (5.7) and (5.8).

Solutions of (5.7)

- Suppose $a = c$. Then (5.7) becomes $a^3(b^2 + 2a^2) = 0$, and has no solution.
- Suppose $a \neq c$. Let us write $B = b^2$, and solve (5.7) as a quadratic equation in B ; the discriminant is $\Delta = (ac)^2(a - 2c)^2$.

- Suppose $a > 2c$. Then $\sqrt{\Delta} = ac(a - 2c)$, and the two solutions are

$$B_1^+ = \frac{a(-a^2 + ac - c^2)}{a - c}, \text{ and } B_1^- = -a(c + a).$$

Let us look at the signs of B_1^+ and B_1^- . The quantity $-a^2 + ac - c^2 = -(a - c)^2 - ac < 0$, hence the sign of B_1^+ is the sign of $c - a$; since $a - 2c > 0$, we have $a - c > 0$, so that $B_1^+ < 0$. Moreover $B_1^- < 0$, which implies that B_1^+ and B_1^- are not solutions for $B = b^2$.

- Suppose $2c > a$. Then $\sqrt{\Delta} = ac(2c - a)$, and the two solutions are

$$B_2^+ = B_1^-, \text{ and } B_2^- = B_1^+.$$

$B_2^+ < 0$ so that it is not a solution for B . The sign of B_2^- is the sign of $c - a$, so that B_2^- is a solution for B when $c > a$.

Solutions of (5.8)

Since $a + c > 0$, (5.8) can be factored as $b^2(a - c) + a(a^2 - ac + c^2) = 0$. When $a = c$ the system has no solution. When $a \neq c$, we obtain

$$b^2 = \frac{a(-a^2 + ac - c^2)}{a - c}.$$

Hence, both equations have the same solutions $a, b, c > 0$, which are exactly those a, b, c satisfying condition (5.1). \square

5.3 Partition function for planar and toroidal graphs

In subsection 5.3.1 we consider two exhaustions of the equilateral triangular lattice \mathbb{T} , one by planar graphs and one by toroidal graphs. Using results of [7], we deduce that the normalized log of the lozenge partition function of these two exhaustions converge to the same value. In subsection 5.3.2, we consider a lozenge-with-diagonals tiling of the plane, and prove a similar result for the normalized log of the quadri-tile partition function. The proof is nevertheless of a different nature, since it uses combinatorial tools.

5.3.1 Triangular lattice case

Consider the equilateral triangular lattice \mathbb{T} . Suppose that all edges of the dual graph \mathbb{T}^* have weight 1. The exhaustion $\{G_n\}$ of \mathbb{T} by planar graphs is that of subsection 5.1.2: G_1 is the hexagon made of six adjacent equilateral triangles of \mathbb{T} , and G_n is the graph made of the $ie_1 + je_2$ translates of G_1 , for every $i, j = 1, \dots, n$ (see figure 5.1). Let us define the exhaustion $\{\bar{G}_n\}$ of \mathbb{T} by toroidal graphs. Define Λ to be the two-dimensional lattice whose basis vectors are e_1 and e_2 , then $\bar{G}_n = \mathbb{T}/n\Lambda$. As a consequence of results of [7], we have

Lemma 5.3

$$\lim_{n \rightarrow \infty} \frac{1}{n^2} \log Z(G_n^*, 1) = \lim_{n \rightarrow \infty} \frac{1}{n^2} \log Z(\bar{G}_n^*, 1). \quad (5.9)$$

Proof:

Edges of \bar{G}_n^* are in three possible orientations, $0^\circ, 60^\circ, 120^\circ$. Let us denote by f_i an edge whose orientation is i° . Because of the symmetries of the graph \bar{G}_n^* , and because all edges have weight 1, the Boltzmann probability $\mu^n(f_i)$ of the edge f_i occurring in a dimer configuration of the graph \bar{G}_n^* is $1/3$. Applying the result of [7] concerning domino tilings to lozenge tilings yields the following. Denote by $\varphi(\bar{G}_n^*)$ the quantity $\frac{1}{n^2} \log Z(\bar{G}_n^*, 1)$, then $\varphi(\bar{G}_n^*)$ converges to the same value as $\varphi(G_n'^*)$, where $\{G_n'\}$ is an exhaustion of \mathbb{T} by planar graphs whose boundary height function approximates a plane of slope $(\lim_{n \rightarrow \infty} \mu^n(e_{120}) - \lim_{n \rightarrow \infty} \mu^n(e_{60}), \lim_{n \rightarrow \infty} \mu^n(e_0) - \lim_{n \rightarrow \infty} \mu^n(e_{120}))$. In our case, this quantity is equal to $(0, 0)$. Moreover, the exhaustion $\{G_n\}$ consists of planar graphs whose boundary height function approximates a plane of slope $(0, 0)$; indeed the lozenge height function is equal to 0 or 1 along the boundary (when normalizing it by a factor 3 to be in the setting of [7]), so that we obtain (5.9). \square

5.3.2 Lozenge-with-diagonals tiling case

Consider the lozenge tiling L_1 of G_1 called the full cube (see figure 4.7, and figure 5.5). Define L to be the lozenge tiling of the plane which consists of copies of L_1 , and let L be the corresponding lozenge-with-diagonals tiling of the plane. Assume there is a weight function ν on the edges of the dual graph L^* , i.e. consider weights a, b, c on edges of type I, II, III and IV respectively. Let L_n be the graph consisting of the $ie_1 + je_2$ translates of L_1 , for $i, j = 1, \dots, n$ (refer to subsection 5.1.2 for the definition of e_1 and e_2), then $\{L_n\}$ defines an exhaustion of L by planar graphs, see figure 5.5. Let Λ be the two-dimensional lattice whose basis vectors are e_1 and e_2 , then $\{\bar{L}_n\}$, with $\bar{L}_n = L/n\Lambda$, defines an exhaustion of L by toroidal graphs.

Proposition 5.4 *Assume that the weights a, b, c satisfy the condition $a^2 + b^2 = c^2$, then*

$$\lim_{n \rightarrow \infty} \frac{1}{n^2} \log Z(L_n^*, \nu) = \lim_{n \rightarrow \infty} \frac{1}{n^2} \log Z(\bar{L}_n^*, \nu).$$

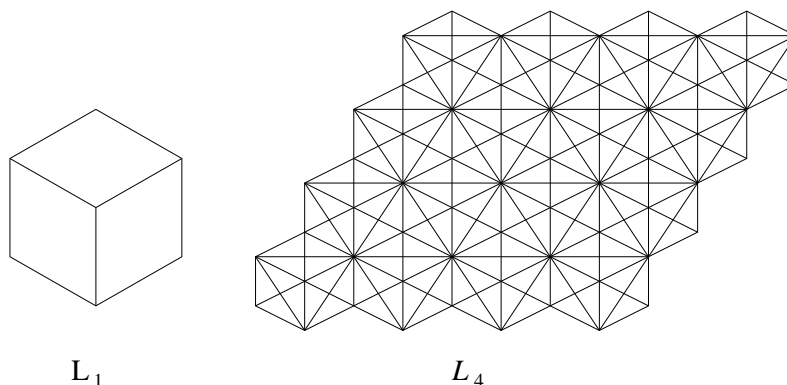


Figure 5.5: The exhaustion $\{L_n\}$ of L .

Proof:

In order to prove proposition 5.4, we need lemmas 5.5 and 5.6 below. Here is the setting for lemma 5.5. Refer to figure 5.6 for an example of the following construction. Fix n , and consider the finite simply connected subgraph G_n of \mathbb{T} of subsection 5.1.2. Let L be any lozenge tiling of G_n , and L be its corresponding lozenge-with-diagonals tiling. The graph L can be winded on the torus, this yields a toroidal graph \bar{L} . Note that its dual graph \bar{L}^* is a bipartite graph on the torus. Denote by L^* the dual graph L^* which contains the dual edges of the boundary edges of L .

Consider a quadri-tiling Q of \bar{L} , then Q corresponds to a perfect matching M which can be unwinded on the graph L^* . This allows us to compute the first height function $h^{\bar{L}}$ on vertices of the quadri-tiling Q unwinded in the plane: fix v_0 and set $h^{\bar{L}}(v_0) = 0$; take the reference flow ω_0 to be a white-to-black flow which flows by $1/3$ along every edge of L^* ; the height function $h^{\bar{L}}$ is then computed in the usual way (refer to subsections 2.2.1 and 4.4.1 for more details).

Note that the height function $h^{\bar{L}}$ is not well defined on vertices of Q winded on \bar{L} : identified vertices may have different heights. Note also, that the height function $h^{\bar{L}}$ on the boundary of Q is periodic, so that one defines the **unnormalized slope** $(\Delta h, \Delta v)$ of a quadri-tiling Q of \bar{L} , by

$$\begin{aligned} h^{\bar{L}}(v_0 + ne_1) - h^{\bar{L}}(v_0) &= \Delta h, \\ h^{\bar{L}}(v_0 + ne_2) - h^{\bar{L}}(v_0) &= \Delta v, \end{aligned}$$

where e_1 and e_2 have been defined in subsection 5.1.2, and are represented in figure 5.1. To simplify the terminology, we shall call $(\Delta h, \Delta v)$ the **slope** of Q (although the slope is usually defined as $\frac{1}{n}(\Delta h, \Delta v)$); Δh (resp. Δv) is also known as the **horizontal** (resp. **vertical**) **height change** of Q .

Since Δh is independent of the path from v_0 to $v_0 + ne_1$, we choose to compute it along the **horizontal path**, which we define to be the boundary edge path of L from v_0 to

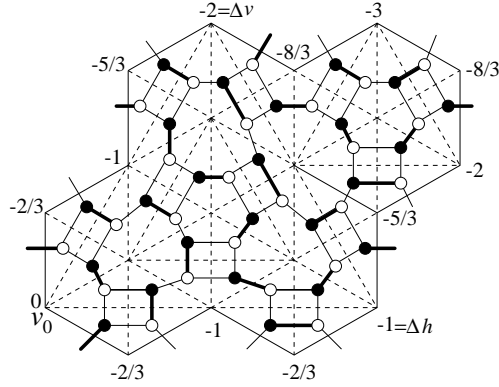


Figure 5.6: Example: $n = 2$, L =dotted lines. Perfect matching of \bar{L}^* unwinded on L^* , and corresponding height function $h^{\bar{L}}$ on the boundary of L .

$v_0 + ne_1$. The **vertical path**, along which we measure the vertical height change, is defined in a symmetric way. Note that both Δh and Δv are integers between $-n$ and n .

Using the bijection between 2-tilings and dimer configurations, we also speak of the slope of a perfect matching M of \bar{L}^* , meaning the slope of the 2-tiling corresponding to M . Let us denote by $(\Delta h(M), \Delta v(M))$ the slope of M .

Consider a weight function ν on the edges of \bar{L}^* , (recall that ν is defined by weights a, b, c on edges of type I, II, III and IV). Define $Z(\bar{L}^*, \nu, (\Delta h, \Delta v))$ to be the weighted sum of dimer configurations of the graph \bar{L}^* , which have slope $(\Delta h, \Delta v)$.

Lemma 5.5 *Assume that the weights a, b, c satisfy the condition $a^2 + b^2 = c^2$, then*

$$\forall (\Delta h, \Delta v), Z(\bar{L}^*, \nu, (\Delta h, \Delta v)) \leq Z(\bar{L}^*, \nu, (0, 0)).$$

Proof:

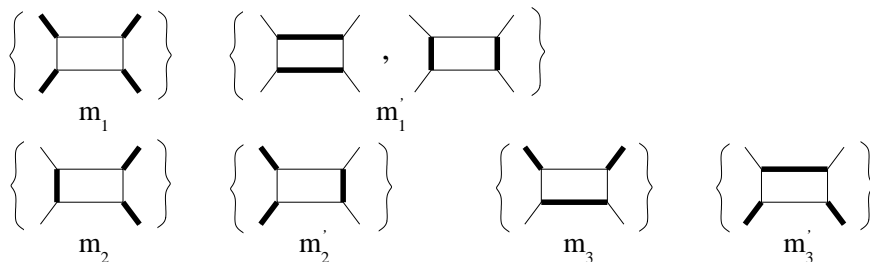
Lemma 5.5 is proved using two intermediate steps.

1. $\forall (\Delta h, \Delta v), Z(\bar{L}^*, \nu, (\Delta h, \Delta v)) = Z(\bar{L}^*, \nu, (-\Delta h, -\Delta v))$.

We say that two perfect matchings of a subgraph of \bar{L}^* are **equivalent**, if they differ by a sequence of dual moves of the sixth quadri-tile move (see section 4.5 for definition). This defines an equivalence relation on perfect matchings of this subgraph.

Note that all perfect matchings of an equivalence class of the graph \bar{L}^* have the same slope, indeed all dual edges crossing the horizontal and vertical paths of L are of type III and IV, and the sixth quadri-tile move only concerns edges of type I and II. Hence the notion of slope of an equivalence class of \bar{L}^* is well defined.

Let ℓ be a lozenge-with-diagonals of \bar{L} , and ℓ^* be its dual graph (with the dual edges of the boundary edges of ℓ). For $i = 1, \dots, 3$ refer to the perfect matchings m_i and m'_i


 Figure 5.7: Complementary perfect matchings of ℓ^* .

of ℓ^* as **complementary** (see figure 5.7), and denote by m_i, m'_i the equivalence class of m_i, m'_i .

Consider an equivalence class M of perfect matchings of \bar{L}^* , and let ℓ be a lozenge-with-diagonals of \bar{L} . Replace the equivalence class M restricted to ℓ^* by its complementary class. Repeating this procedure for every lozenge-with-diagonals ℓ yields an equivalence class of perfect matchings of \bar{L}^* , which we denote by M' .

Let us prove that if a class of perfect matchings M has slope $(\Delta h(M), \Delta v(M))$, then its complementary class M' has slope $(-\Delta h(M), -\Delta v(M))$. We only give the argument for the horizontal height change since the same argument holds for the vertical height change. We start by making two remarks about the horizontal path: it consists of an even number of edges, and the right triangles of L adjacent to its edges are alternately black and white, so that the orientation of its edges alternates. Consider two perfect matchings M of M , and M' of M' , unwinded on L^* . By construction of the complementary matching, the matchings M and M' are disjoint (with respect to edges), moreover the superposition of M and M' contains all dual edges of the horizontal path. Using the above remark, this implies $\Delta h(M) + \Delta h(M') = 0$, hence $\Delta h(M) = -\Delta h(M')$. From this we deduce that there is a bijection between equivalence classes with slope $(\Delta h, \Delta v)$, and those with slope $(-\Delta h, -\Delta v)$.

Let us call **weight** of an equivalence class the weighted sum of its perfect matchings. By the above construction, in order to prove $Z(\bar{L}^*, \nu, (\Delta h, \Delta v)) = Z(\bar{L}^*, \nu, (-\Delta h, -\Delta v))$, it suffices to show that the weight of an equivalence class M , equals that of its complementary class M' . Let ℓ be a lozenge-with-diagonals of \bar{L} . Then the weight of M is equal to the product over all $\ell \in \bar{L}$ of the weights of the equivalence classes of M restricted to ℓ^* , where the c -weight of the edges of type III and IV is replaced by \sqrt{c} (because each of these edges is counted twice). From this we deduce that, when $a^2 + b^2 = c^2$, the weight of M equals the weight of M' . Indeed, when $a^2 + b^2 = c^2$, for every $i = 1, \dots, 3$, the weight of the equivalence class m_i equals the weight of the class m'_i (when the c weights are replaced by \sqrt{c}).

Denote by $\mathcal{M}(\Delta h, \Delta v)$ the set of dimer configurations of the graph \bar{L}^* , which have slope $(\Delta h, \Delta v)$.

2. Definition of an injection $i : \mathcal{M}(\Delta h, \Delta v) \times \mathcal{M}(-\Delta h, -\Delta v) \rightarrow \mathcal{M}(0, 0) \times \mathcal{M}(0, 0)$.

Consider two perfect matchings M_1 of $\mathcal{M}(\Delta h, \Delta v)$, and M_2 of $\mathcal{M}(-\Delta h, -\Delta v)$. Then the superposition $M_1 \cup M_2$ of M_1 and M_2 consists of doubled edges and disjoint cycles. Our first goal is to compute the quantity $(2\Delta h, 2\Delta v) = (\Delta h(M_1) - \Delta h(M_2), \Delta v(M_1) - \Delta v(M_2))$ using cycles of $M_1 \cup M_2$.

Remarks

1. Let C be a cycle of $M_1 \cup M_2$, then edges of type III and IV of C belong to the same perfect matching, that is either to M_1 or to M_2 . As a consequence, if C unwinded on L^* crosses the horizontal and/or the vertical path through edges e_1, \dots, e_m , they all belong to the same perfect matching.
2. Consider the cycles of $M_1 \cup M_2$ unwinded on L^* . Orient them from top to bottom if they wind around the torus, or cclw else. Let C be such a cycle, then edges of M_1 and M_2 alternate in C , so that all edges of M_1 are oriented from white to black, or from black to white; the reverse holds for edges of M_2 .

If uv is an edge of the horizontal path and M is a perfect matching of \bar{L}^* , unwinded on L^* , denote by $\Delta h(M)(uv)$ the height change of M along uv . Let C be a cycle of $M_1 \cup M_2$, define the **contribution of C to $2\Delta h$** to be the sum of the quantities $\Delta h(M_1)(uv) - \Delta h(M_2)(uv)$ over edges uv of the horizontal path which are crossed by the unwinded cycle C . In a similar way we define the **contribution of C to $2\Delta v$** .

Define the oriented winding number of a cycle C to be the triple (s, t, δ) , where s (resp. t) denotes the number of times the cycle winds around the torus vertically (resp. horizontally). When $s = 0$ or $t = 0$, set $\delta = 0$. If $s \neq 0$ and $t \neq 0$, consider the cycle C unwinded on the graph L^* , and consider the part of C which starts from the lower horizontal boundary and exits at the vertical boundary. If it exits at the left boundary, set $\delta = 1$, else if it exits at the right boundary, set $\delta = -1$.

- The contribution to $(2\Delta h, 2\Delta v)$ of a cycle whose oriented winding number is (s, t, δ) is $\pm(s, \delta t)$.

Assume that the oriented winding number of a cycle C is $(0, 0, 0)$, and that C is unwinded on L^* . When travelling along the horizontal path, if one enters the cycle C through an edge uv , one has to exit C through an edge $u'v'$. By remark 1, the dual edges e and e' of uv and $u'v'$ belong to the same perfect matching. By remark 2, this implies that the edges uv and $u'v'$ are oriented in the opposite direction. Hence $\Delta h(M_1)(uv) + \Delta h(M_1)(u'v') = 0$, and $\Delta h(M_2)(uv) + \Delta h(M_2)(u'v') = 0$. The same holds for the vertical height change, and so C contributes $(0, 0)$ to $(2\Delta h, 2\Delta v)$.

Assume that the oriented winding number of C is (s, t, δ) , and that C is unwinded on L^* . Let us assume $s \neq 0$ and $t \neq 0$, if $s = 0$ or $t = 0$, the argument is similar although simpler. When travelling along the horizontal path, one crosses the cycle C , s times through edges $u_1v_1, \dots, u_s v_s$ (more precisely, one crosses C , $s + 2k$ times, but then by the same argument as when C has oriented winding number $(0, 0, 0)$, the $2k$

times contribute $(0, 0)$ to $(2\Delta h, 2\Delta v)$. When travelling along the vertical path, one crosses the cycle C , t times through edges $u'_1v'_1, \dots, u'_tv'_t$. By remark 1, the dual edges e_1, \dots, e_s of u_1v_1, \dots, u_sv_s and the dual edges f_1, \dots, f_t of $u'_1v'_1, \dots, u'_tv'_t$ belong to the same perfect matching, say M_2 . By remark 2, all edges e_i and f_j are oriented from white to black, or from black to white. Let us assume we are in the first case. Then if $\delta = 1$, we obtain

$$\begin{aligned} \sum_{i=1}^s \Delta h(M_1)(u_i v_i) &= s/3, \text{ and } \sum_{i=1}^s \Delta h(M_2)(u_i v_i) = -2s/3, \\ \sum_{j=1}^t \Delta v(M_1)(u'_j v'_j) &= t/3, \text{ and } \sum_{j=1}^t \Delta v(M_2)(u'_j v'_j) = -2t/3. \end{aligned}$$

So that the contribution of the cycle C to $(2\Delta h, 2\Delta v)$ is (s, t) . In a similar way, when $\delta = -1$, we obtain that the contribution of the cycle C to $(2\Delta h, 2\Delta v)$ is $(s, -t)$. We summarize cases $\delta = -1$ and $\delta = 1$ by saying that C contributes $(s, \delta t)$ to $(2\Delta h, 2\Delta v)$. When the edges e_i and f_j go from a black vertex to a white one, C contributes $-(s, \delta t)$ to $(2\Delta h, 2\Delta v)$.

Assume there is a cycle of $M_1 \cup M_2$ whose oriented winding number is $(s, t, \delta) \neq (0, 0, 0)$, then since cycles are disjoint, all cycles of $M_1 \cup M_2$ must have the same oriented winding number. This means that up to a sign, all cycles of $M_1 \cup M_2$ contribute the same quantity to $(2\Delta h, 2\Delta v)$. Moreover, if an edge uv of the horizontal path is crossed by no cycle of $M_1 \cup M_2$, or if it is the dual edge of a doubled edge of $M_1 \cup M_2$, then $\Delta h(M_1)(uv) = \Delta h(M_2)(uv)$, so that in both cases it contributes 0 to $2\Delta h$. The same argument holds for the vertical path. Hence, the only contribution to $(2\Delta h, 2\Delta v)$ comes from cycles of $M_1 \cup M_2$.

To simplify notations, let us suppose Δh and Δv are positive. Then all cycles of $M_1 \cup M_2$ have oriented winding number $(s, t, 1)$, and $(2\Delta h, 2\Delta v) = k(s, t)$ for some positive k . The couple (s, t) is also known as the homology class of a cycle, and since cycles are simple curves, (s, t) has the property that the greatest common divisor between s and t is 1. From this we deduce that k is even. Let us write $(2\Delta h, 2\Delta v) = 2m(s, t)$, where $2m = k$. Then, there are at least $2m$ cycles of $M_1 \cup M_2$ which have oriented winding number $(s, t, 1)$, denote them by C_1, \dots, C_{2m} . Color edges of the matching M_1 red, and edges of the matching M_2 blue. Consider the first m cycles C_1, \dots, C_m and exchange the red and the blue edges of these cycles. In this way, we obtain a red matching M'_1 , and a blue matching M'_2 . Exchanging the color of one of the cycles decreases $\Delta h(M_1)$ by s (resp. $\Delta v(M_1)$ by t), and increases $\Delta h(M_2)$ by s (resp. $\Delta v(M_2)$ by t), hence M'_1 and M'_2 have slope $(0, 0)$. This procedure is reversible, so that the following application is an injection

$$\begin{aligned} i : \mathcal{M}(\Delta h, \Delta v) \times \mathcal{M}(-\Delta h, -\Delta v) &\longrightarrow \mathcal{M}(0, 0) \times \mathcal{M}(0, 0) \\ &\quad (M_1, M_2) \qquad \qquad \qquad \longmapsto \quad (M'_1, M'_2). \end{aligned}$$

3. Proof of lemma 5.5

Using the first step of the proof, we obtain

$$\begin{aligned} Z(\bar{L}^*, \nu, (\Delta h, \Delta v))^2 &= Z(\bar{L}^*, \nu, (\Delta h, \Delta v))Z(\bar{L}^*, \nu, (-\Delta h, -\Delta v)), \\ &= \sum_{M_1 \in \mathcal{M}(\Delta h, \Delta v)} \sum_{M_2 \in \mathcal{M}(-\Delta h, -\Delta v)} \nu(M_1)\nu(M_2). \end{aligned}$$

By construction of the injection i , we have $M_1 \cup M_2 = M'_1 \cup M'_2$, hence

$$\begin{aligned} Z(\bar{L}^*, \nu, (\Delta h, \Delta v))^2 &= \sum_{(M'_1, M'_2)=i(M_1, M_2)} \nu(M'_1)\nu(M'_2), \\ &\leq \sum_{M'_1 \in \mathcal{M}(0,0)} \sum_{M'_2 \in \mathcal{M}(0,0)} \nu(M'_1)\nu(M'_2), \\ &= Z(\bar{L}^*, \nu, (0, 0))^2. \end{aligned}$$

□

Let us place ourselves in the context of proposition 5.4. L_1 is the lozenge tiling of G_1 called the full cube, and L_1 is its corresponding lozenge-with-diagonals tiling. L_n is the tiling consisting of the $ie_1 + je_2$ copies of L_1 , for $i, j = 1, \dots, n$. L is the lozenge-with-diagonals tiling of the plane made of copies of L_1 ; and $\bar{L}_n = L/n\Lambda$, where Λ is the lattice whose basis vectors are e_1 and e_2 .

Lemma 5.6 $\forall n, \forall m \gg n$, we have

1. $\frac{1}{m^2} \log Z(\bar{L}_m^*, \nu) \geq \frac{1}{n^2} \log Z(L_n^*, \nu) + O\left(\frac{n}{m}\right)$.
2. Assume moreover that the weights a, b, c satisfy the condition $a^2 + b^2 = c^2$, then $\frac{1}{m^2} \log Z(L_m^*, \nu) \geq \frac{1}{n^2} \log Z(\bar{L}_n^*, \nu) + O\left(\frac{1}{n}\right)$.

Proof:

Proof of 1.

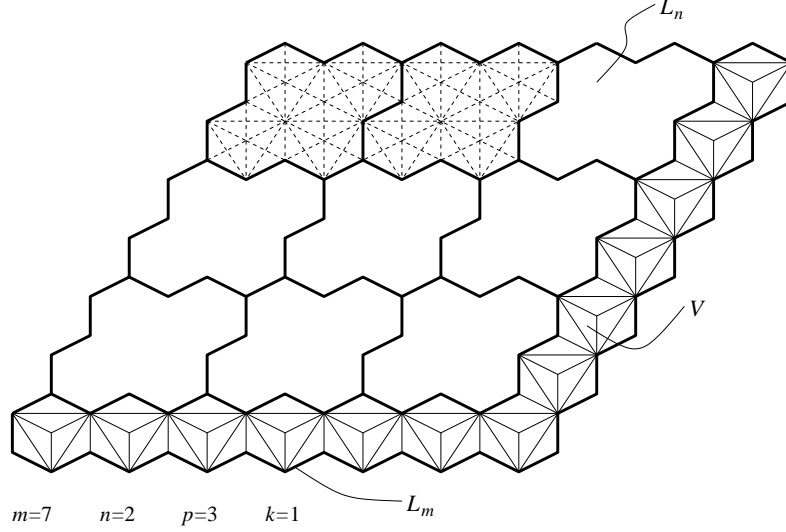
Let $m \gg n$, then m can be written as $pn + k$, for $p \in \mathbb{N}$, and $0 \leq k \leq n - 1$. Let us split the graph L_m as in figure 5.8: L_m consists of p^2 copies of the graph L_n , and of the remaining graph V . Fix a quadri-tiling of V , for example fix a quadri-tiling of L_1 , and take a copy of this quadri-tiling on each copy of L_1 in V , see figure 5.8.

Consider any quadri-tiling on each of the p^2 copies of the graph L_n . In this way, we obtain a quadri-tiling of L_m , which is also a quadri-tiling of \bar{L}_m . Hence,

$$Z(\bar{L}_m^*, \nu) \geq Z(L_n^*, \nu)^{p^2},$$

and we conclude

$$\frac{1}{m^2} \log Z(\bar{L}_m^*, \nu) \geq \frac{p^2}{m^2} \log Z(L_n^*, \nu) = \frac{1}{n^2} \log Z(L_n^*, \nu) + O\left(\frac{n}{m}\right).$$


 Figure 5.8: Splitting of the graph L_m .

Proof of 2.

The toroidal partition function of the graph \bar{L}_n^* can be written as

$$Z(\bar{L}_n^*, \nu) = \sum_{(\Delta h, \Delta v)} Z(\bar{L}_n^*, \nu, (\Delta h, \Delta v)).$$

Using lemma 5.5, this yields

$$Z(\bar{L}_n^*, \nu) \leq |(\Delta h, \Delta v)| Z(\bar{L}_n^*, \nu, (0, 0)), \quad (5.10)$$

where $|(\Delta h, \Delta v)|$ denotes the number of possible slopes for perfect matchings of the graph \bar{L}_n^* . Both Δh and Δv are integers between $-n$ and n , so that $|(\Delta h, \Delta v)| \leq (2n)^2$. Denote by $Z(\bar{L}_n^*, \nu, (0, 0), (c_1, c_2))$ the weighted sum of dimer configurations of the graph \bar{L}_n^* , which have slope $(0, 0)$, and boundary condition c_1 (resp. c_2) for the height function $h^{\bar{L}_n}$ along the horizontal path (resp. vertical path). At each step of the horizontal path, the height function $h^{\bar{L}_n}$ can take 2 possible values, so that $|c_1| \leq 2^{2n}$. The same argument holds for c_2 , hence $|c_1, c_2| \leq 2^{4n}$. Let us denote by (\bar{c}_1, \bar{c}_2) the boundary conditions for $h^{\bar{L}_n}$ which maximize $Z(\bar{L}_n^*, \nu, (0, 0), (c_1, c_2))$. Then,

$$\begin{aligned} Z(\bar{L}_n^*, \nu, (0, 0)) &= \sum_{(c_1, c_2)} Z(\bar{L}_n^*, \nu, (0, 0), (c_1, c_2)), \\ &\leq |c_1, c_2| \max_{(c_1, c_2)} Z(\bar{L}_n^*, \nu, (0, 0), (c_1, c_2)), \\ &\leq 2^{4n} Z(\bar{L}_n^*, \nu, (0, 0), (\bar{c}_1, \bar{c}_2)). \end{aligned} \quad (5.11)$$

Combining equations (5.10) and (5.11) yields,

$$Z(\bar{L}_n^*, \nu) \leq n^2 2^{4n+2} Z(\bar{L}_n^*, \nu, (0, 0), (\bar{c}_1, \bar{c}_2)). \quad (5.12)$$

Let $m \gg n$, then $m - 4n$ can be written as $pn + k$, for $p \in \mathbb{N}$, and $0 \leq k \leq n - 1$. Let us split the graph L_m as in figure 5.9. L_m consists of a graph U made of p^2 copies of the graph L_n , surrounded by a graph V_1 in shape of an annulus, and of a graph V_2 which consists of the right and bottom remaining parts.

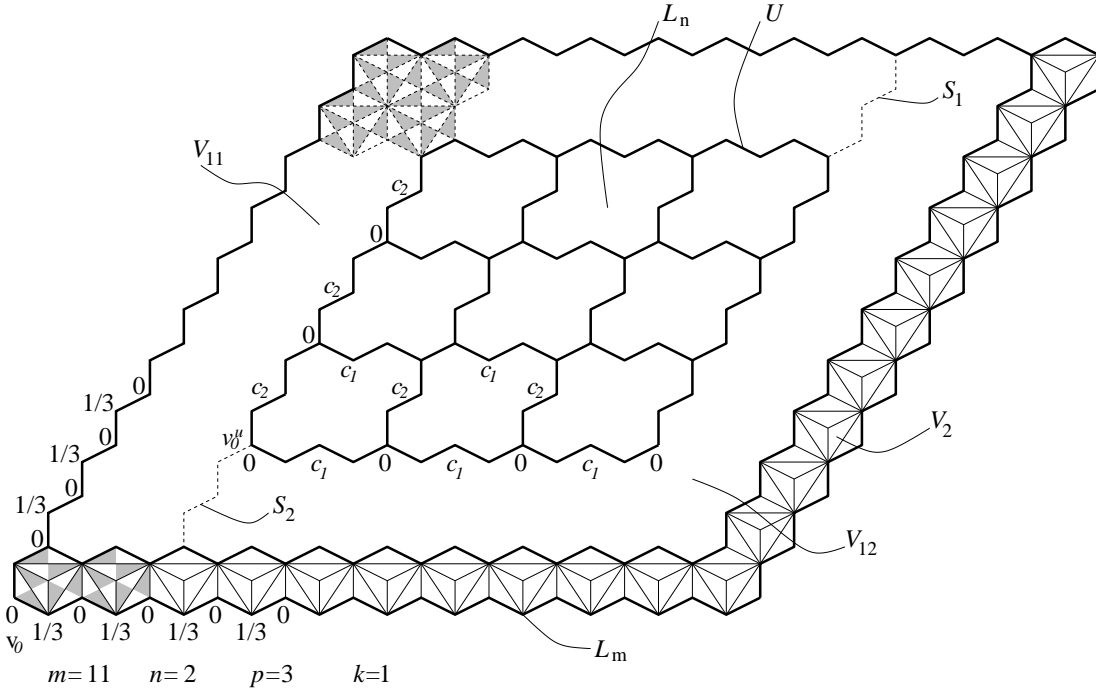


Figure 5.9: Splitting of the graph L_m (the graph V_1 is not at the right scale).

Recall that if G is a finite graph, ∂G denotes the cycle consisting of its boundary edges. Refer to figure 5.9 for notations and for an example. Fix a quadri-tiling of L_1 , and take a copy of this quadri-tiling on each copy of L_1 in V_2 . Consider the vertex v_0 as in figure 5.9, fix $h^{\bar{L}_m}(v_0) = 0$, and compute $h^{\bar{L}_m}$ along ∂V_2 . Then ∂V_2 has planar boundary conditions for $h^{\bar{L}_m}$, that is each edge of ∂V_2 actually bounds a quadri-tile. As a consequence ∂L_m has planar boundary conditions for $h^{\bar{L}_m}$ along its right and bottom part. Let us impose planar boundary conditions along the left and top part of ∂L_m . Since black and white faces of L_m alternate along ∂L_m , $h^{\bar{L}_m}$ is equal to $0, 1/3, -1/3$ along ∂L_m , depending on the choice of bipartite coloring for the faces of L_m .

Let v_0^U be as in figure 5.9, and fix $h^{\bar{L}_m}(v_0^U) = 0$. Consider the boundary condition (\bar{c}_1, \bar{c}_2) on each of the p^2 copies of the graph L_n . This yields a boundary condition for $h^{\bar{L}_m}$ on ∂U , and so a boundary condition on ∂V_1 .

Our goal is now to prove that V_1 with the above boundary condition for $h^{\bar{L}_m}$ is 2-tilable. The proof uses the extension of Thurston's tilability necessary and sufficient condition (see subsection 2.2.2). Let us split V_1 in two as in figure 5.9, in doing so we obtain two simply connected regions V_{11} and V_{12} . Denote by S_1 and S_2 the two paths which have been added in order to obtain V_{11} and V_{12} . Let us fix the height function along S_1 and S_2 by imposing that edges of these two paths bound quadri-tiles. Since black and white vertices alternate along S_1 and S_2 , the height function $h^{\bar{L}_m}$ equals to $1/3, 0$ or $-1/3, 0$ along S_1 and S_2 . Let us prove that V_{11} is 2-tilable, a similar argument holds for V_{12} . By Thurston's condition we need to check that $\forall u, v \in \partial V_{11}$, we have

$$h^{\bar{L}_m}(v) - h^{\bar{L}_m}(u) \leq d(u, v), \quad (5.13)$$

where d denotes the weighted distance, (refer to subsection 2.2.2 for definitions).

- If $u, v \in \partial L_m \cap \partial V_{11}$, or $u, v \in \partial U \cap \partial V_{11}$, then condition (5.13) holds because the graphs L_m and U are 2-tilable.
- If $u \neq v \in S_1$ or S_2 , then $h^{\bar{L}_m}(v) - h^{\bar{L}_m}(u) \leq 1/3 \leq d(u, v)$, so that condition (5.13) holds.
- If $u \in \partial L_m \cap \partial V_{11}$, and $v \in \partial U \cap \partial V_{11}$. Consider a positively oriented path γ from u to v whose weighted length is the distance $d(u, v)$. Then, by construction of the splitting of L_m , γ crosses at least $2n$ copies of the graph L_1 . Moreover, the minimal distance of a path crossing a graph L_1 is $1/3$, hence we deduce,

$$d(u, v) \geq \frac{1}{3}2n.$$

Each copy of the graph L_n with boundary conditions (\bar{c}_1, \bar{c}_2) is 2-tilable, so that its boundary height function satisfies Thurston's condition. The vertex v belongs to one of the graphs L_n . Denote by u' the corner of L_n which is on the same boundary path as v and lies closest to v , then $d(u', v) \leq n/2$. By definition of the boundary condition (\bar{c}_1, \bar{c}_2) , $h^{\bar{L}_m}(u') = 0$, applying Thurston's condition to u', v yields $h^{\bar{L}_m}(v) \leq n/2$. Since $u \in \partial L_m \cap \partial V_{11}$, $h^{\bar{L}_m}(u) \geq -1/3$, we obtain for $n \geq 2$,

$$h^{\bar{L}_m}(v) - h^{\bar{L}_m}(u) \leq \frac{n}{2} + \frac{1}{3} \leq \frac{2n}{3} \leq d(u, v).$$

- Suppose $u \in S_2$, and v belongs to the top part of $\partial U \cap \partial V_{11}$. Denote by v' the right most vertex of $\partial U \cap \partial V_{11}$, then $h^{\bar{L}_m}(v') = 0$. Since $U \setminus V_1$ is tilable, $h^{\bar{L}_m}(v) - h^{\bar{L}_m}(v') \leq d(v', v)$; moreover $d(v', v) \leq d(u, v)$. Combining this yields $h^{\bar{L}_m}(v) - h^{\bar{L}_m}(u) \leq d(u, v)$.

The remaining cases are obtained by similar arguments, and we conclude that the graph V_1 is 2-tilable. Let us consider any quadri-tiling with boundary conditions (\bar{c}_1, \bar{c}_2) on

each of the p^2 copies of L_n in U . This yields a quadri-tiling of U which can be completed in order to obtain a quadri-tiling of L_m with planar boundary conditions. Hence,

$$\begin{aligned} Z(L_m^*, \nu) &\geq Z(\bar{L}_n^*, \nu, (0, 0), (\bar{c}_1, \bar{c}_2))^{p^2}, \text{ so} \\ \frac{1}{m^2} \log Z(L_m^*, \nu) &\geq \frac{p^2}{m^2} \log Z(\bar{L}_n^*, \nu, (0, 0), (\bar{c}_1, \bar{c}_2))^{p^2}, \\ &\geq \frac{p^2}{m^2} (\log(n^{-2} 2^{-4n-2}) + \log Z(\bar{L}_n^*, \nu)), \text{ (by equation (5.12))} \\ &\geq \frac{1}{n^2} \log Z(\bar{L}_n^*, \nu) + O\left(\frac{1}{n}\right). \end{aligned}$$

□

Let us conclude the proof of proposition 5.4. Using the first part of lemma 5.6, we obtain

$$\forall n, \liminf_{m \rightarrow \infty} \frac{1}{m^2} \log Z(\bar{L}_m^*, \nu) \geq \frac{1}{n^2} \log Z(L_n^*, \nu),$$

so

$$\liminf_{m \rightarrow \infty} \frac{1}{m^2} \log Z(\bar{L}_m^*, \nu) \geq \limsup_{n \rightarrow \infty} \frac{1}{n^2} \log Z(L_n^*, \nu).$$

In a similar way, using the second part of lemma 5.6, we obtain

$$\liminf_{m \rightarrow \infty} \frac{1}{m^2} \log Z(L_m^*, \nu) \geq \limsup_{n \rightarrow \infty} \frac{1}{n^2} \log Z(\bar{L}_n^*, \nu).$$

We deduce that

$$\lim_{m \rightarrow \infty} \frac{1}{m^2} \log Z(\bar{L}_m^*, \nu) = \lim_{m \rightarrow \infty} \frac{1}{m^2} \log Z(L_m^*, \nu).$$

□

5.4 Growth rate of the partition function of isoradial dimer models

Let Λ be a 2-dimensional lattice, and let G be an infinite Λ -periodic isoradial graph satisfying condition (*). Suppose that its dual graph G^* is bipartite, B denotes the set of black vertices, W the set of white ones. Assume that the bipartite coloring of the vertices of G^* is preserved by translation by Λ . Consider the critical weight function ν on the edges of G^* . Since G is periodic, a natural exhaustion of G by toroidal graphs is $\{\bar{G}_n\}$, where $\bar{G}_n = G/n\Lambda$. Using a result of [26], we give an explicit formula for the limit (as $n \rightarrow \infty$) of the normalized log of the partition function $Z(\bar{G}_n^*, \nu)$ of the graphs \bar{G}_n^* . In general, the computation of this limit involves elliptic integrals [20, 42, 7], hence it is very satisfying to have such a simple formula in the case of isoradial graphs with critical weights.

5.4.1 Statement of result

Let K be the complex Dirac operator indexed by the vertices of G^* . Kenyon defines the **log of the normalized determinant** of the Dirac operator [26], denoted $\log \det_1 K$ as follows:

$$\text{for every edge } w_i b_i \text{ of } G^*, \quad \frac{\partial \log \det_1 K}{\partial (K(w_i, b_i))} = \frac{1}{|V(\bar{G}_1^*)|} K^{-1}(b_i, w_i), \quad (5.14)$$

where $V(\bar{G}_1^*)$ is the set of vertices of the graph \bar{G}_1^* . The definition is completed by an initial condition for $\log \det_1 K$ (see [26]). Solving the PDE yields,

Theorem 5.7 [26]

$$\log \det_1 K = \frac{2}{|V(\bar{G}_1^*)|} \sum_{i=1}^m \left(\frac{\theta_i}{\pi} \log 2 \sin \theta_i + \frac{1}{\pi} L(\theta_i) \right), \quad (5.15)$$

where $\theta_1, \dots, \theta_m$ are the rhombus angles of the edges e_1, \dots, e_m of \bar{G}_1^* , and L is the Lobachevsky function, $L(x) = -\int_0^x \log 2 \sin t \, dt$.

Equation (5.14) is taken as a definition for $\log \det_1 K$ because, as the graph G^* is infinite, no direct meaning can be given to $\frac{1}{|V(G^*)|} \log |\det K|$, which would be the natural way of defining it. The next proposition yields an interpretation of $\log \det_1 K$ as the limit (as $n \rightarrow \infty$) of $\frac{2}{|V(\bar{G}_n^*)|} \log Z(\bar{G}_n^*, \nu)$; this answers the question of [26] of defining $\log \det_1 K$ via an exhaustion of G^* by finite graphs.

Proposition 5.8

$$\lim_{n \rightarrow \infty} \frac{1}{|V(\bar{G}_n^*)|} \log Z(\bar{G}_n^*, \nu) = \frac{1}{|V(\bar{G}_1^*)|} \sum_{i=1}^m \left(\frac{\theta_i}{\pi} \log 2 \sin \theta_i + \frac{1}{\pi} L(\theta_i) \right). \quad (5.16)$$

where $\theta_1, \dots, \theta_m$ are the rhombus angles of the edges e_1, \dots, e_m of \bar{G}_1^* , and L is the Lobachevsky function, $L(x) = -\int_0^x \log 2 \sin t \, dt$.

Moreover, proposition 5.8 yields an easy way of computing the limit of the normalized log of the partition function of the graphs \bar{G}_n^* : indeed the right hand side of (5.16) only involves the geometry of \bar{G}_1^* , and not the combinatorics of G^* . In general, this limit is hard to compute, involving elliptic integrals. We only expect such a simple formula to hold in the case of isoradial graphs with critical weights.

5.4.2 Proof of proposition 5.8

Some steps of the proof are close to [26].

Refer to section 3.4 for more details on the following definitions. Consider an orientation of the edges of G^* defined as in subsection 3.4.1, and let K be the real Dirac operator indexed by the vertices of G^* , corresponding to this orientation. Let $K_1^n, K_2^n, K_3^n, K_4^n$ be

the Kasteleyn matrices of the graph \bar{G}_n^* . By linear algebra, for every $\ell = 1, \dots, 4$, and for every edge $w_i b_i$ of \bar{G}_n^* , we have

$$\frac{\partial \det \mathbf{K}_\ell^n}{\partial (\mathbf{K}_\ell^n(w_i, b_i))} = (\det \mathbf{K}_\ell^n) ((\mathbf{K}_\ell^n)^{-1}(b_i, w_i)).$$

Denote by $e_1 = w_1 b_1, \dots, e_m = w_m b_m$ the edges of \bar{G}_1^* , and let $\theta_1, \dots, \theta_m$ be the corresponding rhombus angles. Since the graph \bar{G}_n^* is invariant under Λ -translates, we know that for every Λ -translate $w_i^t b_i^t$ of the edge $w_i b_i$, the coefficient $\mathbf{K}_\ell^n(w_i^t, b_i^t) = \pm \mathbf{K}_\ell^n(w_i, b_i)$. The minus sign only occurs when $\ell = 2, 3, 4$, (recall that in the definition of $\mathbf{K}_2^n, \dots, \mathbf{K}_4^n$, the sign of the entries which cross the horizontal and/or the vertical cycle of \bar{G}_n is reversed), but then $(\mathbf{K}_\ell^n)^{-1}(b_i^t, w_i^t) = \pm (\mathbf{K}_\ell^n)^{-1}(b_i, w_i)$. Hence, for every $\ell = 1, \dots, 4$, and for every $i = 1, \dots, m$,

$$\begin{aligned} \frac{\partial \det \mathbf{K}_\ell^n}{\partial \theta_i} &= \sum_{w_i^t b_i^t \text{ translates of } w_i b_i} \frac{\partial \det \mathbf{K}_\ell^n}{\partial (\mathbf{K}_\ell^n(w_i^t, b_i^t))} \frac{\partial (\mathbf{K}_\ell^n(w_i^t, b_i^t))}{\partial \theta_i}, \\ &= n^2 (\det \mathbf{K}_\ell^n) ((\mathbf{K}_\ell^n)^{-1}(b_i, w_i)) \frac{\partial \mathbf{K}_\ell^n(w_i, b_i)}{\partial \theta_i}, \end{aligned} \quad (5.17)$$

where the edges e_1, \dots, e_m do not cross the horizontal and the vertical path of \bar{G}_n . Define the function $\varphi^n(\theta_1, \dots, \theta_m)$ by

$$\varphi^n(\theta_1, \dots, \theta_m) = \frac{1}{|V(\bar{G}_n^*)|} \log Z(\bar{G}_n^*, \nu).$$

By theorem 3.9, we have $Z(\bar{G}_n^*, \nu) = \frac{1}{2}(-\det \mathbf{K}_1^n + \det \mathbf{K}_2^n + \det \mathbf{K}_3^n + \det \mathbf{K}_4^n)$. Moreover, for every $\ell = 1, \dots, 4$, $\mathbf{K}_\ell^n(w_i, b_i) = \mathbf{K}(w_i, b_i)$, so that using (5.17), we obtain for every $i = 1, \dots, m$,

$$\frac{\partial \varphi^n}{\partial \theta_i}(\theta_1, \dots, \theta_m) = \frac{1}{|V(\bar{G}_1^*)|} \left(\frac{\partial \mathbf{K}(w_i, b_i)}{\partial \theta_i} \right) \left(\frac{-\det \mathbf{K}_1^n}{2Z(\bar{G}_n^*, \nu)} (\mathbf{K}_1^n)^{-1}(b_i, w_i) + \sum_{\ell=2}^4 \frac{\det \mathbf{K}_\ell^n}{2Z(\bar{G}_n^*, \nu)} (\mathbf{K}_\ell^n)^{-1}(b_i, w_i) \right). \quad (5.18)$$

The next part of the argument can be found in [21]. The second bracket of equation (5.18) is a weighted average of the four quantities $(\mathbf{K}_\ell^n)^{-1}(b_i, w_i)$, with weights $\pm \frac{1}{2} \det \mathbf{K}_\ell^n / Z(\bar{G}_n^*, \nu)$. These weights are all in the interval $(-1, 1)$ since for every $\ell = 1, \dots, 4$, $2Z(\bar{G}_n^*, \nu) > |\det \mathbf{K}_\ell^n|$. Indeed, $Z(\bar{G}_n^*, \nu)$ counts the weighted sum of dimer configurations of \bar{G}_n^* , whereas $|\det \mathbf{K}_\ell^n|$ counts some configurations with negative sign. Since the weights sum to 1, the weighted average converges to the same value as each $(\mathbf{K}_\ell^n)^{-1}(b_i, w_i)$. By proposition 3.11, for every $\ell = 1, \dots, 4$, $(\mathbf{K}_\ell^n)^{-1}(b_i, w_i)$ converges to $\mathbf{K}^{-1}(b_i, w_i)$ on a subsequence (n_j) of n 's. Hence, for every $\varepsilon > 0$, there exists n_0 such that for $n \geq n_0$, $n \in (n_j)$, equation (5.18) can be written as

$$\frac{\partial \varphi^n}{\partial \theta_i}(\theta_1, \dots, \theta_m) = \frac{1}{|V(\bar{G}_1^*)|} \frac{\partial \mathbf{K}(w_i, b_i)}{\partial \theta_i} \mathbf{K}^{-1}(b_i, w_i) + \varepsilon.$$

A direct computation using the definition of K , and proposition 3.6 yields,

$$\frac{\partial \varphi^n}{\partial \theta_i}(\theta_1, \dots, \theta_m) = \frac{1}{|V(\bar{G}_1^*)|} \frac{\theta_i}{\pi} \cotan \theta_i + \varepsilon.$$

By [26], there is a continuous way to deform the graph G^* so that all rhombus angles tend to 0 or $\pi/2$. The same transformation can be applied to \bar{G}_n^* , for every n . Denote by θ_i^0 the angle θ_i after such a deformation. Let M be the number of angles $\theta_1^0, \dots, \theta_m^0$ which are equal to $\pi/2$. By the argument of [26], for $n \geq n_0$, $n \in (n_j)$, we obtain

$$\varphi^n(\theta_1, \dots, \theta_m) = \frac{1}{|V(\bar{G}_1^*)|} \sum_{i=1}^m \left(\frac{\theta_i}{\pi} \log 2 \sin \theta_i + \frac{1}{\pi} L(\theta_i) \right) - \frac{M}{2|V(\bar{G}_1^*)|} \log 2 + \varphi^n(\theta_1^0, \dots, \theta_m^0) + \varepsilon. \quad (5.19)$$

Let us compute $\varphi^n(\theta_1^0, \dots, \theta_m^0)$. Suppose the above deformation is applied to the graph G^* , then edges corresponding to rhombus angles 0 have weight 0, and those corresponding to rhombus angles $\pi/2$ have weight 2. Removing the 0 weight edges, the deformed graph consists of independent copies of \mathbb{Z} . Applying the deformation to \bar{G}_1^* , we obtain graphs $\mathbb{Z}/m_1\mathbb{Z}, \dots, \mathbb{Z}/m_p\mathbb{Z}$, for even m_1, \dots, m_p , where each $\mathbb{Z}/m_j\mathbb{Z}$ consists of weight 2 edges. We can compute,

$$Z(\bar{G}_n^*, \nu) = (2^{\frac{nm_1}{2}} 2)^n \dots (2^{\frac{nm_p}{2}} 2)^n = 2^{n^2 \frac{M}{2}} 2^{np}.$$

Hence, for every $\varepsilon > 0$, there exists n_1 , such that for every $n \geq n_1$, we have

$$\varphi^n(\theta_1^0, \dots, \theta_m^0) = \frac{M}{2|V(\bar{G}_1^*)|} \log 2 + \varepsilon. \quad (5.20)$$

Combining equations (5.19) and (5.20) yields, for every $n \geq \max\{n_0, n_1\}$, $n \in (n_j)$,

$$\varphi^n(\theta_1, \dots, \theta_m) = \frac{1}{|V(\bar{G}_1^*)|} \sum_{i=1}^m \left(\frac{\theta_i}{\pi} \log 2 \sin \theta_i + \frac{1}{\pi} L(\theta_i) \right) + 2\varepsilon.$$

This implies,

$$\lim'_{n \rightarrow \infty} \varphi^n(\theta_1, \dots, \theta_m) = \frac{1}{|V(\bar{G}_1^*)|} \sum_{i=1}^m \left(\frac{\theta_i}{\pi} \log 2 \sin \theta_i + \frac{1}{\pi} L(\theta_i) \right).$$

where the limit is taken on the subsequence (n_j) . Using theorem 3.5 of [29], we deduce that $\varphi^n(\theta_1, \dots, \theta_m)$ converges (as $n \rightarrow \infty$) to the same limit as the above subsequence. \square

5.5 Proof of theorem 5.1

Let us place ourselves in the context of theorem 5.1. When ν is the critical weight function, the weights a, b, c satisfy condition (5.1) of proposition 5.2. This implies that the total partition function satisfies,

$$\forall n, Z(\partial G_n, \nu) = Z(L^*, \nu) Z(G_n^*, 1),$$

where L is the lozenge-with-diagonals tiling corresponding to any lozenge tiling \mathbf{L} of the graph G_n , $Z(L^*, \nu)$ is the quadri-tile partition function of the graph L^* , and $Z(G_n^*, 1)$ is the lozenge partition function of the graph G_n^* .

Let us take \mathbf{L} to be the lozenge tiling \mathbf{L}_n introduced in subsection 5.3.2: \mathbf{L}_1 is the lozenge tiling called the full cube, and \mathbf{L}_n consists of the $ie_1 + je_2$ copies of \mathbf{L}_1 , for every $i, j = 1, \dots, n$. Then,

$$\forall n, Z(\partial G_n, \nu) = Z(L_n^*, \nu)Z(G_n^*, 1),$$

which implies

$$\lim_{n \rightarrow \infty} \frac{1}{12n^2} \log Z(\partial G_n, \nu) = \lim_{n \rightarrow \infty} \frac{1}{12n^2} \log Z(L_n^*, \nu) + \lim_{n \rightarrow \infty} \frac{1}{12n^2} \log Z(G_n^*, 1).$$

The critical weights satisfy the condition $a^2 + b^2 = c^2$ of proposition 5.4, hence

$$\lim_{n \rightarrow \infty} \frac{1}{12n^2} \log Z(L_n^*, \nu) = \lim_{n \rightarrow \infty} \frac{1}{12n^2} \log Z(\bar{L}_n^*, \nu). \quad (5.21)$$

Since the graph L_n is isoradial, and since the weight function associated to edges of L_n^* is the critical one, we can compute the right hand side of equation (5.21) with the formula of proposition 5.8. The calculation yields

$$\begin{aligned} \lim_{n \rightarrow \infty} \frac{1}{12n^2} \log Z(L_n^*, \nu) &= \frac{1}{12} \left\{ 6 \left(\frac{1}{6} \log 1 + \frac{1}{\pi} L \left(\frac{\pi}{6} \right) + \frac{1}{3} \log \sqrt{3} + \frac{1}{\pi} L \left(\frac{\pi}{3} \right) + \frac{1}{2} \log 2 + \frac{1}{\pi} L \left(\frac{\pi}{2} \right) \right) \right\}, \\ &= \frac{1}{12} \log 3 + \frac{1}{4} \log 2 + \frac{1}{2\pi} L \left(\frac{\pi}{6} \right) + \frac{1}{2\pi} L \left(\frac{\pi}{3} \right), \quad (\text{since } L \left(\frac{\pi}{2} \right) = 0). \end{aligned} \quad (5.22)$$

By lemma 5.3, we have

$$\lim_{n \rightarrow \infty} \frac{1}{12n^2} \log Z(G_n^*, 1) = \lim_{n \rightarrow \infty} \frac{1}{12n^2} \log Z(\bar{G}_n^*, 1). \quad (5.23)$$

The graph G_n is isoradial. Let us compute $\lim_{n \rightarrow \infty} \frac{1}{12n^2} \log Z(\bar{G}_n^*, \sqrt{3})$ with the formula of proposition 5.8 (the critical weight function for the honeycomb lattice \mathbb{T}^* is computed in subsection 4.3.2, it assigns weight $\sqrt{3}$ to every edge of \mathbb{T}^*). The calculations yield,

$$\lim_{n \rightarrow \infty} \frac{1}{12n^2} \log Z(\bar{G}_n^*, \sqrt{3}) = \frac{1}{12} \left\{ 9 \left(\frac{1}{3} \log \sqrt{3} + \frac{1}{\pi} L \left(\frac{\pi}{3} \right) \right) \right\} = \frac{1}{8} \log 3 + \frac{3}{4\pi} L \left(\frac{\pi}{3} \right).$$

The number of edges in a perfect matching of \bar{G}_n^* is $3n^2$, so that

$$\lim_{n \rightarrow \infty} \frac{1}{12n^2} \log Z(\bar{G}_n^*, 1) = \lim_{n \rightarrow \infty} \frac{1}{12n^2} \log Z(\bar{G}_n^*, \sqrt{3}) + \frac{3n^2}{12n^2} \log \left(\frac{1}{\sqrt{3}} \right) = \frac{3}{4\pi} L \left(\frac{\pi}{3} \right). \quad (5.24)$$

Combining equations (5.22) and (5.24) yields,

$$\lim_{n \rightarrow \infty} \frac{1}{12n^2} \log Z(\partial G_n, \nu) = \frac{1}{12} \log 3 + \frac{1}{4} \log 2 + \frac{1}{2\pi} L \left(\frac{\pi}{6} \right) + \frac{5}{4\pi} L \left(\frac{\pi}{3} \right).$$

□

Chapter 6

Explicit Gibbs measure for isoradial dimer models and the case of quadri-tilings

The definition of a Gibbs measure is given in subsection 2.1.3: it is a probability measure on dimer configurations of infinite graphs, which is a natural extension of the Boltzmann measure of finite graphs. A Gibbs measure gives information about local statistics, i.e. about the probability of having a certain set of edges occurring in a dimer configuration. By [29], a dimer model can be in three different phases: solid, gaseous, or liquid; and the determination of the phase is given by the asymptotic edge-to-edge-correlation. This motivates why, after having understood the combinatorics of a dimer model, the second natural step is to obtain an explicit expression for a Gibbs measure.

In [29], Kenyon, Okounkov, Sheffield give an explicit expression for the 2-parameter family of Gibbs measures on doubly periodic graphs which have bipartite duals. This expression involves the limit of the inverse Kasteleyn matrices, a quantity hard to compute in general. In section 6.1 theorem 6.1 states that, when the graph is isoradial with critical weights on the edges of G^* , the limiting inverse Kasteleyn matrices can be replaced by the inverse complex Dirac operator K^{-1} indexed by the vertices of G^* . This answers the question of interpreting the complex Dirac operator in terms of the dimer model on isoradial graphs [26]. Let us recall that $K^{-1}(b, w)$ only depends on the angles of an edge-path from w to b . Using this locality property, theorem 6.1 also gives an expression for a Gibbs measure on graphs that are not necessarily periodic - they are rhombus-with-diagonals tilings. The proof uses a geometric property of rhombus tilings proved in proposition 6.7: every simply connected subgraph of a rhombus tiling can be embedded in a periodic rhombus tiling of the plane. We believe theorem 6.1 to remain true for all isoradial graphs which have bipartite dual graphs. The asymptotic formula for K^{-1} [26] (see also theorem 3.2) combined with the phase description of [29] yields that an isoradial dimer model is always in the liquid phase.

Section 6.2 is about quadri-tilings. First we consider the triangular quadri-tile dimer model with critical weights (see section 4.3 for definitions). Recall that it corresponds to two superposed isoradial dimer models: a quadri-tiling $Q \in \mathcal{Q}$ is a 2-tiling of its underlying lozenge-with-diagonals tiling $L(Q)$, and $L(Q)$ is a 2-tiling of the equilateral triangular lattice \mathbb{T} . Proposition 6.14 gives an explicit expression for a measure on the set of all dimer configurations \mathcal{M} , whose marginals are the Gibbs measures for each of the two dimer models, given by theorem 6.1. Now, let R be a rhombus-with-diagonals tiling of the plane, and let K_R be the complex Dirac operator indexed by the vertices of R^* . Theorem 6.15 states that when $|b - w| \rightarrow \infty$, then $K_R^{-1}(b, w)$ only depends on the rhombi to which b and w belong. This is a surprising fact since in general $K_R^{-1}(b, w)$ depends on the angles of an edge-path from w to b . This allows us to deduce asymptotic properties of the Gibbs measure μ_R on $\mathcal{M}(R^*)$, and of the total measure on \mathcal{M} .

6.1 Explicit Gibbs measure for the isoradial dimer model

In the whole of this section, we let G be an infinite isoradial graph satisfying (*). Suppose that its dual graph G^* is bipartite, B denotes the set of black vertices, and W the set of white ones. Recall that $\mathcal{M}(G^*)$ denotes the set of dimer configurations of G^* . Assume the critical weight function ν is assigned to the edges of G^* . Let K be the complex Dirac operator indexed by the vertices of G^* , and let K^{-1} be the inverse complex Dirac operator, (see section 3.2 for definitions).

Subsection 6.1.1 consists in the statement of theorem 6.1: it gives an explicit expression for a Gibbs measure on $\mathcal{M}(G^*)$ as a function of K and K^{-1} , in the case where G is either periodic or is a rhombus-with-diagonals tiling. The proof of theorem 6.1 in the periodic case is given in subsection 6.1.2. In subsection 6.1.3, we prove a geometry property of rhombus tilings. This property is needed for the proof of theorem 6.1 in the case of an aperiodic rhombus-with-diagonals tiling, which is the subject of subsection 6.1.4.

6.1.1 Explicit Gibbs measure

If $e_1 = w_1 b_1, \dots, e_k = w_k b_k$ is a subset of edges of G^* , define the **cylinder set** $\{e_1, \dots, e_k\}$ of G^* to be the set of dimer configurations of G^* which contain the edges e_1, \dots, e_k . Let \mathcal{A} be the field consisting of the empty set and of the finite disjoint unions of cylinders. Denote by $\sigma(\mathcal{A})$ the σ -field generated by \mathcal{A} .

Theorem 6.1 *Assume one of the following*

1. G is periodic,
2. G is a rhombus-with-diagonals tiling of the plane (which might not be periodic),

then there exists a unique probability measure μ on $(\mathcal{M}(G^), \sigma(\mathcal{A}))$ that satisfies*

$$\mu(e_1, \dots, e_k) = \left(\prod_{i=1}^k K(w_i, b_i) \right) \det_{1 \leq i, j \leq k} (K^{-1}(b_i, w_j)). \quad (6.1)$$

Moreover μ is a Gibbs measure.

The conclusion of theorem 6.1 using assumption 1. (resp. assumption 2.) is proved in subsection 6.1.2 (resp. subsection 6.1.4).

Remark 6.2

1. Let G_1 be a finite simply connected subgraph of G , and let K^1 be the sub-matrix of K indexed by the vertices of G_1^* . Then by [26], the probability that a subset of edges $\{w_1b_1, \dots, w_kb_k\}$ of G_1^* occurs in a dimer configuration chosen with respect to the Boltzmann measure μ^1 , is given by

$$\left(\prod_{i=1}^k K^1(w_i, b_i) \right) \det_{1 \leq i, j \leq k} ((K^1)^{-1}(b_i, w_j)).$$

In that respect, our definition of the measure μ is a natural extension of the Boltzmann measure to $\mathcal{M}(G^*)$.

2. We believe theorem 6.1 to be true for all infinite isoradial graphs satisfying condition (*). Removing the periodicity assumption for a general graph implies solving a geometric problem of the kind of subsection 6.1.3 in a more general setting.

Example of computation: the probability of a single edge

Let $e = wb$ be an edge of G^* , then by theorem 6.1 the probability of the edge e occurring in a dimer configuration of the graph G^* is given by

$$\mu(e) = K(w, b)K^{-1}(b, w).$$

Let w, x, b, y be the vertices of the rhombus $R(wb)$ in cclw (counterclockwise) order. Denote by $e^{i\alpha}$ the complex vector $y - w$, and by $e^{i\beta}$ the complex vector $x - w$; let θ be the rhombus angle of the edge wb . By definition of the complex Dirac operator, we have

$$K(w, b) = i(e^{i\beta} - e^{i\alpha}). \tag{6.2}$$

Moreover, w, x, b is an edge path of \tilde{R} from w to b , hence using the definition of $f_{wb}(z)$ we obtain,

$$K^{-1}(b, w) = \frac{1}{4\pi^2 i} \int_C \frac{\log z}{(z - e^{i\alpha})(z - e^{i\beta})} dz = \frac{1}{2\pi} \left(\frac{2i\theta}{e^{i\alpha} - e^{i\beta}} \right). \tag{6.3}$$

From equations (6.2) and (6.3), we deduce

$$\mu(e) = \theta/\pi. \tag{6.4}$$

6.1.2 Proof of theorem 6.1 under assumption 1.

Under assumption 1, theorem 6.1 is a direct consequence of lemmas 6.3, 6.5 and 6.6 below. We refer the reader to section 3.4 for details of definitions of this subsection. Let Λ be the 2-dimensional lattice which acts periodically on G . Suppose that the bipartite coloring of the vertices of G^* is preserved by translations by Λ (this is possible by eventually replacing Λ by 2Λ). Define an orientation of the edges of G^* as in subsection 3.4.1, and let K be the real Dirac operator indexed by the vertices of G^* , corresponding to this orientation. Consider the toroidal graph $\bar{G}_n = G/n\Lambda$, then its dual graph \bar{G}_n^* is bipartite. Let μ^n be the Boltzmann measure on the set of dimer configurations $\mathcal{M}(\bar{G}_n^*)$ of \bar{G}_n^* . Let $e_1 = w_1 b_1, \dots, e_k = w_k b_k$ be a subset of edges of G^* , and suppose that n is large enough so that these edges are contained in \bar{G}_n^* .

Lemma 6.3

$$\lim_{n \rightarrow \infty} \mu^n(e_1, \dots, e_k) = \left(\prod_{i=1}^k K(w_i, b_i) \right) \det_{1 \leq i, j \leq k} (K^{-1}(b_i, w_j)). \quad (6.5)$$

Proof:

Let K_1^n, \dots, K_4^n be the Kasteleyn matrices of the graph \bar{G}_n^* . Suppose that n is large enough so that the edges e_1, \dots, e_k are contained in \bar{G}_n^* , and so that they do not cross the horizontal and vertical cycle of \bar{G}_n . Then we have the following theorem of Kenyon [21] (see also subsection 3.4.2).

Theorem 6.4 [21] *The probability $\mu^n(e_1, \dots, e_k)$ of the edges e_1, \dots, e_k occurring in a dimer configuration of \bar{G}_n^* is given by*

$$\left(\prod_{i=1}^k K(w_i, b_i) \right) \left(-\frac{\det K_1^n}{2Z(\bar{G}_n^*, \nu)} \det_{1 \leq i, j \leq k} ((K_1^n)^{-1}(b_i, w_j)) + \sum_{\ell=2}^4 \frac{\det K_\ell^n}{2Z(\bar{G}_n^*, \nu)} \det_{1 \leq i, j \leq k} ((K_\ell^n)^{-1}(b_i, w_j)) \right). \quad (6.6)$$

The next part of the argument can be found in [21] (it is also used in the proof of proposition 5.8). The second bracket of equation (6.6) is a weighted average of the four quantities $\det_{1 \leq i, j \leq k} ((K_\ell^n)^{-1}(b_i, w_j))$, with weights $\pm \frac{1}{2} \det K_\ell^n / Z(\bar{G}_n^*, \nu)$. These weights are all in the interval $(-1, 1)$ since, for every $\ell = 1, \dots, 4$, $2Z(\bar{G}_n^*, \nu) > |\det K_\ell^n|$. Indeed, $Z(\bar{G}_n^*, \nu)$ counts the weighted sum of dimer configurations of \bar{G}_n^* , whereas $|\det K_\ell^n|$ counts some configurations with negative sign. Since the weights sum to 1, the weighted average converges to the same value as each $\det_{1 \leq i, j \leq k} ((K_\ell^n)^{-1}(b_i, w_j))$.

By proposition 3.11, for every $\ell = 1, \dots, 4$, $\det_{1 \leq i, j \leq k} ((K_\ell^n)^{-1}(b_i, w_j))$ converges to $\det_{1 \leq i, j \leq k} (K^{-1}(b_i, w_j))$ on a subsequence of n 's. Hence $\mu^n(e_1, \dots, e_k)$ converges to the right hand side of (6.5) on a subsequence of n 's. By Sheffield's theorem [40], this is the unique limit of the Boltzmann measures μ^n , so that we have convergence for every n . \square

Lemma 6.5 *There exists a unique probability measure μ on $(\mathcal{M}(G^*), \sigma(\mathcal{A}))$ that satisfies*

$$\mu(e_1, \dots, e_k) = \left(\prod_{i=1}^k \mathsf{K}(w_i, b_i) \right) \det_{1 \leq i, j \leq k} (\mathsf{K}^{-1}(b_i, w_j)). \quad (6.7)$$

Moreover, μ is a Gibbs measure.

Proof:

The edges of the graph G^* form a countable set. For every $i \in \mathbb{N}$, define $f_i : \mathcal{M}(G^*) \rightarrow \{0, 1\}$ by

$$f_i(M) = \begin{cases} 1 & \text{if the edge } e_i \text{ belongs to } M, \\ 0 & \text{else.} \end{cases}$$

Fix $k \in \mathbb{N}$, and a k -tuple (s_1, \dots, s_k) of distinct elements of \mathbb{N} . Let $H \in \mathcal{B}\{0, 1\}^k$, where $\mathcal{B}\{0, 1\}^k$ denotes the Borel σ -field of $\{0, 1\}^k$, and define a **cylinder of rank k** by

$$A_{(s_1, \dots, s_k)}(H) = \{M \in \mathcal{M}(G^*) \mid (f_{s_1}(M), \dots, f_{s_k}(M)) \in H\}.$$

Then $A_{(s_1, \dots, s_k)}(H)$ can be written as a disjoint union of cylinder sets,

$$A_{(s_1, \dots, s_k)}(H) = \bigcup_{i=1}^m \{e_{t_{i1}}, \dots, e_{t_{i\ell_i}}\},$$

(recall that for every i , $\{e_{t_{i1}}, \dots, e_{t_{i\ell_i}}\}$ denotes the set of dimer configurations of G^* containing the edges $e_{t_{i1}}, \dots, e_{t_{i\ell_i}}$). Define

$$\mu_{(s_1, \dots, s_k)}(H) = \sum_{i=1}^m \left(\left(\prod_{j=1}^{\ell_i} \mathsf{K}(w_{t_{ij}}, b_{t_{ij}}) \right) \det_{1 \leq j, k \leq \ell_i} (\mathsf{K}^{-1}(b_{t_{ij}}, w_{t_{ik}})) \right).$$

Then, by lemma 6.3, $\mu_{(s_1, \dots, s_k)}(H) = \lim_{n \rightarrow \infty} \mu^n(A_{(s_1, \dots, s_k)}(H))$. From this we deduce that for every k , and for every k -tuple (s_1, \dots, s_k) , $\mu_{(s_1, \dots, s_k)}$ is a probability measure on $\mathcal{B}\{0, 1\}^k$. Moreover, we deduce that the system of measures $\{\mu_{(s_1, \dots, s_k)} : (s_1, \dots, s_k) \text{ is a } k\text{-tuple of distinct elements of } \mathbb{N}\}$ satisfy Kolmogorov's two consistency conditions. Applying Kolmogorov's extension theorem, we obtain the existence of a unique measure μ , which satisfies (6.7).

Using the fact that the measure μ of a cylinder set is the limit of the Boltzmann measures, we deduce that the measure μ is a Gibbs measure. \square

Lemma 6.6 *For every subset of edges $e_1 = w_1 b_1, \dots, e_k = w_k b_k$ of G^* , we have:*

$$\left(\prod_{i=1}^k \mathsf{K}(w_i, b_i) \right) \det_{1 \leq i, j \leq k} (\mathsf{K}^{-1}(b_i, w_j)) = \left(\prod_{i=1}^k K(w_i, b_i) \right) \det_{1 \leq i, j \leq k} (K^{-1}(b_i, w_j)).$$

Proof:

By definition of the determinant, we have

$$\left(\prod_{i=1}^k \mathbb{K}(w_i, b_i) \right)_{1 \leq i, j \leq k} \det (\mathbb{K}^{-1}(b_i, w_j)) = \sum_{\sigma \in \mathcal{S}_n} \text{sgn } \sigma \left(\prod_{i=1}^k \mathbb{K}(w_i, b_i) \right) \mathbb{K}^{-1}(b_1, w_{\sigma(1)}) \dots \mathbb{K}^{-1}(b_k, w_{\sigma(k)}),$$

where \mathcal{S}_n is the set of permutations of n elements. A permutation $\sigma \in \mathcal{S}_n$ can be written as a product of disjoint cycles, so let us treat the case of each cycle separately. Refer to subsection 3.3.2 for the definition of the function f_{wx} below.

• Suppose that in the product there is a 1-cycle, that is a point j such that $\sigma(j) = j$. Then, using remark 3.4 and proposition 3.6, we obtain

$$\begin{aligned} \mathbb{K}(w_j, b_j) &= f_{w_j b_j}(0) K(w_j, b_j), \\ \mathbb{K}^{-1}(b_j, w_j) &= \overline{f_{w_j b_j}(0)} K^{-1}(b_j, w_j). \end{aligned}$$

Moreover, $\overline{f_{w_j b_j}(0)} = f_{w_j b_j}(0)^{-1}$, hence

$$\mathbb{K}(w_j, b_j) \mathbb{K}^{-1}(b_j, w_j) = K(w_j, b_j) K^{-1}(b_j, w_j). \quad (6.8)$$

• Suppose that in the product there is an ℓ -cycle, with $\ell \neq 1$. To simplify notations, let us assume $\sigma(1) = 2, \dots, \sigma(\ell) = 1$, and let us prove the following (indices are written cyclically, i.e. $\ell + 1 \equiv 1$),

$$\prod_{j=1}^{\ell} \mathbb{K}(w_j, b_j) \mathbb{K}^{-1}(b_j, w_{j+1}) = \prod_{j=1}^{\ell} K(w_j, b_j) K^{-1}(b_j, w_{j+1}). \quad (6.9)$$

Again, using remark 3.4 and proposition 3.6, we obtain

$$\prod_{j=1}^{\ell} \mathbb{K}(w_j, b_j) \mathbb{K}^{-1}(b_j, w_{j+1}) = \prod_{j=1}^{\ell} K(w_j, b_j) K^{-1}(b_j, w_{j+1}) f_{w_j b_j}(0) f_{w_{j+1} b_j}(0)^{-1}.$$

Using the definition of the function f_{wx} , and the fact that it is well defined yields

$$\prod_{j=1}^{\ell} f_{w_j b_j}(0) f_{w_{j+1} b_j}(0)^{-1} = \prod_{j=1}^{\ell} f_{w_j b_j}(0) f_{b_j w_{j+1}}(0) = \prod_{j=1}^{\ell} f_{w_j w_{j+1}}(0) = f_{w_1 w_1}(0) = 1.$$

This proves equation (6.9). Combining equations (6.8), (6.9), and the fact that every permutation is a product of cycles, we obtain lemma 6.6. \square

\square

6.1.3 Geometric property of rhombus tilings

Consider a rhombus-with-diagonals tiling of the plane R . When R is periodic, it satisfies assumption 1. of theorem 6.1, and the proof is that of subsection 6.1.2. A new difficulty comes in when R is not periodic. In order to prove theorem 6.1, we need the following geometric property of rhombus tilings, stated in proposition 6.7 below. The proof of this proposition is the object of this subsection. Note that all rhombus-with-diagonals tilings are assumed to use finitely many different rhombi, up to isometry.

Proposition 6.7 *Let R be a rhombus tiling of the plane, then any finite simply connected subgraph P of R can be embedded in a periodic rhombus tiling S of the plane.*

Proof:

Proposition 6.7 is a direct consequence of lemmas 6.8, 6.9, 6.11 below. \square

The notion of **train-track** has been introduced by Mercat [35], see also Kenyon and Schlenker [26, 31]. A train-track of a rhombus tiling is a path of rhombi (each rhombus being adjacent along an edge to the previous rhombus) which does not turn: on entering a rhombus, it exits across the opposite edge. Train-tracks are assumed to be maximal in the sense that they extend in both directions as far as possible. Thus train-tracks of rhombus tilings of the plane are bi-infinite. Each rhombus in a train-track has an edge parallel to a fixed unit vector e , called the **transversal direction** of the train-track. Let us denote by t_e the train-track of transversal direction e . In an oriented train-track (i.e. the edges of the two parallel boundary paths of the train-track have the same given orientation), we choose the direction of e so that when the train-track runs in the direction given by the orientation, e points from the right to the left. The vector e is called the **oriented transversal direction** of the oriented train-track. A train-track cannot cross itself, and two different train-tracks can cross at most once. A finite simply connected subgraph P of a rhombus tiling of the plane R is **train-track-convex**, if every train-track of R that intersects P crosses the boundary of P twice exactly.

Lemma 6.8 *Let R be a rhombus tiling of the plane, then any finite simply connected subgraph P of R can be completed by a finite number of rhombi of R in order to become train-track-convex.*

Proof:

Let e_1, \dots, e_m be the boundary edges of P . Every rhombus of P belongs to two train-tracks of R , each of which can be continued in both directions up to the boundary of P . In both directions the intersection of each of the train-tracks and the boundary of P is an edge parallel to the transversal direction of the train-track. Thus, to take into account all train-tracks of R that intersect P , it suffices to consider for every i the train-track t_{e_i} associated to the boundary edge e_i of P . Consider the following algorithm (see figure 6.1).

Set $Q_1 = P$.

For $i = 1, \dots, m$, do the following:

Consider the train-track t_{e_i} , and let $2n_i$ be the number of times t_{e_i} intersects the boundary of Q_i .

- If $n_i > 1$: there are $n_i - 1$ portions of t_{e_i} that are outside of Q_i , denote them by $t_{e_i}^1, \dots, t_{e_i}^{n_i-1}$. Then, since Q_i is simply connected, for every j , $R \setminus (Q_i \cup t_{e_i}^j)$ is made of two disjoint sub-graphs of R , one of which is finite (it might be empty in the case where one of the two parallel boundary paths of $t_{e_i}^j$ is part of the boundary path of Q_i). Denote by $g_{e_i}^j$ the simply connected subgraph of R made of the finite subgraph of $R \setminus (Q_i \cup t_{e_i}^j)$ and of $t_{e_i}^j$. Denote by $b_{e_i}^j$ the portion of the boundary of Q_i which bounds $g_{e_i}^j$. Replace Q_i by $Q_{i+1} = Q_i \cup (\cup_{j=1}^{n_i-1} g_{e_i}^j)$. By this construction t_{e_i} intersects the boundary of Q_{i+1} exactly twice, and Q_{i+1} is simply connected.
- If $n_i = 1$: set $Q_{i+1} = Q_i$.

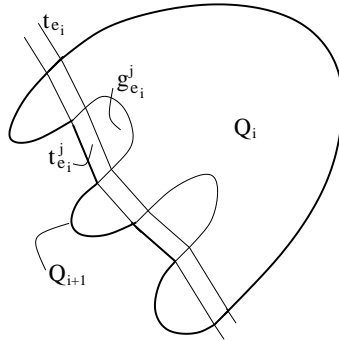


Figure 6.1: One step of the algorithm.

Let us show that at every step the train-tracks of R that intersect Q_i and Q_{i+1} are the same. By construction, boundary edges of Q_{i+1} are boundary edges of Q_i and of $t_{e_i}^j$, for every j . Let f be an edge on the boundary of Q_{i+1} , but not of Q_i , that is f is on the boundary of $t_{e_i}^j$ for some j , thus t_f crosses $g_{e_i}^j$. Since two train-tracks cross at most once, t_f has to intersect $b_{e_i}^j$, which means t_f also crosses Q_i . From this we also conclude that if a train-track intersects the boundary of Q_i twice, then it also intersects the boundary of Q_{i+1} twice.

Thus all train-tracks that intersect Q_{m+1} cross its boundary exactly twice, and Q_{m+1} contains P . \square

Lemma 6.9 *Let R be a rhombus tiling of the plane. Then any finite simply connected train-track-convex subgraph P of R can be completed by a finite number of rhombi in order to become a convex polygon Q , whose opposite boundary edges are parallel.*

Proof:

Let e_1, \dots, e_m be the boundary edges of P oriented cclw. Since P is train-track-convex, the train-tracks t_{e_1}, \dots, t_{e_m} intersect the boundary of P twice, so that there are pairs of parallel boundary edges. Let us assume that the transversal directions of the train-tracks are all distinct (if this is not the case, one can always perturb the graph a little so that it happens). Let us also denote by t_{e_1}, \dots, t_{e_m} the portions of the bi-infinite train-tracks of R in P . In what follows, indices will be denoted cyclically, that is $e_j = e_{m+j}$. Write x_j (resp. y_j) for the initial (resp. end) vertex of an edge e_j .

Let e_i, e_{i+1} be two adjacent boundary edges of P . Consider the translate e_{i+1}^t of e_{i+1} so that the initial vertex of e_{i+1}^t is adjacent to the initial vertex of e_i . Then we define the **turning angle from e_i to e_{i+1}** (also called exterior angle) to be the angle $\widehat{e_i e_{i+1}^t}$, and we denote it by $\theta_{e_i, e_{i+1}}$. If e_i, e_j are two boundary edges, then the **turning angle from e_i to e_j** is defined by $\sum_{\alpha=i}^{j-1} \theta_{e_\alpha, e_{\alpha+1}}$, and is denoted by θ_{e_i, e_j} .

Property 6.10

1. $\sum_{\alpha=1}^m \theta_{e_\alpha, e_{\alpha+1}} = 2\pi$.
2. If e_i, e_j are two boundary edges, and if $\gamma = \{f_1, \dots, f_n\}$ is an oriented edge-path in P from y_i to x_j , then $\theta_{e_i, e_j} = \theta_{e_i, f_1} + \sum_{\alpha=1}^{n-1} \theta_{f_\alpha, f_{\alpha+1}} + \theta_{f_n, e_j}$.
3. If e_i is a boundary edge of P , and e_k is the second boundary edge at which t_{e_i} intersects the boundary of P , then $\theta_{e_i, e_k} = \pi$. Thus e_k and e_i are oriented in the opposite direction, and we denote e_k by e_i^{-1} .
4. P is convex, if and only if every train-track of P crosses every other train-track of P .

We first end the proof of lemma 6.9, and then prove properties 1. to 4.

Note that properties 1. and 2. are true for any finite simply connected subgraph of R . The number of train-tracks intersecting P is $n = m/2$, so that if every train-track crosses every other train-track, the total number of crossings is $n(n-1)/2$. Consider the following algorithm (see figure 6.2 for an example).

Set $Q_1 = P$, $n_1 =$ the number of train-tracks that cross in Q_1 .

For $i = 1, 2, \dots$ do the following:

1. If $n_i = n(n-1)/2$: then by property 4, Q_i is convex.
2. If $n_i < n(n-1)/2$: then by property 4, $\theta_{e_{j_i}, e_{j_i+1}} < 0$ for some $j_i \in \{1, \dots, m\}$. Add the rhombus ℓ_{j_i} of parallel directions e_{j_i}, e_{j_i+1} along the boundary of Q_i . Set $Q_{i+1} = Q_i \cup \ell_{j_i}$, and rename the boundary

edges e_1, \dots, e_m in cclw order. Then the number of train-tracks that cross in Q_{i+1} is $n_i + 1$, set $n_{i+1} = n_i + 1$. Note that if property 4. is true for Q_i , it stays true for Q_{i+1} , and note that the same train-tracks intersect Q_i and Q_{i+1} .

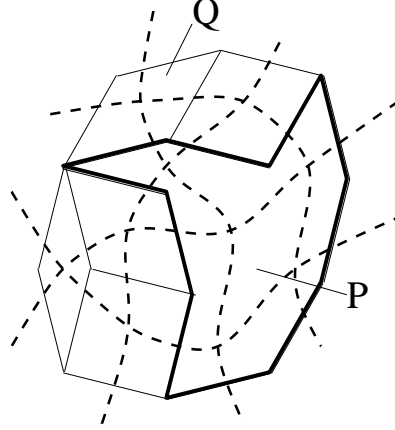


Figure 6.2: Example of application of the algorithm.

For the algorithm to be able to add the rhombus ℓ_j at every step, we need to check that:

$$\forall i, \theta_{e_{j_i-1}, e_{j_i+1}} > -\pi, \text{ and } \theta_{e_{j_i}, e_{j_i+2}} > -\pi. \quad (6.10)$$

Assume we have proved that for any finite simply connected train-track-convex sub-graph P of R we have:

$$\forall i, j, \theta_{e_i, e_j} > -\pi. \quad (6.11)$$

Then properties 1. and 2. imply that if (6.11) is true for Q_i it stays true for Q_{i+1} , moreover (6.11) implies (6.10). So let us prove (6.11) by induction on the number of rhombi contained in P . If P is a rhombus, then (6.11) is clear. Now assume P is made of k rhombi. Consider the train-tracks in P adjacent to the boundary (every boundary edge e of P belongs to a rhombus of P which has parallel directions e and f ; for every boundary edge e , the train-track of transversal direction f is the train-track adjacent to the boundary). Denote the train-tracks adjacent to the boundary by t_1, \dots, t_p in cclw order, and write f_β for the oriented transversal direction of t_β (when the boundary edge-path of P is oriented cclw). Consider two adjacent boundary edges e_i, e_{i+1} of P that don't belong to the same boundary train-track. That is e_i belongs to t_β , and e_{i+1} to $t_{\beta+1}$. Then either $\widehat{f_\beta f_{\beta+1}} < 0$ or $\widehat{f_\beta f_{\beta+1}} > 0$, in the second case t_β and $t_{\beta+1}$ cross and their intersection is a rhombus ℓ_β of P . ℓ_β has boundary edges e_i, e_{i+1} , and $f_{\beta+1} = e_i^{-1}, f_\beta^{-1} = e_{i+1}^{-1}$. Now property 1. implies that $\sum_{\beta=1}^{p-1} \widehat{f_\beta f_{\beta+1}} = 2\pi$, so that there always exists β_0 such that $\widehat{f_{\beta_0} f_{\beta_0+1}} > 0$. Removing ℓ_{β_0} from P and using the

assumption that P is train-track convex, we obtain a graph P' made of $k - 1$ rhombi which is train-track-convex. By induction, $\theta_{e,f} > -\pi$ for every boundary edge of P' , and using property 2, we conclude that this stays true for P .

Denote by Q the convex polygon obtained from P by the algorithm, and assume that opposite boundary edges are not parallel. Then there are indices i and j such that e_i comes before e_j , and e_j^{-1} comes before e_i^{-1} . This implies that $\theta_{e_i, e_j} = -\theta_{e_j^{-1}, e_i^{-1}}$, so that one of the two angles is negative, which means Q can not be convex. Thus we have a contradiction, and we conclude that opposite boundary edges of Q are parallel.

Proof of properties 1. to 4.

1. and 2. are straightforward.

3. When computing θ_{e_i, e_k} along the boundary edge-path of t_{e_i} we obtain π , so by property 2. we deduce that $\theta_{e_i, e_k} = \pi$ in P .

4. P is convex if and only if, for every i , $\theta_{e_i, e_{i+1}} > 0$, which is equivalent to saying that, for every $i \neq j$, $\theta_{e_i, e_j} > 0$. Therefore property 4. is equivalent to proving that $\theta_{e_i, e_j} > 0$, for every $i \neq j$, if and only if every train-track of P crosses every other train-track of P .

Assume there are two distinct train-tracks t_{e_ℓ} and t_{e_k} that don't cross in P . Then, in cclw order around the boundary of P , we have either $e_\ell, e_k^{-1}, e_k, e_\ell^{-1}$, or $e_\ell, e_k, e_k^{-1}, e_\ell^{-1}$. It suffices to solve the second case, the first case being similar. By property 1, $\theta_{e_\ell, e_k} + \theta_{e_k, e_k^{-1}} + \theta_{e_k^{-1}, e_\ell^{-1}} + \theta_{e_\ell^{-1}, e_\ell} = 2\pi$. Moreover by property 3, $\theta_{e_k, e_k^{-1}} = \theta_{e_\ell^{-1}, e_\ell} = \pi$, which implies $\theta_{e_\ell, e_k} = -\theta_{e_k^{-1}, e_\ell^{-1}}$. Since all train-tracks have different transversal directions, either θ_{e_ℓ, e_k} or $\theta_{e_k^{-1}, e_\ell^{-1}}$ is negative.

Now take two boundary edges e_i, e_j of P (with $i \neq j$, and $e_j \neq e_i^{-1}$), and assume the train-tracks t_{e_i}, t_{e_j} cross inside P . Then in cclw order around the boundary of P , we have either $e_i, e_j^{-1}, e_i^{-1}, e_j$, or $e_i, e_j, e_i^{-1}, e_j^{-1}$. It suffices to solve the second case since the first case can be deduced from the second one. The intersection of t_{e_i} and t_{e_j} is a rhombus ℓ . Let \tilde{e}_j^{-1} (resp. \tilde{e}_i^{-1}) be the boundary edge of ℓ parallel and closest to e_j (resp. e_i), oriented in the opposite direction, then $\theta_{\tilde{e}_j^{-1}, \tilde{e}_i^{-1}} < 0$. Let γ_j (resp. γ_i) be the boundary edge-path of t_{e_j} (resp. t_{e_i}) from y_j to \tilde{x}_j (resp. from \tilde{y}_i to x_i), and let Q be the subgraph of R whose boundary is $e_i, e_{i+1}, \dots, e_j, \gamma_j, \tilde{e}_j^{-1}, \tilde{e}_i^{-1}, \gamma_i$. Since t_{e_i} and t_{e_j} intersect the boundary of P twice, they also intersect the boundary of Q twice. Moreover t_{e_i} and t_{e_j} don't cross in Q , so that $\theta_{e_i, e_j} = -\theta_{\tilde{e}_j^{-1}, \tilde{e}_i^{-1}} > 0$.

□

□

Lemma 6.11 *Any convex $2n$ -gon Q whose opposite boundary edges are parallel and of the same length can be embedded in a periodic tiling of the plane by Q and rhombi.*

Proof:

Let $e_1, \dots, e_n, e_1^{-1}, \dots, e_n^{-1}$ be the boundary edges of the polygon Q oriented cclw. If $n \leq 3$, then Q is either a rhombus or a hexagon, and it is straightforward that the plane can be tiled periodically with Q .

If $n > 4$, for $k = 1, \dots, n-3$, do the following (see figure 6.3): along e_{n-k} add the finite train-track $\tilde{t}_{e_{n-k}}$ of transversal direction e_{n-k} , going away from Q , whose boundary edges starting from the boundary of Q are:

$$e_1, \underbrace{e_2, e_1}, \underbrace{e_3, e_2, e_1}, \dots, \underbrace{e_{n-k-2}, \dots, e_1}.$$

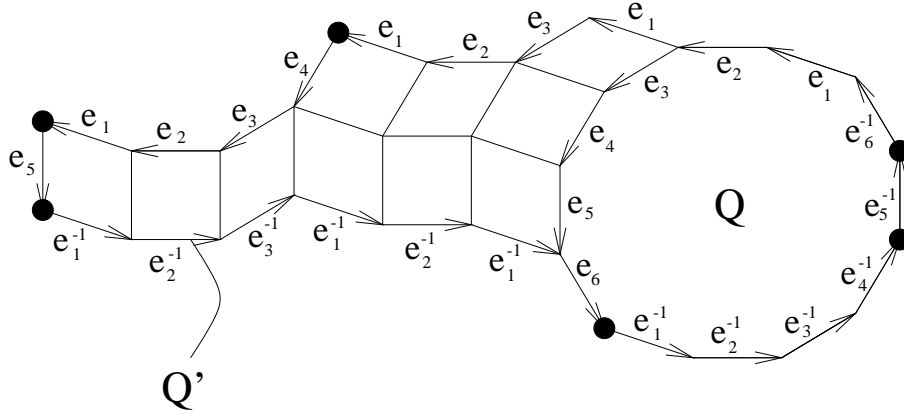


Figure 6.3: Fundamental domain of a periodic tiling of the plane by dodecagons and rhombi.

Since the polygon Q is convex, the rhombi that are added are well defined, moreover the intersection of \tilde{t}_{e_i} and the boundary of Q is the edge e_i , and \tilde{t}_{e_i} doesn't cross \tilde{t}_{e_j} , when $i \neq j$. So we obtain a new polygon Q' made of Q and rhombi, whose boundary edge-path is $\gamma_1, \dots, \gamma_6$, (when starting from the edge e_n^{-1} of Q), where:

$$\gamma_1 = e_n^{-1}, e_1, \underbrace{e_2, e_1}, \underbrace{e_3, e_2, e_1}, \dots, \underbrace{e_{n-3}, \dots, e_1},$$

$$\gamma_2 = e_{n-2}, \dots, e_1,$$

$$\gamma_3 = e_{n-1},$$

$$\gamma_4 = \underbrace{e_1^{-1}, \dots, e_{n-3}^{-1}}, \dots, \underbrace{e_1^{-1}, e_2^{-1}}, e_1^{-1}, e_n,$$

$$\gamma_5 = e_1^{-1}, \dots, e_{n-2}^{-1},$$

$$\gamma_6 = e_{n-1}^{-1}.$$

Noting that $\gamma_4 = \gamma_1^{-1}, \gamma_5 = \gamma_2^{-1}, \gamma_6 = \gamma_3^{-1}$, and using the fact that the plane can be tiled periodically with hexagons which have parallel opposite boundary edges, we deduce that the plane can be tiled with Q' , that is it can be tiled periodically by Q and rhombi. \square

6.1.4 Proof of theorem 6.1 under assumption 2.

Let R be a non periodic rhombus-with-diagonals tiling of the plane, and let \bar{R} be its corresponding rhombus tiling. Denote by K the complex Dirac operator indexed by the vertices of the dual graph R^* .

Consider a subset of edges e_1, \dots, e_k of R^* , and let P be a simply connected subgraph of \bar{R} such that P^* contains these edges (P^* is the dual graph of the rhombus-with-diagonals tiling P corresponding to P). By proposition 6.7, there exists a periodic rhombus tiling of the plane S that contains P . Let us assign the critical weight function to edges of S^* . Denote by Λ the lattice which acts periodically on S , and suppose that the dual graph \bar{S}_n^* of the toroidal graph $\bar{S}_n = S/n\Lambda$ is bipartite. Let μ_S^n be the Boltzmann measure on dimer configurations $\mathcal{M}(\bar{S}_n^*)$ of \bar{S}_n^* . Then we have,

Lemma 6.12

$$\lim_{n \rightarrow \infty} \mu_S^n(e_1, \dots, e_k) = \left(\prod_{i=1}^k K(w_i, b_i) \right)_{1 \leq i, j \leq k} \det (K^{-1}(b_i, w_j)).$$

Proof:

Denote by K_S the Dirac operator indexed by the vertices of S^* . Then combining lemmas 6.3 and 6.6 yields

$$\lim_{n \rightarrow \infty} \mu_S^n(e_1, \dots, e_k) = \left(\prod_{i=1}^k K_S(w_i, b_i) \right)_{1 \leq i, j \leq k} \det (K_S^{-1}(b_i, w_j)).$$

Since P is simply connected, for every $i, j = 1, \dots, k$, it contains a path of \tilde{R} (the set of rhombi associated to edges of R^*) from w_j to b_i . Moreover by theorem 3.1, $K^{-1}(b_i, w_j)$ only depends on such a path, hence $K_S^{-1}(b_i, w_j) = K^{-1}(b_i, w_j)$. We also have $\forall i = 1, \dots, k, K_S(w_i, b_i) = K(w_i, b_i)$, so that we deduce lemma 6.12. \square

The next part of the proof is close to the proof of lemma 6.5. Let us use the same notations. Fix $k \in \mathbb{N}$, and a k -tuple (s_1, \dots, s_k) of distinct elements of \mathbb{N} . Let $H \in \mathcal{B}\{0, 1\}^k$, and $A_{(s_1, \dots, s_k)}(H)$ be the corresponding cylinder of rank k ; recall that it can be written as

$$A_{(s_1, \dots, s_k)}(H) = \bigcup_{i=1}^m \{e_{t_{i1}}, \dots, e_{t_{i\ell_i}}\}.$$

Define

$$\mu_{(s_1, \dots, s_k)}(H) = \sum_{i=1}^m \left(\left(\prod_{j=1}^{\ell_i} K(w_{t_{ij}}, b_{t_{ij}}) \right) \det_{1 \leq j, k \leq \ell_i} (K^{-1}(b_{t_{ij}}, w_{t_{ik}})) \right).$$

Let P be a finite simply connected subgraph of R such that, for every $i = 1, \dots, m$, P^* contains the edges $e_{t_{i1}}, \dots, e_{t_{i\ell_i}}$. Let S be a periodic rhombus tiling of the plane that contains P (given by proposition 6.7). Then, by lemma 6.12, $\mu_{(s_1, \dots, s_k)}(H) = \lim_{n \rightarrow \infty} \mu_S^n(A_{(s_1, \dots, s_k)}(H))$. From this we deduce that for every k , and for every k -tuple (s_1, \dots, s_k) , $\mu_{(s_1, \dots, s_k)}$ is a probability measure on $\mathcal{B}\{0, 1\}^k$. Moreover, we deduce that the system of measures $\{\mu_{(s_1, \dots, s_k)} : (s_1, \dots, s_k) \text{ is a } k\text{-tuple of distinct elements of } \mathbb{N}\}$ satisfy Kolmogorov's two consistency conditions. Applying Kolmogorov's extension theorem, we obtain the existence of a unique measure μ , which satisfies (6.1). \square

6.2 The case of quadri-tilings

In subsection 6.2.1, we give an explicit expression for a total measure on the set of all quadri-tilings of the triangular quadri-tile dimer model, whose marginals are the quadri-tiling Gibbs measure and the lozenge Gibbs measure. In subsection 6.2.2, we consider a rhombus-with-diagonals tiling R , and the complex Dirac operator K_R indexed by the vertices of R^* . We derive a very simple asymptotic formula for K_R^{-1} , and deduce asymptotic properties of the quadri-tiling Gibbs measure and of the total measure.

6.2.1 Total measure for the triangular quadri-tile dimer model

Let L be any lozenge-with-diagonals tiling of the plane, and suppose that the critical weight function is associated to edges of L^* . Let μ_L be the Gibbs measure on $\mathcal{M}(L^*)$ given by theorem 6.1.

Consider the equilateral triangular lattice \mathbb{T} , then \mathbb{T} is a periodic isoradial graph whose dual graph \mathbb{T}^* (the honeycomb lattice) is bipartite. Assume that the critical weight function is associated to edges of \mathbb{T}^* , and let ν be the Gibbs measure on $\mathcal{M}(\mathbb{T}^*)$ given by theorem 6.1 (this measure is the same as the one given in [21]).

Recall that \mathcal{M} is the set of dimer configurations corresponding to quadri-tilings of the triangular quadri-tile dimer model (see section 4.3). In this subsection, we start by defining a σ -algebra $\sigma(\mathcal{B})$ on \mathcal{M} . Then we give an explicit expression for a probability measure μ on $(\mathcal{M}, \sigma(\mathcal{B}))$, whose marginals are the measures μ_L and ν .

Recall that \mathcal{L} is the set of lozenge-with-diagonals tilings of the plane, up to isometry. Define \mathcal{L}^* to be the graph (which is not planar) obtained by superposing the dual graphs L^* of lozenge-with-diagonals tilings $L \in \mathcal{L}$. Although some edges of \mathcal{L}^* have length 0, we think of them as edges of the one skeleton of the graph, so that to every edge of \mathcal{L}^* there corresponds a unique quadri-tile in a lozenge-with-diagonals tiling of \mathcal{L} . Let e be an edge of \mathcal{L}^* , and let q_e be the corresponding quadri-tile, then q_e is made of two

adjacent right triangles. If the two triangles share the hypotenuse edge, they belong to two adjacent lozenges; else if they share a leg, they belong to the same lozenge. Let us call these lozenge(s) the **lozenge(s) associated to the edge** e , and denote it/them by l_e (that is l_e consists of either one or two lozenges). Let k_e be the edge(s) of \mathbb{T}^* corresponding to the lozenge(s) l_e .

Consider a dimer configuration $M \in \mathcal{M}$, then M is in bijection with a quadri-tiling which we denote by Q_M . Let $L(Q_M)$ be the underlying lozenge-with-diagonals tiling of Q_M , and recall that $\mathbf{L}(Q_M)$ denotes the corresponding lozenge tiling.

Let e_1, \dots, e_m be a subset of edges of \mathcal{L}^* , and k_1, \dots, k_n be a subset of edges of \mathbb{T}^* . We define the **cylinder set** $\{e_1, \dots, e_m, k_1, \dots, k_n\}$ of \mathcal{M} by,

$$\{M \in \mathcal{M} \mid M \text{ contains } e_1, \dots, e_m, \text{ and } \mathbf{L}(Q_M)^* \text{ contains } k_1, \dots, k_n\}.$$

Remark 6.13

1. If the edges k_{e_1}, \dots, k_{e_m} are not included in the set of edges k_1, \dots, k_n , then

$$\{e_1, \dots, e_m, k_1, \dots, k_n\} = \emptyset.$$

2. Every cylinder set of \mathcal{M} can be expressed as a finite disjoint union of cylinders whose edges are edges of \mathcal{L}^* exclusively.
3. Every cylinder whose edges are edges of \mathcal{L}^* can be expressed as a finite disjoint union of cylinders, each of which has the property that the lozenges associated to its edges form a connected path of lozenges.

Let us call **connected cylinder** any cylinder which has the property of the third point of remark 6.13. Consider \mathcal{B} the field consisting of the empty set and of finite disjoint unions of connected cylinders. Denote by $\sigma(\mathcal{B})$ the σ -field generated by \mathcal{B} .

Let e_1, \dots, e_m be a subset of edges of \mathcal{L}^* which has the property that $\{e_1, \dots, e_m\}$ is a connected cylinder.

Proposition 6.14 *There exists a unique probability measure μ on $(\mathcal{M}, \sigma(\mathcal{B}))$ that satisfies*

$$\mu(e_1, \dots, e_m) = \mu_L(e_1, \dots, e_m) \nu(k_{e_1}, \dots, k_{e_m}), \quad (6.12)$$

where L is the lozenge-with-diagonals tiling corresponding to any lozenge tiling \mathbf{L} which contains the lozenges l_{e_1}, \dots, l_{e_m} .

Proof:

Expression (6.12) is well defined, i.e. independent of the lozenge tiling \mathbf{L} which contains the lozenges l_{e_1}, \dots, l_{e_m} . Indeed, by definition of a connected cylinder set, the lozenges associated to the edges e_1, \dots, e_m form a connected path of lozenges, say γ . Let \mathbf{L} be a lozenge tiling that contains γ , and denote by K_L the complex Dirac operator indexed by the vertices of the graph L^* . Then $K_L^{-1}(b_i, w_j)$ is independent of the lozenge tiling

L which contains γ , indeed $K_L^{-1}(b_i, w_j)$ only depends on an edge-path of \tilde{R} from w_j to b_i , and since L contains γ which is connected, we can choose the edge-path to be the same for all lozenge-with-diagonals tilings L . We then use the fact that ν and μ^L are probability measures to prove the two conditions of Kolmogorov's extension theorem. \square

6.2.2 Asymptotics of the quadri-tile Gibbs measure and of the total measure

Let R be a rhombus tiling of the plane which uses finitely many different rhombi up to isometry, and let R be the corresponding rhombus-with-diagonals tiling. Consider the complex Dirac operator K_R indexed by the vertices of the dual graph R^* . We establish that asymptotically (as $|b - w| \rightarrow \infty$), $K_R^{-1}(b, w)$ only depends on the rhombi to which the vertices b and w belong, and else is independent of the graph R . Let μ_R be the Gibbs measure on $\mathcal{M}(R^*)$ given by theorem 6.1, and let μ be the total measure on \mathcal{M} . Then, from the asymptotic property of K_R^{-1} , we deduce asymptotic properties of the measures μ_R and μ .

Refer to figure 6.4 for the following notations. Let ℓ'_1, ℓ'_2 be two disjoint side-length two rhombi in the plane, and let ℓ_1, ℓ_2 be the corresponding rhombi with diagonals. Assume ℓ_1 and ℓ_2 have a fixed black and white bipartite coloring of their faces. Let r_1 and r_2 be the dual graphs of ℓ_1 and ℓ_2 (r_1 and r_2 are rectangles), with the corresponding bipartite coloring of the vertices. Let w be a white vertex of r_1 , and b a black vertex of r_2 , then w (resp. b) belongs to a boundary edge e_1 of ℓ_1 (resp. e_2 of ℓ_2). By property 4.2, to the bipartite coloring of the faces of ℓ_1 and ℓ_2 , there corresponds a bipartite coloring of the vertices of ℓ'_1 and ℓ'_2 . Let x_1 (resp. x_2) be the black vertex of the edge e_1 (resp. e_2). Orient the edge wx_1 from w to x_1 , and let $e^{i\theta_1}$ be the corresponding vector. Orient the edge x_2b from x_2 to b , and let $e^{i\theta_2}$ be the corresponding vector. Assume ℓ'_1 and ℓ'_2 belong to a rhombus tiling of the plane R . Moreover, suppose that the bipartite coloring of the vertices of R^* is compatible with the bipartite coloring of the vertices of r_1 and r_2 .

Then we have the following asymptotics for the inverse complex Dirac operator K_R^{-1} indexed by the vertices of R^* .

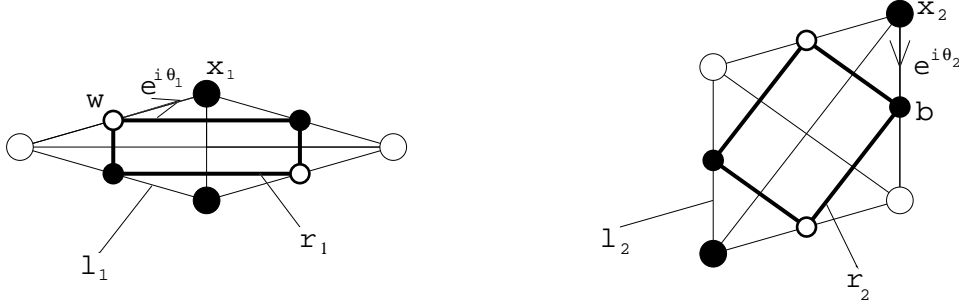
Theorem 6.15 $K_R^{-1}(b, w)$ is given by

$$\frac{1}{2\pi} \left(\frac{1}{b-w} + \frac{e^{-i(\theta_1+\theta_2)}}{\bar{b}-\bar{w}} \right) + \frac{1}{2\pi} \left(\frac{e^{2i\theta_1} + e^{2i\theta_2}}{(b-w)^3} + \frac{e^{-i(3\theta_1+\theta_2)} + e^{-i(\theta_1+3\theta_2)}}{(\bar{b}-\bar{w})^3} \right) + O\left(\frac{1}{|b-w|^3}\right),$$

where θ_1 and θ_2 are defined above.

Proof:

Let us define an edge-path from w to b in \tilde{R} . Consider the bipartite coloring of the


 Figure 6.4: Rhombi with diagonals ℓ_1, ℓ_2 and their dual graphs r_1, r_2 .

vertices of R (given by property 4.2) associated to the bipartite coloring of the vertices of R^* . We define the graph N as follows. Vertices of N are black vertices of R , and two vertices of N are connected by an edge if they belong to the same rhombus in R . N is connected because R is. Each face of N is inscribable in a circle of radius two. The circumcenter of a face of N is the intersection of the rhombi in R , to which the edges on the boundary cycle of the face belong. Thus the circumcenter is in the closure of the face, and so faces of N are convex. Note that the vertices x_1 and x_2 are vertices of the graph N .

Denote by (x, y) the line segment from a vertex x to a vertex y of N . An edge uv of N is called a **forward-edge** for the segment (x, y) if $\langle v - u, y - x \rangle \geq 0$. An edge-path v_1, \dots, v_k of N is called a **forward-path** for the segment (x, y) , if all the edges $v_i v_{i+1}$ are forward-edges for (x, y) . Similarly to what has been done in [26], let us define a forward-path of N for the segment (x_1, x_2) , from x_1 to x_2 (see figure 6.5). Let F_1, \dots, F_ℓ be the faces of N whose interior intersect (x_1, x_2) (if some edge of N lies exactly on (x_1, x_2) , perturb the segment (x_1, x_2) slightly, using instead a segment $(x_1 + \varepsilon_1, x_2 + \varepsilon_2)$ for two generic infinitesimal translations $(\varepsilon_1, \varepsilon_2)$). Note that the number of such faces is finite because the rhombus tiling of the plane R has only finitely many different rhombi. Then for $j = 1, \dots, \ell - 1$, $F_j \cap F_{j+1}$ is an edge e_{j+1} of N crossing (x_1, x_2) . Set $v_1 = x_1$, $v_\ell = x_2$, and for $j = 1, \dots, \ell - 2$, define v_{j+1} to be the vertex of e_{j+1} such that the edge e_{j+1} oriented towards v_{j+1} is a forward-edge for (x_1, x_2) . Then, for $j = 1, \dots, \ell - 1$, the vertices v_j and v_{j+1} belong to the face F_j . Take an edge-path from v_j to v_{j+1} on the boundary cycle of F_j , such that it is a forward-path for (x_1, x_2) . Such a path exists because faces of N are convex. Thus, we have built a forward-path of N for (x_1, x_2) , from x_1 to x_2 . Denote by $u_1 = x_1, u_2, \dots, u_{k-1}, u_k = x_2$ the vertices of this path.

Let us now define an edge-path of \tilde{R} from w to b . Note that the edges wx_1 and x_2b are edges of \tilde{R} . For $j = 1, \dots, k - 1$, define the following edge-path of \tilde{R} from u_j to u_{j+1} (see figure 6.6). Remember that $u_j u_{j+1}$ is the diagonal of a rhombus of R , say ℓ'_j . Let r_j be the dual graph of ℓ'_j . Let u_j^1 be the black vertex in r_j adjacent to u_j , let u_j^2 be the crossing of the diagonals of ℓ'_j , and let u_j^3 be the white vertex in r_j adjacent to u_{j+1} . Then the path $u_j, u_j^1, u_j^2, u_j^3, u_{j+1}$ is an edge-path of \tilde{R} . Thus

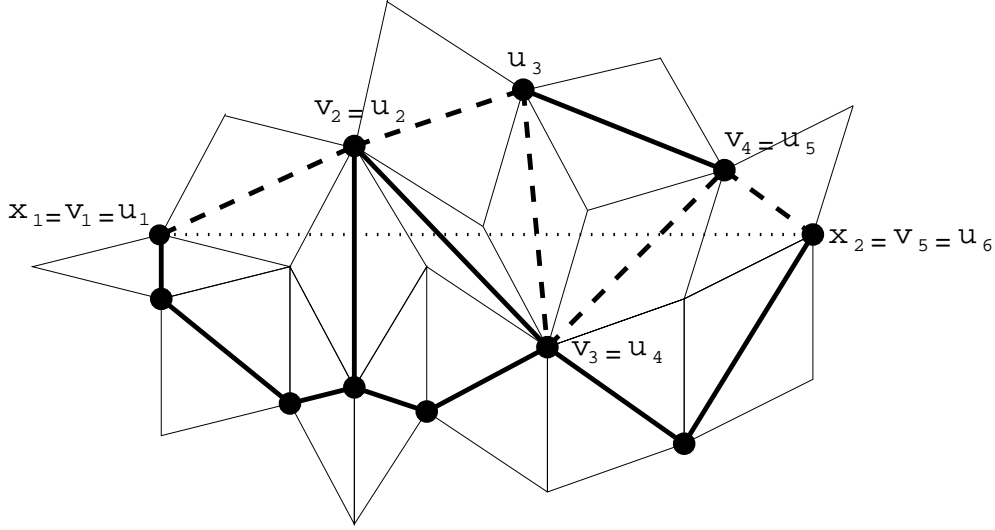


Figure 6.5: forward-path from x_1 to x_2 for the segment (x_1, x_2) .

$w, x_1 = u_1, u_1^1, u_1^2, u_1^3, u_2, \dots, u_{k-1}, u_{k-1}^1, u_{k-1}^2, u_{k-1}^3, u_k = x_2, b$ is an edge-path of \tilde{R} , from w to b . Orient the edges in the path towards the black vertices of R^* , and away from the white vertices of R^* .

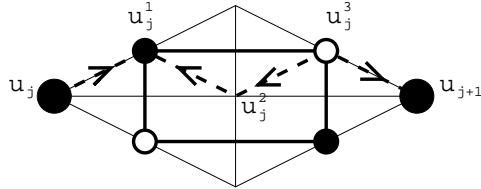


Figure 6.6: Edge-path of \tilde{R} from u_j to u_{j+1} .

Let $e^{i\beta_j^1}, e^{i\beta_j^2}, e^{i\alpha_j^1}, e^{i\alpha_j^2}$ be the vectors corresponding respectively to the edges $u_j u_j^1, u_j^3 u_{j+1}, u_j^2 u_j^1, u_j^3 u_j^2$. Without loss of generality, suppose that $x_2 - x_1$ is real and positive. Then for $j = 1, \dots, k-1$, and $\ell = 1, 2$, we have:

$$\cos \beta_j^\ell - \cos \alpha_j^\ell = \frac{\langle u_{j+1} - u_j, x_2 - x_1 \rangle}{2|x_2 - x_1|}.$$

Since u_1, \dots, u_k is a forward-path for (x_1, x_2) , this quantity is positive, thus $\cos \beta_j^\ell \geq \cos \alpha_j^\ell$.

Moreover, since there is only a finite number of different rhombi in R , $k = O(|b-w|)$. For the same reason, there is a finite number of angles β_j^ℓ , and they are all in $[-\pi + \Delta, \pi + \Delta]$, for some small $\Delta > 0$ (in the general case where the angle of the vector $x_2 - x_1$ is θ_0 ,

the angles β_j^ℓ would be in the interval $[\theta_0 - \pi + \Delta, \theta_0 + \pi + \Delta]$. Thus by theorem 4.3 of [26], we have:

$$K_R^{-1}(b, w) = \frac{1}{2\pi} \left(\frac{1}{b-w} + \frac{\gamma}{\bar{b}-\bar{w}} \right) + \frac{1}{2\pi} \left(\frac{\xi_2}{(b-w)^3} + \frac{\gamma\bar{\xi}_2}{(\bar{b}-\bar{w})^3} \right) + O\left(\frac{1}{|b-w|^3}\right), \quad (6.13)$$

where $\gamma = e^{-i(\theta_1+\theta_2)} \prod_{j=1}^{k-1} \prod_{\ell=1}^2 e^{i(-\beta_j^\ell + \alpha_j^\ell)}$, and $\xi_2 = e^{2i\theta_1} + e^{2i\theta_2} + \sum_{j=1}^{k-1} \sum_{\ell=1}^2 e^{2i\beta_j^\ell} - e^{2i\alpha_j^\ell}$.

Note that this theorem is stated in subsection 3.2.2 where, to simplify notations, we have omitted the second order term. This term appears in [26], and we state in (6.13), since it implies precision of the second order for theorem 6.15.

For $j = 1, \dots, k-1$, we have $\alpha_j^2 \equiv (\beta_j^1 + \pi) \pmod{[2\pi]}$, and $\beta_j^2 \equiv (\alpha_j^1 + \pi) \pmod{[2\pi]}$, thus:

$$\begin{aligned} \prod_{\ell=1}^2 e^{i(-\beta_j^\ell + \alpha_j^\ell)} &= e^{i(-\beta_j^1 + \alpha_j^1)} e^{i(-\alpha_j^1 - \pi + \beta_j^1 + \pi)} = 1, \\ \sum_{\ell=1}^2 e^{2i\beta_j^\ell} - e^{2i\alpha_j^\ell} &= e^{2i\beta_j^1} - e^{2i\alpha_j^1} + e^{2i(\alpha_j^1 + \pi)} - e^{2i(\beta_j^1 + \pi)} = 0. \end{aligned}$$

Therefore $\gamma = e^{-i(\theta_1+\theta_2)}$, $\xi_2 = e^{2i\theta_1} + e^{2i\theta_2}$, which proves the theorem. \square

Let R be a rhombus tiling of the plane, and let R^* be the corresponding rhombus-with-diagonals tiling. Recall that μ_R is the Gibbs measure on $\mathcal{M}(R^*)$ given by theorem 6.1. Consider a subset of edges $e_1 = w_1 b_1, \dots, e_k = w_k b_k$ of R^* .

Corollary 6.16 *When $\forall j \neq i$, $|w_j - b_i| \rightarrow \infty$, $\mu_R(e_1, \dots, e_k)$ only depends on the rhombi of R to which the vertices b_i and w_j belong, and else is independent of the structure of the graph R .*

Proof:

This is a consequence of the explicit formula for $\mu_R(e_1, \dots, e_k)$ of theorem 6.1, and of the asymptotic formula for the inverse complex Dirac operator K_R^{-1} of theorem 6.15. \square

Recall that the non planar graph \mathcal{L}^* is obtained by superposing the dual graphs L^* of all lozenge-with-diagonals tilings $L \in \mathcal{L}$. Let $e_1 = w_1 b_1, \dots, e_k = w_k b_k$ be a subset of edges of \mathcal{L}^* , and define \mathcal{L}^E to be the set of lozenge-with-diagonals tilings of the plane that contain the lozenges associated to the edges e_1, \dots, e_k .

Corollary 6.17 *When $\forall j \neq i$, $|w_j - b_i| \rightarrow \infty$, $\mu_L(e_1, \dots, e_k)$ is independent of $L \in \mathcal{L}^E$.*

Proof:

As in subsection 6.2.1, we choose an embedding of \mathcal{L}^* so that every edge of \mathcal{L}^* uniquely

determines the lozenge(s) it belongs to. Corollary 6.17 is then a restatement of corollary 6.16. \square

Recall that μ is the total measure for the triangular quadri-tile dimer model, given by proposition 6.14. Let l_{e_1}, \dots, l_{e_k} be the lozenges associated to the edges e_1, \dots, e_k of \mathcal{L}^* , and let k_{e_1}, \dots, k_{e_k} be the corresponding edges of \mathbb{T}^* .

Corollary 6.18 *When $\forall j \neq i, |w_j - b_i| \rightarrow \infty$, and for every $L \in \mathcal{L}^E$, we have $\mu(e_1, \dots, e_k) = \mu_L(e_1, \dots, e_k)\nu(k_{e_1}, \dots, k_{e_k})$.*

Proof:

This is a consequence of the explicit formula for $\mu(e_1, \dots, e_k)$ of proposition 6.14, and of corollary 6.17. \square

Chapter 7

Height fluctuations for isoradial dimer models

Consider an infinite isoradial graph G whose dual graph G^* is bipartite. Suppose that the critical weight function is assigned to edges of G^* . Consider the height function h on 2-tilings of G given in section 3.5, then 2-tilings of G can be interpreted as discrete surfaces that are projected to the plane. Assume that G is either periodic, or is a rhombus-with-diagonals tiling of the plane, and let μ be the Gibbs measure of theorem 6.1, on the set of dimer configurations $\mathcal{M}(G^*)$ of G^* . An interesting question is to understand the fluctuations of the discrete surfaces, when the dimer configurations are chosen with respect to the measure μ (theorem 7.2).

In section 7.1, we define the Gaussian free field in the plane: it is a Gaussian random distribution whose covariance function is given by the Dirichlet energy.

Let us multiply the edge-lengths of the graph G by a real factor ε , this yields a new graph G^ε . Let h be the unnormalized height function on 2-tilings of G^ε . Theorem 7.2 of section 7.2 states that the height function h converges weakly in distribution to a Gaussian free field. Section 7.3 consists in the proof of theorem 7.2.

A direct application of theorem 7.2 yields the convergence of the height function of domino tilings, lozenge tilings and quadri-tilings of the plane to a Gaussian free field. Recall from chapter 6 that an isoradial dimer model is always in the liquid phase. We believe the result of theorem 7.2 to hold for all dimer models in the liquid phase.

7.1 Gaussian free field in the plane

In this section, we define the Gaussian free field in the plane. It is a random distribution whose covariance function is given by the Dirichlet energy.

7.1.1 Green's function of the plane, and Dirichlet energy

The **Green's function of the plane**, denoted by g , is the kernel of the Laplace equation in the plane, it satisfies $\Delta_x g(x, y) = \delta_x(y)$, where δ_x is the Dirac distribution at x . Up to an additive constant, g is given by

$$g(x, y) = -\frac{1}{2\pi} \log |x - y|.$$

Define the following bilinear form

$$\begin{aligned} G : C_{c,0}^\infty(\mathbb{R}^2) \times C_{c,0}^\infty(\mathbb{R}^2) &\longrightarrow \mathbb{R} \\ (\varphi_1, \varphi_2) &\longmapsto G(\varphi_1, \varphi_2) = \int_{\mathbb{R}^2} \int_{\mathbb{R}^2} g(x, y) \varphi_1(x) \varphi_2(y) dx dy. \end{aligned}$$

$G(\varphi, \varphi)$ is called the **Dirichlet energy** of φ . Let us consider the topology induced by the L^∞ norm on $C_{c,0}^\infty(\mathbb{R}^2)$.

Lemma 7.1 *G is a continuous, positive definite, bilinear form.*

Proof:

G is continuous

This is a consequence of the fact that for every $\varphi_1, \varphi_2 \in C_{c,0}^\infty(\mathbb{R}^2)$, the function $g(x, y)$ is integrable.

G is positive definite

For $i = 1, 2$, denote by $K_i = \text{supp}(\varphi_i)$, and let $f_i(x) = \int_{\mathbb{R}^2} g(x, y) \varphi_i(y) dy$. Let us prove that

$$G(\varphi_1, \varphi_2) = \int_{\mathbb{R}^2} \nabla f_1(x) \cdot \nabla f_2(x) dx. \quad (7.1)$$

For any $R > 0$, Green's formula implies

$$\int_{B(0,R)} \nabla f_1(x) \cdot \nabla f_2(x) dx = - \int_{B(0,R)} \Delta f_1(x) f_2(x) dx + \int_{S(0,R)} f_2(x) \nabla f_1(x) \cdot n(x) ds. \quad (7.2)$$

Assume R is large enough so that $K_1, K_2 \subset B(0, R)$. The first term of the right hand side of (7.2) satisfies

$$\begin{aligned} - \int_{B(0,R)} \Delta f_1(x) f_2(x) dx &= - \int_{B(0,R)} \Delta_x \left(\int_{K_1} g(x, y) \varphi_1(y) dy \right) \left(\int_{K_2} g(x, y) \varphi_2(y) dy \right) dx, \\ &= \int_{K_1} \int_{K_2} g(x, y) \varphi_1(x) \varphi_2(y) dy dx = G(\varphi_1, \varphi_2). \end{aligned}$$

In order to evaluate the second term of the right hand side of (7.2), let us compute

$$\begin{aligned}
 \nabla f_1(x) \cdot n(x) &= -\frac{1}{2\pi} \int_{K_1} \varphi_1(y) \nabla \log |x-y| \cdot n(x) dy, \\
 &= -\frac{1}{2\pi} \int_{K_1} \varphi_1(y) \frac{|x|}{|x-y|^2} dy, \\
 &= -\frac{1}{2\pi} \int_{K_1} \varphi_1(y) \left(\frac{|x|}{|x-y|^2} - \frac{1}{|x|} \right) dy - \frac{1}{2\pi} \int_{K_1} \varphi_1(y) \frac{1}{|x|} dy, \\
 &= -\frac{1}{2\pi} \int_{K_1} \varphi_1(y) \left(\frac{|x|}{|x-y|^2} - \frac{1}{|x|} \right) dy \quad (\text{since } \varphi_1 \text{ is a mean 0 function}).
 \end{aligned}$$

$\forall x \in S(0, R)$, $\forall y \in K_1$, we have $\frac{|x|}{|x-y|^2} - \frac{1}{|x|} = O\left(\frac{1}{R^2}\right)$, hence $|\nabla f_1(x) \cdot n(x)| = O\left(\frac{1}{R^2}\right)$; $\forall x \in S(0, R)$, we also have $|f_2(x)| = O(\log R)$, thus the second term of the right hand side of (7.2) is $O\left(\frac{\log R}{R}\right)$. Taking the limit as $R \rightarrow \infty$ in (7.2), we obtain (7.1).

Let us assume $G(\varphi_1, \varphi_1) = 0$. By equality (7.1) this is equivalent to $\int_{\mathbb{R}^2} |\nabla f_1(x)|^2 dx = 0$, hence $\nabla f_1 \equiv (0, 0)$. Since $\varphi_1(x) = \Delta f_1(x) = \operatorname{div}(\nabla f_1(x))$, we deduce $\varphi_1 \equiv 0$. \square

7.1.2 Random distributions

The following definitions are taken from [17]. A **random function** F associates to every function $\varphi \in C_{c,0}^\infty(\mathbb{R}^2)$ a real random variable $F\varphi$. For $\varphi_1, \dots, \varphi_k \in C_{c,0}^\infty(\mathbb{R}^2)$, we suppose that the joint probabilities $a_n \leq F\varphi_n < b_n$, $1 \leq n \leq k$ are given, and we ask that they satisfy the compatibility relation. A random function F is **linear** if $\forall \varphi_1, \varphi_2 \in C_{c,0}^\infty(\mathbb{R}^2)$,

$$F(\alpha\varphi_1 + \beta\varphi_2) = \alpha F\varphi_1 + \beta F\varphi_2.$$

It is **continuous** if convergence of the functions φ_{n_j} to φ_j ($1 \leq j \leq k$) implies

$$\lim_{n \rightarrow \infty} (F\varphi_{n_1}, \dots, F\varphi_{n_k}) = (F\varphi_1, \dots, F\varphi_k),$$

that is, if $P(x)$ (resp. $P_n(x)$) is the probability measure corresponding to the random variable $(F\varphi_1, \dots, F\varphi_k)$ (resp. $(F\varphi_{n_1}, \dots, F\varphi_{n_k})$), then for any bounded continuous function f

$$\lim_{n \rightarrow \infty} \int f(x_1, \dots, x_k) dP_n(x) = \int f(x_1, \dots, x_k) dP(x).$$

A **random distribution** F is a random function which is linear and continuous. It is said to be **Gaussian** if for every linearly independent functions $\varphi_1, \dots, \varphi_k \in C_{c,0}^\infty(\mathbb{R}^2)$, the random vector $(F\varphi_1, \dots, F\varphi_k)$ is Gaussian.

Two random distributions F and G are said to be **independent** if for any functions $\varphi_1, \dots, \varphi_k \in C_{c,0}^\infty(\mathbb{R}^2)$, the random vectors $(F\varphi_1, \dots, F\varphi_k)$ and $(G\varphi_1, \dots, G\varphi_k)$ are independent.

7.1.3 Gaussian free field in the plane

Theorem 7.2 [4] *If $G : C_{c,0}^\infty(\mathbb{R}^2) \times C_{c,0}^\infty(\mathbb{R}^2) \rightarrow \mathbb{R}$ is a bilinear, continuous, positive definite form, then there exists a Gaussian random distribution F , whose covariance function is given by*

$$\mathbb{E}(F\varphi_1 F\varphi_2) = G(\varphi_1, \varphi_2).$$

Using lemma 7.1, and theorem 7.2, we define a **Gaussian free field in the plane** to be a Gaussian random distribution whose covariance function is

$$\mathbb{E}(F\varphi_1 F\varphi_2) = -\frac{1}{2\pi} \int_{\mathbb{R}^2} \int_{\mathbb{R}^2} \log|x-y|\varphi_1(x)\varphi_2(y) dx dy.$$

See also [14, 41] for other ways of the defining the Gaussian free field.

7.2 Gaussian fluctuations for the height function of the isoradial dimer model

For the remaining of this chapter, we let G be an infinite isoradial graph satisfying (*). Suppose that G is either periodic, or is a rhombus-with-diagonals tiling of the plane (which might not be periodic), and ask that its dual graph G^* is bipartite. Assume the critical weight function ν is assigned to the edges of G^* . Let K be the complex Dirac operator indexed by the vertices of G^* , and let K^{-1} be the inverse complex Dirac operator, (see section 3.2 for definitions). Consider the Gibbs measure μ on the set of dimer configurations $\mathcal{M}(G^*)$ of the graph G^* , given by theorem 6.1.

Recall the definition of the reference flow $\omega_0 \in \Omega(G^*)$, in the case of isoradial graphs: for every edge wb of G^* , if θ_{wb} is the rhombus angle of the edge wb , then ω_0 flows by θ_{wb}/π from w to b . This flow ω_0 defines a height function h on vertices of 2-tilings of G (see section 3.5). Denote by G^ε the graph G whose edge-lengths have been multiplied by ε , and define

$$\begin{aligned} H^\varepsilon : C_{c,0}^\infty(\mathbb{R}^2) &\rightarrow \mathbb{R} \\ \varphi &\mapsto H^\varepsilon \varphi = \varepsilon^2 \sum_{v \in V(G^\varepsilon)} \varphi(v)h(v), \end{aligned}$$

where $V(G^\varepsilon)$ denotes the set of vertices of the graph G^ε , and the height function h is unnormalized. The next theorem states the convergence of H^ε to $\frac{1}{\sqrt{\pi}}$ times a Gaussian free field. It is proved in section 7.3.

Theorem 7.3 *Consider a graph G satisfying the above assumptions, then H^ε converges weakly in distribution to $\frac{1}{\sqrt{\pi}}$ times a Gaussian free field, that is for every $\varphi_1, \dots, \varphi_k \in C_{c,0}^\infty(\mathbb{R}^2)$, $(H^\varepsilon \varphi_1, \dots, H^\varepsilon \varphi_k)$ converges in law (as $\varepsilon \rightarrow 0$) to $\frac{1}{\sqrt{\pi}}(F\varphi_1, \dots, F\varphi_k)$, where F is a Gaussian free field.*

7.3 Proof of theorem 7.3

Since the random vector $(F\varphi_1, \dots, F\varphi_k)$ is Gaussian, to prove convergence of $(H^\varepsilon\varphi_1, \dots, H^\varepsilon\varphi_k)$ to $(F\varphi_1, \dots, F\varphi_k)$, it suffices to prove convergence of the moments of $(H^\varepsilon\varphi_1, \dots, H^\varepsilon\varphi_k)$ to those of $(F\varphi_1, \dots, F\varphi_k)$; that is we need to show that for every k -tuple of positive integers (m_1, \dots, m_k) , we have

$$\lim_{\varepsilon \rightarrow 0} \mathbb{E}_\mu[(H^\varepsilon\varphi_1)^{m_1} \dots (H^\varepsilon\varphi_k)^{m_k}] = \mathbb{E}[(F\varphi_1)^{m_1} \dots (F\varphi_k)^{m_k}]. \quad (7.3)$$

In subsection 7.3.1, we prove two properties of the height function h . Then, in subsection 7.3.2, we prove a formula for the limit (as $\varepsilon \rightarrow 0$) of the k^{th} moment of h . In subsection 7.3.3, we use this formula to prove convergence of $\mathbb{E}[(H^\varepsilon\varphi)^k]$ to $\mathbb{E}[(F\varphi)^k]$. One obtains equation (7.3) by choosing φ to be a suitable linear combination of the φ_i 's.

Consider the orientation of the edges of G induced by the bipartite coloring of the vertices of G^* : edges around the black faces of G are oriented cclw, edges around the white faces of G are then oriented cw.

7.3.1 Properties of the height function

Let u, v be two vertices of G , and let γ be an edge-path of G from u to v . First, consider edges of γ which are oriented in the direction of the path, that is edges which have a black face of G on the left, and denote by f_1, \dots, f_n their dual edges. Hence an edge f_j consists of a black vertex on the left of γ , and of a white one on the right. Similarly, consider edges of γ which are oriented in the opposite direction, and denote by e_1, \dots, e_m their dual edges, hence an edge e_i consists of a white vertex on the left of γ , and of a black one on the right. Let \mathbb{I}_e be the indicator function of $\mathcal{M}(G^*)$: $\mathbb{I}_e(M) = 1$ if the edge e belongs to the dimer configuration M of G^* , and 0 else.

Lemma 7.4

$$h(v) - h(u) = \sum_{j=1}^m (\mathbb{I}_{e_j} - \mu(e_j)) + \sum_{j=1}^n (-\mathbb{I}_{f_j} + \mu(f_j)).$$

Proof:

Let e_j be the dual edge of an edge $u_j v_j$ of γ oriented from v_j to u_j . Denote by θ_j the rhombus angle of the edge e_j , then by lemma 2.5,

$$h(v_j) - h(u_j) = \begin{cases} -\frac{\theta_j}{\pi} + 1 & \text{if the edge } e_j \text{ belongs to the dimer configuration of } G^*, \\ -\frac{\theta_j}{\pi} & \text{else.} \end{cases}$$

Hence $h(v_j) - h(u_j) = (-\frac{\theta_j}{\pi} + 1)\mathbb{I}_{e_j} - \frac{\theta_j}{\pi}(1 - \mathbb{I}_{e_j}) = \mathbb{I}_{e_j} - \frac{\theta_j}{\pi}$. Moreover, we know from equation (6.4) that $\mu(e_j) = \theta_j/\pi$, so

$$h(v_j) - h(u_j) = \mathbb{I}_{e_j} - \mu(e_j).$$

Similarly, when f_j is the dual edge of an edge $u'_j v'_j$ of γ oriented from u'_j to v'_j , we obtain $h(v'_j) - h(u'_j) = -\mathbb{I}_{f_j} + \mu(f_j)$, and we conclude

$$h(v) - h(u) = \sum_{j=1}^m h(v_j) - h(u_j) + \sum_{j=1}^n h(v'_j) - h(u'_j) = \sum_{j=1}^m (\mathbb{I}_{e_j} - \mu(e_j)) + \sum_{j=1}^n (-\mathbb{I}_{f_j} + \mu(f_j)).$$

□

Lemma 7.5

$$\mathbb{E}_\mu[h(v) - h(u)] = 0.$$

Proof:

By lemma 7.4 we have

$$\begin{aligned} \mathbb{E}_\mu[h(v) - h(u)] &= \sum_{j=1}^m \mathbb{E}_\mu[\mathbb{I}_{e_j} - \mu(e_j)] + \sum_{j=1}^n \mathbb{E}_\mu[-\mathbb{I}_{f_j} + \mu(f_j)] \\ &= \sum_{j=1}^m (\mu(e_j) - \mu(e_j)) + \sum_{j=1}^n (-\mu(f_j) + \mu(f_j)) = 0. \end{aligned}$$

□

7.3.2 Moment formula

Let $u_1, \dots, u_k, v_1, \dots, v_k$ be distinct points of \mathbb{R}^2 , and let $\gamma_1, \dots, \gamma_k$ be pairwise disjoint paths such that γ_j runs from u_j to v_j . Let $u_j^\varepsilon, v_j^\varepsilon$ be black vertices of G^ε lying within $O(\varepsilon)$ of u_j and v_j respectively. Then, we have

Proposition 7.6 *For every $k \in \mathbb{N}$, $k \geq 2$*

$$\lim_{\varepsilon \rightarrow 0} \mathbb{E}_\mu[(h(v_1^\varepsilon) - h(u_1^\varepsilon)) \dots (h(v_k^\varepsilon) - h(u_k^\varepsilon))] = \frac{(-i)^k}{(2\pi)^k} \sum_{\varepsilon=0,1} (-1)^{k\varepsilon} \left(\int_{\gamma_1} \dots \int_{\gamma_k} \det_{\substack{i,j \in [1,k] \\ i \neq j}} \left(\frac{1}{z_i^\varepsilon - z_j^\varepsilon} \right) dz_1^\varepsilon \dots dz_k^\varepsilon \right), \tag{7.4}$$

where $z_i^0 = z_i$ and $z_i^1 = \bar{z}_i$.

Proof:

Let $\gamma_1^\varepsilon, \dots, \gamma_k^\varepsilon$ be pairwise disjoint paths of G^ε , such that γ_j^ε runs from u_j^ε to v_j^ε and approximates γ_j within $O(\varepsilon)$. For every j , denote by f_{js}^ε the dual edge of the s^{th} edge of the path γ_j^ε , which is oriented in the direction of the path: f_{js}^ε consists of a black vertex on the left of γ_j^ε , and of a white one on the right. Denote by e_{jt} the dual edge

of the t^{th} edge of the path γ_j^ε , which is oriented in the opposite direction: e_{jt} consists of a black vertex on the right of γ_j^ε , and of a white one on the left. Using lemma 7.4, we obtain

$$\begin{aligned}
 & \mathbb{E}_\mu[(h(v_1^\varepsilon) - h(u_1^\varepsilon)) \dots (h(v_k^\varepsilon) - h(u_k^\varepsilon))] = \\
 &= \mathbb{E}_\mu \left[\sum_{t_1} (\mathbb{I}_{e_{1t_1}} - \mu(e_{1t_1})) - \sum_{s_1} (\mathbb{I}_{f_{1s_1}} - \mu(f_{1s_1})) \right] \dots \left[\sum_{t_k} (\mathbb{I}_{e_{kt_k}} - \mu(e_{kt_k})) - \sum_{s_k} (\mathbb{I}_{f_{ks_k}} - \mu(f_{ks_k})) \right], \\
 &= \sum_{t_1, \dots, t_k} \mathbb{E}_\mu [\mathbb{I}_{e_{1t_1}} - \mu(e_{1t_1})] \dots [\mathbb{I}_{e_{kt_k}} - \mu(e_{kt_k})] - \dots + (-1)^k \sum_{s_1, \dots, s_k} \mathbb{E}_\mu [\mathbb{I}_{f_{1s_1}} - \mu(f_{1s_1})] \dots [\mathbb{I}_{f_{ks_k}} - \mu(f_{ks_k})], \\
 &= \sum_{\delta_1, \dots, \delta_k \in \{0,1\}} \sum_{t_1^{\delta_1}, \dots, t_k^{\delta_k}} (-1)^{\delta_1 + \dots + \delta_k} \mathbb{E}_\mu [\mathbb{I}_{e_{1t_1^{\delta_1}}} - \mu(e_{1t_1^{\delta_1}})] \dots [\mathbb{I}_{e_{kt_k^{\delta_k}}} - \mu(e_{kt_k^{\delta_k}})], \tag{7.5}
 \end{aligned}$$

$$\text{where } t_j^{\delta_j} = \begin{cases} t_j & \text{if } \delta_j = 0 \\ s_j & \text{if } \delta_j = 1 \end{cases}, \quad e_{jt_j^{\delta_j}} = e_{jt_j^{\delta_j}} = \begin{cases} e_{jt_j} & \text{if } \delta_j = 0 \\ f_{js_j} & \text{if } \delta_j = 1 \end{cases}.$$

For the time being, let us drop the second subscript. Write $e_j = w_j b_j$ and $f_j = w'_j b'_j$, the letters w, b are used respectively for the white and the black vertex. Moreover, let us introduce the notation $w_j^{\delta_j}$, where $w_j^{\delta_j} = w_j$ if $\delta_j = 0$, and $w_j^{\delta_j} = w'_j$ if $\delta_j = 1$, similarly we introduce the notation $b_j^{\delta_j}$. Hence we can write a generic term of (7.5) as

$$(-1)^{\delta_1 + \dots + \delta_k} \mathbb{E}_\mu [(\mathbb{I}_{w_1^{\delta_1} b_1^{\delta_1}} - \mu(w_1^{\delta_1} b_1^{\delta_1})) \dots (\mathbb{I}_{w_k^{\delta_k} b_k^{\delta_k}} - \mu(w_k^{\delta_k} b_k^{\delta_k}))].$$

Lemma 7.7 [21]

$$\begin{aligned}
 & (-1)^{\delta_1 + \dots + \delta_k} \mathbb{E}_\mu [(\mathbb{I}_{w_1^{\delta_1} b_1^{\delta_1}} - \mu(w_1^{\delta_1} b_1^{\delta_1})) \dots (\mathbb{I}_{w_k^{\delta_k} b_k^{\delta_k}} - \mu(w_k^{\delta_k} b_k^{\delta_k}))] = \\
 &= (-1)^{\delta_1 + \dots + \delta_k} a_E \begin{vmatrix} 0 & K^{-1}(b_1^{\delta_1}, w_2^{\delta_2}) & \dots & K^{-1}(b_1^{\delta_1}, w_k^{\delta_k}) \\ K^{-1}(b_2^{\delta_2}, w_1^{\delta_1}) & 0 & & \vdots \\ \vdots & & & K^{-1}(b_{k-1}^{\delta_{k-1}}, w_k^{\delta_k}) \\ K^{-1}(b_k^{\delta_k}, w_1^{\delta_1}) & \dots & K^{-1}(b_k^{\delta_k}, w_{k-1}^{\delta_{k-1}}) & 0 \end{vmatrix}, \tag{7.6}
 \end{aligned}$$

where $a_E = \prod_{j=1}^k K(w_j^{\delta_j}, b_j^{\delta_j})$, and K is the complex Dirac operator indexed by the vertices of G^* .

A typical term in the expansion of (7.6) is

$$(-1)^{\delta_1 + \dots + \delta_k} a_E \operatorname{sgn} \sigma K^{-1}(b_1^{\delta_1}, w_{\sigma(1)}^{\delta_{\sigma(1)}}) \dots K^{-1}(b_k^{\delta_k}, w_{\sigma(k)}^{\delta_{\sigma(k)}}), \tag{7.7}$$

where $\sigma \in \widetilde{S}_k$, and \widetilde{S}_k is the set of permutations of k elements, with no fixed points. To simplify notations, let us assume σ is a k -cycle, hence (7.7) becomes

$$(-1)^{\delta_1 + \dots + \delta_k} a_E \operatorname{sgn} \sigma K^{-1}(b_1^{\delta_1}, w_2^{\delta_2}) \dots K^{-1}(b_k^{\delta_k}, w_1^{\delta_1}). \tag{7.8}$$

Lemma 7.8 *When ε is small, and for every $\delta_1, \dots, \delta_k \in \{0, 1\}$,*

$$\varepsilon^k a_E = (-i)^k (-1)^{\delta_1 + \dots + \delta_k} dz_1^{\delta_1} \dots dz_k^{\delta_k}. \quad (7.9)$$

Proof:

Let $u_j v_j$ be an edge of the path γ_j^ε where u_j precedes v_j . We can write

$$u_j v_j = \varepsilon \ell(u_j v_j) e^{i\theta_j}, \quad (7.10)$$

where $\ell(u_j v_j)$ is the length of the edge $u_j v_j$ in G , and θ_j is the direction from u_j to v_j . Let us first consider the case of an edge $u_j v_j$ oriented in the direction of the path, that is the dual edge $w'_j b'_j$ of $u_j v_j$ has its black vertex on the left of γ_j^ε . By definition of the complex Dirac operator, we have $K(w'_j, b'_j) = \ell(u_j v_j) e^{i\theta_j} e^{i\frac{\pi}{2}}$. Next we consider the case of an edge $u_j v_j$ oriented in the opposite direction, that is its dual edge $w_j b_j$ has its black vertex on the right of γ_j^ε . Again, using the definition of the complex Dirac operator, we obtain $K(w_j, b_j) = \ell(u_j v_j) e^{i\theta_j} e^{-i\frac{\pi}{2}}$. We summarize the two cases by the following equation

$$K(w_j^{\delta_j}, b_j^{\delta_j}) = (-i)(-1)^{\delta_j} \ell(u_j v_j) e^{i\theta_j}. \quad (7.11)$$

When ε is small we replace $u_j v_j$ by $dz_j^{\delta_j}$. Thus combining equations (7.10) and (7.11) we obtain equation (7.9). \square

Lemma 7.9 *When ε is small and up to a term of order $O(\varepsilon)$, equation (7.8) equals*

$$\frac{(-i)^k}{(2\pi)^k} \sum_{\varepsilon_1, \dots, \varepsilon_k \in \{0, 1\}} [f_{w_2^{\delta_2} b_1^{\delta_1}}(0)]^{\varepsilon_1} \dots [f_{w_1^{\delta_1} b_k^{\delta_k}}(0)]^{\varepsilon_k} F_{\varepsilon_1}(b_1^{\delta_1}, w_2^{\delta_2}) \dots F_{\varepsilon_k}(b_k^{\delta_k}, w_1^{\delta_1}) dz_1^{\delta_1} \dots dz_k^{\delta_k}, \quad (7.12)$$

where $F_0(z, w) = \frac{1}{z - w}$, $F_1(z, w) = F_0(\bar{z}, \bar{w})$, and the functions f_{wb} are defined in section 3.2.

Proof:

Let us drop the superscripts δ_i . Plugging relation (7.9) in (7.8), we obtain

$$(7.8) = (-i)^k \operatorname{sgn} \sigma K^{-1}(b_1, w_2) \dots K^{-1}(b_k, w_1) \frac{1}{\varepsilon^k} dz_1 \dots dz_k. \quad (7.13)$$

Moreover, for every $i \neq j$, $\lim_{\varepsilon \rightarrow 0} \frac{|b_i - w_j|}{\varepsilon} = \infty$, so that by theorem 3.2 we have

$$K^{-1}(b_i, w_j) = \frac{\varepsilon}{2\pi} (F_0(b_i, w_j) + f_{w_j b_i}(0) F_1(b_i, w_j)) + O(\varepsilon^2). \quad (7.14)$$

Equation (7.12) is then (7.13) where the elements $K^{-1}(b_i, w_j)$ have been replaced by (7.14) and expanded out. \square

In what follows, all that we say is true whether the edge $w_j^{\delta_j} b_j^{\delta_j}$ has its black vertex on the right or on the left of the path γ_j^ε , that is whether $\delta_j = 0$ or 1. So to simplify notations, let us write $\{t_j\}$ instead of $\{\delta_j \in \{0, 1\}, t_j^{\delta_j}\}$, hence $\{t_j\}$ is the set of indices which run along the path γ_j^ε . Keeping in mind that our aim is to take the limit as $\varepsilon \rightarrow 0$, we replace the vertices b_j and w_j in the argument of the function F_{ε_j} by one common vertex denoted by z_j . Define

$$H(\varepsilon_1, \dots, \varepsilon_k) = \sum_{t_1, \dots, t_k} [f_{w_{2t_2} b_{1t_1}}(0)]^{\varepsilon_1} \dots [f_{w_{1t_1} b_{kt_k}}(0)]^{\varepsilon_k} F_{\varepsilon_1}(z_{1t_1}, z_{2t_2}) \dots F_{\varepsilon_k}(z_{kt_k}, z_{1t_1}) dz_{1t_1} \dots dz_{kt_k}.$$

Lemma 7.10

1. If $(\varepsilon_1, \dots, \varepsilon_k) = (0, \dots, 0)$, then

$$\lim_{\varepsilon \rightarrow 0} H(0, \dots, 0) = \int_{\gamma_1} \dots \int_{\gamma_k} F_0(z_1, z_2) \dots F_0(z_k, z_1) dz_1 \dots dz_k.$$

2. If $(\varepsilon_1, \dots, \varepsilon_k) = (1, \dots, 1)$, then

$$\lim_{\varepsilon \rightarrow 0} H(1, \dots, 1) = (-1)^k \int_{\gamma_1} \dots \int_{\gamma_k} F_0(\bar{z}_1, \bar{z}_2) \dots F_0(\bar{z}_k, \bar{z}_1) d\bar{z}_1 \dots d\bar{z}_k.$$

3. Assume there exists $i \neq j \in \{1, \dots, k\}$ such that $\varepsilon_i = 0$, $\varepsilon_j = 1$, then

$$\lim_{\varepsilon \rightarrow 0} |H(\varepsilon_1, \dots, \varepsilon_k)| = 0.$$

Proof:

Here are some preliminary notations. Dropping the second subscript, we consider an edge $u_j v_j$ of one of the paths γ_i^ε , where u_j precedes v_j . Let us denote by $w_j b_j$ the dual edge of the edge $u_j v_j$, and let $\varepsilon e^{i\alpha_j} = v_j - w_j$, $\varepsilon e^{i\beta_j} = b_j - v_j$. With these notations, we have $dz_j = \varepsilon(e^{i\alpha_j} - e^{i\beta_j})$ (see figure 7.1).

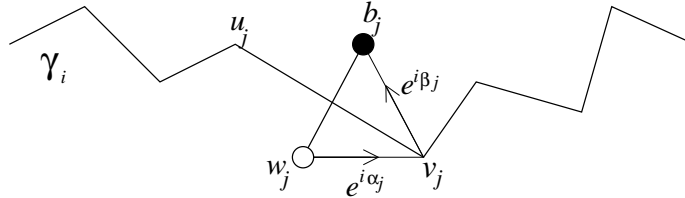


Figure 7.1: Notations

Moreover, define

$$J(\varepsilon_1, \dots, \varepsilon_k) = [f_{w_2 b_1}(0)]^{\varepsilon_1} \dots [f_{w_1 b_k}(0)]^{\varepsilon_k} dz_1 \dots dz_k.$$

Proof of 1.

$$J(0, \dots, 0) = dz_1 \dots dz_k,$$

so that

$$H(0, \dots, 0) = \sum_{t_1, \dots, t_k} F_0(z_{1t_1}, z_{2t_2}) \dots F_0(z_{kt_k}, z_{1t_1}) dz_{1t_1} \dots dz_{kt_k}.$$

Since the paths γ_j are disjoint, the function $F_0(z_1, z_2) \dots F_0(z_k, z_1)$ is integrable, and taking the limit as $\varepsilon \rightarrow 0$, we obtain 1.

Proof of 2.

$$J(1, \dots, 1) = f_{w_2 b_1}(0) \dots f_{w_1 b_k}(0) dz_1 \dots dz_k.$$

Fix a vertex v of G^* . Then, by definition of the function f_{wv} ,

$$\begin{aligned} J(1, \dots, 1) &= f_{w_2 v}(0) f_{v b_1}(0) \dots f_{w_1 v}(0) f_{v b_k}(0) dz_1 \dots dz_k, \\ &= f_{w_1 v}(0) f_{v b_1}(0) \dots f_{w_k v}(0) f_{v b_k}(0) dz_1 \dots dz_k, \\ &= f_{w_1 b_1}(0) \dots f_{w_k b_k}(0) dz_1 \dots dz_k. \end{aligned}$$

For every j , we have $f_{w_j b_j}(0) = e^{-i(\beta_j + \alpha_j)}$. Moreover, recall that $dz_j = \varepsilon(e^{i\alpha_j} - e^{i\beta_j})$, so that $-d\bar{z}_j = e^{-i(\beta_j + \alpha_j)} dz_j$, and we deduce

$$J(1, \dots, 1) = (-1)^k d\bar{z}_1 \dots d\bar{z}_k.$$

This implies,

$$H(1, \dots, 1) = (-1)^k \sum_{t_1, \dots, t_k} F_0(\bar{z}_{1t_1}, \bar{z}_{2t_2}) \dots F_0(\bar{z}_{kt_k}, \bar{z}_{1t_1}) d\bar{z}_{1t_1} \dots d\bar{z}_{kt_k}.$$

Taking the limit as $\varepsilon \rightarrow 0$, we obtain 2.

Proof of 3.

Consider $0 < \ell < k$, and assume $\varepsilon_1 = \dots = \varepsilon_{\ell-1} = 0$, $\varepsilon_\ell = \dots = \varepsilon_k = 1$. Let us prove that $\lim_{\varepsilon \rightarrow 0} |H(0, \dots, 0, 1, \dots, 1)| = 0$. Note that up to a permutation of indices, the argument is the same for the other cases.

$$J(0, \dots, 0, 1, \dots, 1) = f_{w_{\ell+1} b_\ell}(0) \dots f_{w_1 b_k}(0) dz_1 \dots dz_k.$$

As above, let v be a vertex of G^* . Then,

$$J(0, \dots, 0, 1, \dots, 1) = (f_{v b_\ell}(0) dz_\ell) (f_{w_1 v}(0) dz_1) dz_2 \dots dz_{\ell-1} d\bar{z}_{\ell+1} \dots d\bar{z}_k.$$

Introducing the following notation

$$\begin{aligned} H_1 &= F(z_{2t_2}, z_{3t_3}) \cdots F(z_{\ell-2t_{\ell-2}}, z_{\ell-1t_{\ell-1}}) F(\bar{z}_{\ell+1t_{\ell+1}}, \bar{z}_{\ell+2t_{\ell+2}}) \cdots F(\bar{z}_{k-1t_{k-1}}, \bar{z}_{kt_k}), \\ H_2 &= F(z_{1t_1}, z_{2t_2}) F(\bar{z}_{kt_k}, \bar{z}_{1t_1}), \\ H_3 &= F(z_{\ell-1t_{\ell-1}}, z_{\ell t_\ell}) F(\bar{z}_{\ell t_\ell}, \bar{z}_{\ell+1t_{\ell+1}}), \end{aligned}$$

we obtain $H(0, \dots, 0, 1, \dots, 1) =$

$$= \sum_{t_2, \dots, t_\ell, \dots, t_k} H_1 \left(\sum_{t_1} H_2 f_{w_{1t_1} v}(0) dz_{1t_1} \right) \left(\sum_{t_\ell} H_3 f_{vb_{\ell t_\ell}}(0) dz_{\ell t_\ell} \right) dz_{2t_2} \cdots dz_{\ell-1t_{\ell-1}} d\bar{z}_{\ell+1t_{\ell+1}} \cdots d\bar{z}_{kt_k}.$$

Let us prove

$$\sum_{t_\ell} f_{vb_{\ell t_\ell}}(0) dz_{\ell t_\ell} = O(\varepsilon). \quad (7.15)$$

Dropping the second subscript, let $u_1, v_1 = u_2, v_2 = u_3, \dots, v_{m-1} = u_m, v_m$ be the edge-path γ_ℓ^ε . Denote by ξ the quantity $f_{vu_1}(0)$, then

$$f_{vb_j}(0) = \xi e^{i(\beta_1 - \alpha_1)} \cdots e^{i(\beta_{j-1} - \alpha_{j-1})} e^{-i\alpha_j}.$$

Since $dz_j = \varepsilon(e^{i\alpha_j} - e^{i\beta_j})$, we obtain

$$f_{vb_j}(0) dz_j = \varepsilon \xi \left[\left(e^{i(\beta_1 - \alpha_1)} \cdots e^{i(\beta_{j-1} - \alpha_{j-1})} \right) - \left(e^{i(\beta_1 - \alpha_1)} \cdots e^{i(\beta_{j-1} - \alpha_{j-1})} e^{i(\beta_j - \alpha_j)} \right) \right],$$

hence

$$\begin{aligned} \sum_{t_\ell} f_{vb_{\ell t_\ell}}(0) dz_{\ell t_\ell} &= \sum_{j=1}^m f_{vb_j}(0) dz_j, \\ &= \varepsilon \xi \left[1 - e^{i(\beta_1 - \alpha_1)} + \sum_{j=2}^m e^{i(\beta_1 - \alpha_1)} \cdots e^{i(\beta_{j-1} - \alpha_{j-1})} - (e^{i(\beta_1 - \alpha_1)} \cdots e^{i(\beta_{j-1} - \alpha_{j-1})} e^{i(\beta_j - \alpha_j)}) \right], \\ &= \varepsilon \xi [1 - (e^{i(\beta_1 - \alpha_1)} \cdots e^{i(\beta_m - \alpha_m)}), \text{ (telescopic sum)}]. \end{aligned}$$

We deduce $|\sum_{t_\ell} f_{vb_{\ell t_\ell}}(0) dz_{\ell t_\ell}| \leq 2\varepsilon$, and (7.15) is proved.

In a similar way we prove $\sum_{t_1} f_{w_{1t_1} v}(0) dz_{1t_1} = O(\varepsilon)$.

Using Taylor expansion in ε for H_2 and H_3 , we deduce that $(\sum_{t_1} H_2 f_{w_{1t_1} v}(0) dz_{1t_1})$ and $(\sum_{t_\ell} H_3 f_{vb_{\ell t_\ell}}(0) dz_{\ell t_\ell})$ are $O(\varepsilon)$. Since the function H_1 is integrable, we conclude that $H(0, \dots, 0, 1, \dots, 1)$ is $O(\varepsilon^2)$ and so 3. is proved. \square

Rewriting the second subscript, and summing equation (7.8) over the paths $\gamma_1^\varepsilon, \dots, \gamma_k^\varepsilon$, we obtain (by lemma 7.9 and 7.10):

$$\begin{aligned} \lim_{\varepsilon \rightarrow 0} \operatorname{sgn} \sigma \sum_{\delta_1, \dots, \delta_k \in \{0,1\}} \sum_{t_1^{\delta_1} \dots t_k^{\delta_k}} (-1)^{\delta_1 + \dots + \delta_k} a_E K^{-1}(b_{1t_1^{\delta_1}}, w_{2t_2^{\delta_2}}) \cdots K^{-1}(b_{kt_k^{\delta_k}}, w_{1t_1^{\delta_1}}) = \\ = \frac{(-i)^k}{(2\pi)^k} \operatorname{sgn} \sigma \sum_{\varepsilon=0,1} (-1)^{\varepsilon k} \left(\int_{\gamma_1} \cdots \int_{\gamma_k} F_0(z_1^\varepsilon, z_2^\varepsilon) \cdots F_0(z_k^\varepsilon, z_1^\varepsilon) dz_1^\varepsilon \cdots dz_k^\varepsilon \right), \end{aligned} \quad (7.16)$$

where $z_i^0 = z_i$ and $z_i^1 = \bar{z}_i$. When σ is a product of disjoint cycles, we can treat each cycle separately and the result is the product of terms like (7.16). Thus when we sum over all permutations with no fixed points, we obtain equation (7.4) of proposition 7.6. \square

Proposition 7.11

- When k is odd, $\lim_{\varepsilon \rightarrow 0} \mathbb{E}_\mu[(h(v_1^\varepsilon) - h(u_1^\varepsilon)) \dots (h(v_k^\varepsilon) - h(u_k^\varepsilon))] = 0$.
- When k is even, $\lim_{\varepsilon \rightarrow 0} \mathbb{E}_\mu[(h(v_1^\varepsilon) - h(u_1^\varepsilon)) \dots (h(v_k^\varepsilon) - h(u_k^\varepsilon))] =$

$$= \left(\frac{1}{\pi}\right)^{k/2} \sum_{\tau \in \mathcal{T}_k} g(u_{\tau(1)}, v_{\tau(1)}, u_{\tau(2)}, v_{\tau(2)}) \dots g(u_{\tau(k-1)}, v_{\tau(k-1)}, u_{\tau(k)}, v_{\tau(k)}),$$

where $g(u, v, u', v') = g(v, v') + g(u, u') - g(v, u') - g(u, v')$, g is the Green's function of the plane, and \mathcal{T}_k is the set of all $(k-1)!!$ pairings of $\{1, \dots, k\}$.

Proof:

Let us cite the following lemma from [24].

Lemma 7.12 [24] *Let M be the $k \times k$ matrix $M = (m_{ij})$, with $m_{ii} = 0$, and $m_{ij} = \frac{1}{x_i - x_j}$, when $i \neq j$. Then when k is odd, $\det M = 0$, and when k is even*

$$\det M = \sum_{\tau \in \mathcal{T}_k} \frac{1}{(x_{\tau(1)} - x_{\tau(2)})^2 \dots (x_{\tau(k-1)} - x_{\tau(k)})^2}.$$

Combining proposition 7.6 and lemma 7.12, when $k = 2$, we obtain

$$\begin{aligned} \lim_{\varepsilon \rightarrow 0} \mathbb{E}_\mu[(h(v_1^\varepsilon) - h(u_1^\varepsilon))(h(v_2^\varepsilon) - h(u_2^\varepsilon))] &= \\ &= -\frac{1}{4\pi^2} \left(\int_{\gamma_1} \int_{\gamma_2} \frac{1}{(z_1 - z_2)^2} dz_1 dz_2 + \int_{\gamma_1} \int_{\gamma_2} \frac{1}{(\bar{z}_1 - \bar{z}_2)^2} d\bar{z}_1 d\bar{z}_2 \right), \\ &= -\frac{1}{2\pi^2} \log \left| \frac{(v_1 - v_2)(u_1 - u_2)}{(v_1 - u_2)(u_1 - v_2)} \right|, \\ &= \frac{1}{\pi} g(u_1, v_1, u_2, v_2). \end{aligned}$$

The case of a general even k is an easy but notationally cumbersome extension of the case $k = 2$. \square

7.3.3 Proof of theorem 7.3

Proposition 7.13

$$\lim_{\varepsilon \rightarrow 0} \mathbb{E}_\mu[(H^\varepsilon \varphi)^k] = \frac{1}{\pi^k} \mathbb{E}[(F\varphi)^k] = \begin{cases} 0 & \text{when } k \text{ is odd,} \\ (k-1)!! \frac{1}{\pi^{k/2}} G(\varphi, \varphi)^{k/2} & \text{when } k \text{ is even.} \end{cases} \quad (7.17)$$

Proof:

The second equality is just the k^{th} moment of a mean 0, variance $\frac{1}{\pi} G(\varphi, \varphi)$, Gaussian variable. So let us prove equality between the first and the last term.

Consider u_1, \dots, u_k distinct points of \mathbb{R}^2 , and for every j , let u_j^ε be a vertex of G^ε lying within $O(\varepsilon)$ of u_j . Define

$$H_{u_j}^\varepsilon \varphi = \sum_{v^\varepsilon \in G^\varepsilon} \varepsilon^2 \varphi(v^\varepsilon) (h(v^\varepsilon) - h(u_j^\varepsilon)) = \sum_{v^\varepsilon \in K^\varepsilon} \varepsilon^2 \varphi(v^\varepsilon) (h(v^\varepsilon) - h(u_j^\varepsilon)),$$

where $K^\varepsilon = G^\varepsilon \cap K$, and $K = \text{supp}(\varphi)$, then since we sum over a finite number of vertices,

$$\begin{aligned} \mathbb{E}_\mu[H_{u_1}^\varepsilon \varphi \dots H_{u_k}^\varepsilon \varphi] &= \mathbb{E}_\mu \left[\sum_{v_1^\varepsilon \in K^\varepsilon} \varepsilon^2 \varphi(v_1^\varepsilon) (h(v_1^\varepsilon) - h(u_1^\varepsilon)) \dots \sum_{v_k^\varepsilon \in K^\varepsilon} \varepsilon^2 \varphi(v_k^\varepsilon) (h(v_k^\varepsilon) - h(u_k^\varepsilon)) \right], \\ &= \sum_{v_1^\varepsilon \in K^\varepsilon} \dots \sum_{v_k^\varepsilon \in K^\varepsilon} (\varepsilon^2)^k \varphi(v_1^\varepsilon) \dots \varphi(v_k^\varepsilon) \mathbb{E}_\mu[(h(v_1^\varepsilon) - h(u_1^\varepsilon)) \dots (h(v_k^\varepsilon) - h(u_k^\varepsilon))] \end{aligned} \quad (7.18)$$

Lemma 7.14 *As $\varepsilon \rightarrow 0$, the Riemann sum (7.18) converges to*

$$\int \dots \int \varphi(v_1) \dots \varphi(v_k) \lim_{\varepsilon \rightarrow 0} \mathbb{E}_\mu[(h(v_1^\varepsilon) - h(u_1^\varepsilon)) \dots (h(v_k^\varepsilon) - h(u_k^\varepsilon))] dv_1 \dots dv_k,$$

where $\lim_{\varepsilon \rightarrow 0} \mathbb{E}_\mu[(h(v_1^\varepsilon) - h(u_1^\varepsilon)) \dots (h(v_k^\varepsilon) - h(u_k^\varepsilon))]$ is given by proposition 7.11.

Proof:

In what follows, all that we say is true whether $\delta_j = 0$ or 1, so to simplify notations, as before, let us write $\{t_j\}$ instead of $\{\delta_j \in \{0, 1\}, t_j^{\delta_j}\}$, hence $\{t_j\}$ is the set of indices which run along the path γ_j^ε . Combining equations (7.5), (7.7) and (7.9) yields,

$$\begin{aligned} \mathbb{E}_\mu[h(v_1^\varepsilon) - h(u_1^\varepsilon)] \dots [h(v_k^\varepsilon) - h(u_k^\varepsilon)] &= \\ &= (-i)^k \sum_{t_1, \dots, t_k} \sum_{\sigma \in \widetilde{S}_k} \text{sgn } \sigma K^{-1}(b_{1t_1}, w_{\sigma(1)t_{\sigma(1)}}) \dots K^{-1}(b_{kt_k}, w_{\sigma(k)t_{\sigma(k)}}) \frac{1}{\varepsilon^k} dz_{1t_1} \dots dz_{kt_k}. \end{aligned} \quad (7.19)$$

It suffices to consider the case where σ is a k -cycle, other cases are treated similarly. Indices are denoted cyclically (i.e. $k+1 \equiv 1$). There is a singularity in (7.19) as soon as $v_j^\varepsilon = v_{j+1}^\varepsilon$ for some indices j . Hence, we need to prove that for ε small enough,

$$\sum_{v_1^\varepsilon} \dots \sum_{v_k^\varepsilon} (\varepsilon^2)^k |\varphi(v_1^\varepsilon) \dots \varphi(v_k^\varepsilon)| \sum_{t_1, \dots, t_k} |K^{-1}(b_{1t_1}, w_{2t_2}) \dots K^{-1}(b_{kt_k}, w_{1t_1})| \frac{1}{\varepsilon^k} dz_{1t_1} \dots dz_{kt_k}, \quad (7.20)$$

is $o(1)$, when the sum is over vertices $v_1^\varepsilon, \dots, v_k^\varepsilon$ that satisfy

$$|v_1^\varepsilon - v_2^\varepsilon| \leq \delta, \dots, |v_m^\varepsilon - v_{m+1}^\varepsilon| \leq \delta, |v_{m+1}^\varepsilon - v_{m+2}^\varepsilon| > \delta, \dots, |v_k^\varepsilon - v_1^\varepsilon| > \delta,$$

for some $1 \leq m < k - 1$. Let $0 < \beta < 1$, up to a renaming of indices, this amounts to considering vertices $v_1^\varepsilon, \dots, v_k^\varepsilon$ in $\Theta_1 \cap \Theta_2 \cap \Theta_3$, where

$$\begin{aligned} \Theta_1 &= \{v_1^\varepsilon, \dots, v_m^\varepsilon \mid \{1 \leq i \leq m, 0 \leq |v_i^\varepsilon - v_{i+1}^\varepsilon| \leq \varepsilon^\beta\}, \\ \Theta_2 &= \{v_{m+1}^\varepsilon, \dots, v_n^\varepsilon \mid m+1 \leq j \leq n, \varepsilon^\beta \leq |v_j^\varepsilon - v_{j+1}^\varepsilon| \leq \delta\}, \\ \Theta_3 &= \{v_{n+1}^\varepsilon, \dots, v_k^\varepsilon \mid n+1 \leq \ell \leq k, |v_\ell^\varepsilon - v_{\ell+1}^\varepsilon| > \delta\}, \end{aligned}$$

for some $1 \leq m < n < k - 1$.

Since u_1, \dots, u_k are distinct vertices of \mathbb{R}^2 , and since equation (7.20) does not depend on the path γ_j^ε from u_j^ε to v_j^ε , let us choose the paths $\gamma_1^\varepsilon, \dots, \gamma_k^\varepsilon$ as follows. Note that it suffices to consider the part of the path γ_j^ε where the vertices b_{jt_j} and w_{jt_j} are within distance δ from v_j^ε . Let us write $|t_j| \leq \delta$ to denote indices t_j which refer to vertices of γ_j^ε that are at distance at most δ from v_j^ε . Take γ_j^ε to approximate a straight line within $O(\varepsilon)$, from v_j^ε to $v_j^\varepsilon + \delta$. Moreover, ask that if one continues the lines of γ_j^ε and γ_{j+1}^ε away from u_j^ε and u_{j+1}^ε , they intersect and form an angle θ_j . Let us use the definition of the paths γ_j^ε , and consider the three following cases. Whenever it is not confusing, we shall drop the second subscript. C denotes a generic constant, $A \sim B$ means A and B are of the same order.

- $v_1^\varepsilon, \dots, v_m^\varepsilon \in \Theta_1$.

By remark 7.15 below, we have $|K^{-1}(b_i, w_{i+1})| \leq C$. This implies,

$$\sum_{|t_1| \leq \delta, \dots, |t_m| \leq \delta} |K^{-1}(b_{1t_1}, w_{2t_2}) \dots K^{-1}(b_{mt_m}, w_{m+1t_{m+1}})| \frac{1}{\varepsilon^m} dz_{1t_1} \dots dz_{mt_m} \leq \left(\frac{C\delta}{\varepsilon}\right)^m.$$

- $v_{n+1}^\varepsilon, \dots, v_k^\varepsilon \in \Theta_3$.

By definition of the paths γ_ℓ^ε , $|b_\ell - w_{\ell+1}| > \delta$, so that $\lim_{\varepsilon \rightarrow 0} \frac{|b_\ell - w_{\ell+1}|}{\varepsilon} = \infty$. Using theorem 3.2 yields $\frac{1}{\varepsilon} |K^{-1}(b_\ell, w_{\ell+1})| = O\left(\frac{1}{|b_\ell - w_{\ell+1}|}\right) \leq \frac{C}{\delta}$. Hence,

$$\sum_{|t_{n+1}| \leq \delta, \dots, |t_k| \leq \delta} |K^{-1}(b_{n+1t_{n+1}}, w_{n+2t_{n+2}}) \dots K^{-1}(b_{kt_k}, w_{1t_1})| \frac{1}{\varepsilon^{k-n}} dz_{n+1t_{n+1}} \dots dz_{kt_k} \leq \left(\frac{C}{\delta}\right)^{k-n}.$$

- $v_{m+1}^\varepsilon, \dots, v_n^\varepsilon \in \Theta_2$.

Let $\varepsilon^\beta \leq L \leq \delta$, and define the annulus, $A(v_j^\varepsilon, L) = \{v \in G^\varepsilon \mid L \leq |v - v_j^\varepsilon| \leq L + \varepsilon\}$.

By definition of the paths γ_j^ε , if $v_j^\varepsilon \in A(v_{j+1}^\varepsilon, L)$, we have $\lim_{\varepsilon \rightarrow 0} \frac{|b_j - w_{j+1}|}{\varepsilon} = \infty$ (since $\beta < 1$). Using theorem 3.2 yields

$$\frac{1}{\varepsilon} |K^{-1}(b_j, w_{j+1})| = O\left(\frac{1}{|b_j - w_{j+1}|}\right) \leq \frac{1}{\min_{\{w_{j+1} \in \gamma_{j+1}^\varepsilon\}} |b_j - w_{j+1}|} = \frac{C}{x_j + CL} \sin \theta_j,$$

where x_j is the distance from v_j^ε to b_j . Let us replace $\sin \theta_j$ by C . Hence, if for $m+1 \leq j \leq n$, $v_j^\varepsilon \in A(v_{j+1}, L_j)$, we obtain

$$\begin{aligned} & \sum_{|t_{m+1}| \leq \delta, \dots, |t_n| \leq \delta} |K^{-1}(b_{m+1+t_{m+1}}, w_{m+2t_{m+2}}) \dots K^{-1}(b_{nt_n}, w_{n+1t_{n+1}})| \frac{1}{\varepsilon^{n-m}} dz_{m+1t_{m+1}} \dots dz_{nt_n} \leq \\ & \leq \sum_{|t_{m+1}| \leq \delta, \dots, |t_n| \leq \delta} \frac{C}{x_{m+1t_{m+1}} + CL_{m+1}} \dots \frac{C}{x_{nt_n} + CL_n} dx_{m+1t_{m+1}} \dots dx_{nt_n}, \\ & \sim C \prod_{j=m+1}^n \log \left(\frac{\delta + CL_j}{CL_j} \right). \end{aligned}$$

Let Ξ be the sum (7.20) over vertices $v_1^\varepsilon, \dots, v_k^\varepsilon \in \Theta_1 \cap \Theta_2 \cap \Theta_3$. Denote by $M = \sup_{v \in \mathbb{R}^2} |\varphi(v)|$. Then, $\Xi \leq \Xi_1 \Xi_2 \Xi_3$, where

$$\begin{aligned} \Xi_1 &= CM^m \left[\sum_{v_1^\varepsilon, \dots, v_m^\varepsilon \in \Theta_1} \varepsilon^{2m} \left(\frac{\delta}{\varepsilon} \right)^m \right], \\ \Xi_2 &= \left[\sum_{v_{n+1}^\varepsilon, \dots, v_k^\varepsilon \in \Theta_2} \varepsilon^{2(k-n)} |\varphi(v_{n+1}^\varepsilon)| \dots |\varphi(v_k^\varepsilon)| \left(\frac{1}{\delta} \right)^{k-n} \right], \\ \Xi_3 &= CM^{n-m} \left[\sum_{L_{m+1}=0}^{\delta} \dots \sum_{L_n=0}^{\delta} \varepsilon^{n-m} L_{m+1} \dots L_n \log \left(\frac{\delta + CL_{m+1}}{L_{m+1}} \right) \dots \log \left(\frac{\delta + CL_n}{L_n} \right) dL_{m+1} \dots dL_n \right]. \end{aligned}$$

Moreover,

$$\begin{aligned} \Xi_1 &\leq CM^m \delta^m \varepsilon^{m(2\beta-1)}, \\ \Xi_2 &\leq \left(\frac{1}{\delta} \right)^{k-n} \sum_{v_{n+1}^\varepsilon, \dots, v_k^\varepsilon \in \mathbb{R}^2} \varepsilon^{2(k-n)} |\varphi(v_{n+1}^\varepsilon)| \dots |\varphi(v_k^\varepsilon)| \leq M^{k-n} \left(\frac{1}{\delta} \right)^{k-n}, \\ \Xi_3 &\sim CM^{n-m} (\delta \log \delta)^{n-m}. \end{aligned}$$

Hence, $\Xi \leq CM^k \delta^{2n-k} \varepsilon^{m(2\beta-1)}$. Let us take $\beta = 2/3 < 1$, then $m(2\beta - 1) > 0$. If $2n - k \geq 1$, then $\Xi = o(1)$. If $2n - k \leq 0$, take $\varepsilon \leq \delta^{\frac{k-2n+1}{m(2\beta-1)}}$, and $\Xi = o(1)$.

Remark 7.15 Let G^* be a bipartite isoradial graph, and let K^{-1} be the corresponding inverse Dirac operator, then for every black vertex b and every white vertex w of G^* , we have

$$|K^{-1}(b, w)| \leq C$$

for some constant C which only depends on the graph G^* .

Proof:

By theorem 3.1, K^{-1} is given by

$$K^{-1}(b, w) = \frac{1}{4\pi^2 i} \int_C f_{wb}(z) \log z \, dz,$$

Refer to theorem 3.1 for the definition of C . Without loss of generality suppose $\theta_0 = 0$. As in [26], let us homotope the curve C to the curve from $-\infty$ to the origin and back to $-\infty$ along the two sides of the negative real axis. On the two sides of this ray, $\log z$ differs by $2\pi i$, hence

$$K^{-1}(b, w) = \frac{1}{2\pi} \int_{-\infty}^0 f_{wb}(t) dt, \text{ where } f_{wb}(t) = \frac{1}{(t - e^{i\theta_1})(t - e^{i\theta_2})} \prod_{j=1}^k \frac{(t - e^{i\alpha_j})}{(t - e^{i\beta_j})}.$$

Refer to [26] for the choice of path from w to b , that is for the definition of the angles $\theta_1, \theta_2, \alpha_j, \beta_j$. These angles have the property that for all j , $\cos \alpha_j \leq \cos \beta_j$, so

$$\left| \frac{t - e^{i\theta_j}}{t - e^{i\beta_j}} \right| \leq 1.$$

For every $e^{i\theta} \in \{e^{i\theta} \mid \theta \in [\theta_0 - \pi + \Delta, \theta_0 + \pi - \Delta]\}$, and for every $t < 0$, we have $|t - e^{i\theta}|^2 \geq |t - e^{i(\pi+\Delta)}|^2 = |t + e^{i\Delta}|^2$. Moreover for every $t \in \mathbb{R}$, we have $|t + e^{i\Delta}|^2 \geq \sin^2 \Delta$, and $|t + e^{i\Delta}|^2 \geq (t + 1)^2$, thus

$$\int_{-\infty}^0 |f_{wb}(t)| dt \leq \int_{-\infty}^{-2} \frac{1}{(t+1)^2} dt + \int_{-2}^0 \frac{1}{\sin^2 \Delta} dt = 1 + \frac{2}{\sin^2 \Delta}.$$

Hence $|K^{-1}(b, w)| \leq \mathcal{C}$, where $\mathcal{C} = \frac{1}{2\pi} \left(1 + \frac{2}{\sin^2 \Delta}\right)$. □

□

We end the proof of proposition 7.13 with the following

Lemma 7.16

$$1. \int \dots \int \varphi(v_1) \dots \varphi(v_k) \lim_{\varepsilon \rightarrow 0} \mathbb{E}_\mu[(h(v_1^\varepsilon) - h(u_1^\varepsilon)) \dots (h(v_k^\varepsilon) - h(u_k^\varepsilon))] dz_1 \dots dz_k =$$

$$= \begin{cases} 0 & \text{when } k \text{ is odd,} \\ (k-1)!! \frac{1}{\pi^{k/2}} G(\varphi, \varphi)^{k/2} & \text{when } k \text{ is even.} \end{cases}$$

$$2. \lim_{\varepsilon \rightarrow 0} \mathbb{E}_\mu[H_{u_1}^\varepsilon \varphi \dots H_{u_k}^\varepsilon \varphi] = \lim_{\varepsilon \rightarrow 0} \mathbb{E}_\mu[(H^\varepsilon \varphi)^k].$$

Proof:

1. is deduced from the formula of proposition 7.11, and from the fact that φ is a mean 0 function. 2. is a consequence of the fact that φ is a mean 0 function, and of estimates of the kind of those of lemma 7.14. □

□

Bibliography

- [1] R. J. Baxter, Exactly solved models in statistical mechanics. *Academic Press, London* (1982).
- [2] P. Billingsley, Probability and measure. Second edition. *Wiley* (1986).
- [3] H. W. J. Blöte, H. J. Hilhorst, Roughening transitions and the zero-temperature triangular Ising anti-ferromagnet. *J. Phys. A* **15** (1982), L631-L637.
- [4] Bochner, Harmonic analysis and the theory of probabilities. *Univ. of California Press* (1960).
- [5] O. Bodini, M. Latapy, Generalized tilings with height functions.
- [6] E. G. D. Cohen, J. de Boer, Z. W. Salsburg, *Physica* **21** (1955), 137.
- [7] H. Cohn, R. Kenyon, J. Propp, A variational principle for domino tilings. *J. Amer. Math. Soc.* **14** (2001), no 2, 297-346.
- [8] O. Darrigol, The Origins of the Entropy Concept. *Séminaire Poincaré* 2 (2003), 1-12.
- [9] G. David, C. Tomei, The problem of the calissons. *Amer. Math. Monthly* **96** (1989), no 5, 429-431.
- [10] G. Duff, D. Naylor, *Differential Equations of Applied Mathematics*, John Wiley and sons, New York (1966).
- [11] B. de Tiliere, Quadri-tilings of the plane. math.PR/0403324.
- [12] N. Elkies, G. Kuperberg, M. Larsen, and J. Propp, Alternating-sign matrices and domino tilings. *J. Algebraic Combin.* **1** (1992), no 2, 111-132.
- [13] R. H. Fowler, G. S. Rushbrooke, Statistical theory of perfect solutions. *Trans. Faraday. Soc.* **33** (1937), 1272-1294.
- [14] J. Glimm, A. Jaffe, Quantum physics. A functional integral point of view. *Springer-Verlag, New York-Berlin*, (1981).

- [15] H. S. Green, C. A. Hurst, Order-Disorder Phenomena, *Interscience, New York* (1964).
- [16] E. A. Guggenheim, Mixtures. *Clarendon Press, Oxford England* (1952), chap X.
- [17] I.M. Guelfand, N.Y. Vilenkin, Les distributions, Tome 4 : Applications de l'analyse harmonique. *Dunod, Paris* (1967).
- [18] P.W. Kasteleyn, The statistics of dimers on a lattice, I. The number of dimer arrangements on a quadratic lattice. *Physica* **27** (1961), 1209-1225.
- [19] P.W. Kasteleyn, Dimer statistics and phase transitions. *J. Mathematical Phys.* **4** (1963), 287-293.
- [20] P.W. Kasteleyn, Graph theory and crystal physics. *Graph Theory and Theoretical Physics, Academic Press, London*, (1967), 43-110.
- [21] R. Kenyon, Local statistics of lattice dimers. *Ann. Inst. H. Poincaré, Probab. Statist.* **33** (1997), no 5, 591-618.
- [22] R. Kenyon, An introduction to the dimer model. math.CO/0310326.
- [23] R. Kenyon, The planar dimer model with boundary: a survey. *CRM Monogr. Ser.* **13**, Amer. Math. Soc., Providence, (2000), 307-328.
- [24] R. Kenyon, Conformal invariance of domino tilings. *Ann. Probab.* **28** (2000), no 2, 759-795.
- [25] R. Kenyon, Dominos and the Gaussian free field. *Ann. Probab.* **29** (2001), no 3, 1128-1137.
- [26] R. Kenyon, The Laplacian and Dirac operators on critical planar graphs. *Invent. Math.* **150** (2002), no 2, 409-439.
- [27] R. Kenyon, Height fluctuations in the honeycomb dimer model. math-ph/0405052.
- [28] R. Kenyon, A. Okounkov, Harnack curves. math-ph/0311005.
- [29] R. Kenyon, A. Okounkov, S. Sheffield, Dimers and amoebas. math-ph/0311005.
- [30] R. Kenyon, J. Propp, D. Wilson, Trees and matchings. *Electron. J. Combin.* **7** (2000), Research Paper 25, 34 pp (electronic).
- [31] R. Kenyon, J-M. Schlenker, Rhombic embeddings of planar graphs. *Trans. Amer. Math. Soc.* (2003).
- [32] G. Kuperberg, An exploration of the permanent-determinant method. *Electron. J. Combin.* **5** (1998), Research Paper 46, 34 pp. (electronic).

-
- [33] L. S. Levitov, Equivalence of the dimer resonating-valence-bond problem to the quantum roughening problem. *Phys. Rev. Lett.* **64** (1990), 92-94.
- [34] L. Lovász, M. D. Plummer, Matching theory. *North-Holland Mathematics Studies* **121** (1986), North-Holland Publishing Co.
- [35] C. Mercat, Exponentials form a basis of discrete holomorphic functions on a compact. *Bull. Soc. Math. France* **132** (2004), no 2, 305-326.
- [36] C. Mercat, Discrete period matrices and related topics. math-ph/0111043.
- [37] T. Muir, A treatise on the theory of determinants. Dover publications New, York, (1960).
- [38] L. Onsager, A two-dimensional model with an order-disorder transition. *Phys. Rev.* **65** (1944), 117-149.
- [39] J. Propp, Lattice structure of orientations of graphs. math.CO/0209005.
- [40] S. Sheffield, PhD Thesis. *Stanford University* (2003).
- [41] S. Sheffield, Gaussian Free Field for mathematicians. math.PR/0312099.
- [42] H. N. V. Temperley, M. E. Fisher, Dimer problem in statistical mechanics - An exact result. *Phil. Mag.* **6** (1961), 1061-1063.
- [43] G. Tesler, Matchings in graphs on non-orientable surfaces. *J. Combin. Theory Ser. B* **78** (2000), no. 2, 198-231.
- [44] W.P. Thurston, Conway's tiling groups, *Amer. Math. Monthly* **97** (1990), no 8, 757-773.

N° d'impression :
4^{ème} trimestre 2004

Résumé

Le modèle de dimères modélise la répartition de molécules diatomiques à la surface d'un cristal. Nous nous plaçons dans le cas où le réseau représentant la surface du cristal est infini périodique et vérifie une condition géométrique appelée *isoradialité*, nous supposons que les arêtes du réseau sont munies de la fonction de poids *critique* (les poids modélisent la température extérieure). Le modèle a alors un comportement "critique", au sens où il n'a que 2 phases possibles, solide ou liquide, au lieu de 3 en général (il n'a pas de phase gazeuse). Les trois résultats principaux sur le modèle de dimères isoradial sont les suivants. Nous prouvons une formule explicite pour le taux de croissance de la fonction de partition de l'exhaustion naturelle du réseau infini. Puis, nous démontrons une formule explicite pour la mesure de Gibbs d'énergie libre minimale. L'originalité et l'intérêt de ces deux formules résident dans le fait qu'elles ne dépendent que de la géométrie locale du graphe et sont donc très simples d'utilisation. Nous pensons que cette propriété de localité est caractéristique du cas isoradial. D'autre part, les configurations de dimères ont une interprétation géométrique en tant que surfaces discrètes décrites par une fonction de hauteur. Nous montrons que lorsque les surfaces sont distribuées selon la mesure de Gibbs d'énergie libre minimale, la fonction de hauteur converge vers un champ libre Gaussien. Comme cas particulier de modèles de dimères isoradiaux, nous retrouvons les cas classiques de réseau \mathbb{Z}^2 et hexagonal avec mesure uniforme.

Nous introduisons le modèle de *quadri-pavages triangulaires*, où les quadri-pavages sont des pavages par quadrilatères obtenus à partir de triangles rectangles. Nous montrons que ce modèle est superposition de deux modèles de dimères sur des graphes isoradiaux, et l'interprétons géométriquement comme surfaces de dimension 2 dans un espace de dimension 4. Nous étudions ce modèle dans sa phase "critique". Nous montrons une formule explicite pour le taux de croissance de la fonction de partition *totale* et pour une mesure sur l'espace de *tous* les quadri-pavages (ceci nécessite d'étendre le résultat du cas isoradial à une famille de graphes non périodiques). C'est le premier modèle d'interfaces aléatoires en dimension $2 + 2$ sur lequel des résultats de ce type ont pu être obtenus.

Mots Clés : mécanique statistique, dimères, pavages, graphes isoradiaux, fonction de partition, mesure de Gibbs, champ libre Gaussien, quadri-pavages.

MSC2000 : 82B20.